




2018

## Inhibition of Mutant EGFR in NSCLC Promotes Endothelin-1-Mediated NSCLC Disease Progression

Stephen Ollosi  
*Loyola University Chicago*

Follow this and additional works at: [https://ecommons.luc.edu/luc\\_theses](https://ecommons.luc.edu/luc_theses)

 Part of the [Molecular Biology Commons](#)

---

### Recommended Citation

Ollosi, Stephen, "Inhibition of Mutant EGFR in NSCLC Promotes Endothelin-1-Mediated NSCLC Disease Progression" (2018). *Master's Theses*. 3698.  
[https://ecommons.luc.edu/luc\\_theses/3698](https://ecommons.luc.edu/luc_theses/3698)

This Thesis is brought to you for free and open access by the Theses and Dissertations at Loyola eCommons. It has been accepted for inclusion in Master's Theses by an authorized administrator of Loyola eCommons. For more information, please contact [ecommons@luc.edu](mailto:ecommons@luc.edu).



This work is licensed under a [Creative Commons Attribution-Noncommercial-No Derivative Works 3.0 License](#).  
Copyright © 2018 Stephen Ollosi

LOYOLA UNIVERSITY CHICAGO

INHIBITION OF MUTANT EGFR IN NSCLC PROMOTES  
ENDOTHELIN-1-MEDIATED NSCLC DISEASE PROGRESSION

A THESIS SUBMITTED TO  
THE FACULTY OF THE GRADUATE SCHOOL  
IN CANDIDACY FOR THE DEGREE OF  
MASTER OF SCIENCE

PROGRAM IN BIOCHEMISTRY AND MOLECULAR BIOLOGY

BY  
STEPHEN L. OLLOSI  
CHICAGO, IL  
AUGUST 2018

## ACKNOWLEDGMENTS

I would like to thank all of the people who made this dissertation possible, starting with the great professors in the Biochemistry and Molecular Biology Department at Loyola University Chicago, Stritch School of Medicine. Dr. Takeshi Shimamura provided an excellent resource for me from the beginning of my time here, and steered my thinking about the role of endothelin in NSCLC. Dr. Mitchell Denning and Dr. Nancy Zeleznik-Le provided me with much guidance throughout the entire process of my thesis and directed me in the right direction when needed.

My friends in the Biochemistry and Molecular Biology Department and outside of it have provided me with healthy competition and helped create an academic environment in which I could complete the work necessary for this thesis. Together, the great people in this school perform amazing work which is admirable in any organization.

## TABLE OF CONTENTS

ACKNOWLEDGMENTS	iii
LIST OF TABLES	vi
LIST OF FIGURES	vii
LIST OF ABBREVIATIONS	ix
ABSTRACT	xi
CHAPTER ONE: INTRODUCTION	1
Overview of Lung Cancer	1
EGFR Kinase Domain Mutation in NSCLC	3
Resistance to EGFR TKI Treatment	6
Acquired Resistance	7
EMT Overview	12
Endothelin-1 Overview	13
EDN1 and Vasoconstriction	14
VEGF Signaling Overview	16
EGFR TKI Plus VEGFR2 Inhibition in the Clinic	18
CHAPTER TWO: MATERIALS AND METHODS	21
Cell Lines and Cell Culture	21
Luminex Multiplex Assay	23
Cell Counting	23
Lentiviral Production and Transduction	24
Conditioned Media Preparation	26
<i>In vitro</i> Angiogenesis	26
Image Analysis	27
Western Blot Analysis	27
Murine Xenograft	28
IHC Sample Preparation	28
Immunohistochemical Staining	28
Microvessel Density Determination	29

CHAPTER THREE: RESULTS	31
Induction of EMT in EGFR Mutation-Positive NSCLC Cell Lines	31
Admix of Epithelial HCC827 and Mesenchymal ER23 Cell Types Confer a Growth Advantage <i>In Vivo</i> but No Growth Advantage is Seen in Epithelial and Mesenchymal Admix <i>In Vitro</i> in Multiple Cell Lines	33
HCC827/ER23 50/50 Admix at Time of Implantation Results in an Epithelial Dominated Tumor at 24 Days	36
The EMT Process Results in Differential Expression of Several Pro-Angiogenic and Growth Factors	38
Induction of EMT or EGFR Inhibition Results in a Significant Increase in EDN1 Secretion and Decrease in VEGF-A Secretion	40
Epithelial/Mesenchymal Admix Conditioned Media Confers Greater Differentiation Potential in Cultured HUVEC Endothelial Cells Compared to Epithelial or Mesenchymal Pure Culture Conditioned Media	43
Sunitinib/Zibotentan Combination Therapy Effectively Inhibits Tube Formation <i>In Vitro</i>	47
The Expression of EDNRA and Phosphorylated VEGFR2 in HUVEC Cells is Increased Under 8H Stimulation by Admix Conditioned Media and Sunitinib Abrogates VEGFR Phosphorylation	49
NSCLC Cell Lines with an EDN1 Over-Expression or Knock-Down Phenotype Maintain VEGF-A Secretion <i>In Vitro</i> and EDN1 Secretion was Associated with Significantly Lower Tumor Growth	51
EDN1 Expressing Tumors Show Significantly Greater EGFR TKI Resistance <i>In Vivo</i>	53
The Presence of EDN1 Secreting Cells in Admix Tumors or an Over-Expression Model Promotes Significantly Reduced Microvessel Density	55
Phosphorylated EGFR is Maintained in Gefitinib Treated Mesenchymal and Admix Tumors	58
CHAPTER FOUR: DISCUSSION	61
REFERENCE LIST	78
VITA	86

## LIST OF TABLES

Table 1. List of shRNA Sequences Used in Study	25
--	----

## LIST OF FIGURES

Figure 1. Induction of EMT in EGFR Mutation-Positive NSCLC Cell Lines	32
Figure 2. Admix of Epithelial HCC827 and Mesenchymal ER23 Cell Types Confers a Growth Advantage <i>In Vivo</i> but No Growth Advantage is Seen in Epithelial and Mesenchymal Admix <i>In Vitro</i> in Multiple Cell Lines.	35
Figure 3. HCC827/ER23 50/50 Admix at Time of Implantation Results in an Epithelial Dominated Tumor at 24 Days.	37
Figure 4. EMT Process Results in Differential Expression of Several Pro-Angiogenic and Growth Factors.	39
Figure 5. Induction of EMT or EGFR Inhibition Results in a Significant Increase in EDN1 Secretion and Decrease in VEGF-A Secretion.	42
Figure 6. Epithelial/Mesenchymal Admix Conditioned Media Confers Greater Differentiation Potential in Cultured HUVEC Cells Compared to Epithelial or Mesenchymal Pure Culture Conditions.	44
Figure 7. <i>In Vitro</i> Angiogenesis Analyzed by Tube Formation Assay.	46
Figure 8. <i>In Vitro</i> Inhibition of Angiogenesis Analyzed by Tube Formation Assay.	48

Figure 9. HUVEC Cells Express EDNRA and Phosphorylated VEGFR2 is Up-Regulated Under 8H Stimulation by Admix Conditioned Media While Being Effectively Abrogated by 10nM Sunitinib Treatment.	50
Figure 10. NSCLC Cells Lines Harboring EGFR Kinase Domain Mutations Maintain VEGF-A Secretion <i>In Vitro</i> when EDN1 is Either Over-Expressed or Knocked Down and Result in a Slower or Faster Growing Tumor Respectively <i>In Vivo</i> .	52
Figure 11. Mesenchymal or Epithelial/Mesenchymal Admix Tumors and Tumors Overexpressing EDN1 Result in Significantly Greater EGFR TKI Resistance <i>In Vivo</i> .	54
Figure 12. Epithelial/Mesenchymal Admix Conditions Result in Significantly Lower Blood Vessel Density Which Can be Abrogated Through Knockdown of EDN1 in Mesenchymal Cells.	52
Figure 13. Total EGFR is Comparable in Untreated Conditions While Total EGFR is Maintained in Gefitinib Treated Mesenchymal ER23 and Admix Tumors.	59
Figure 14. Phosphorylated EGFR is Maintained in Gefitinib Treated Mesenchymal and Admix Conditions.	60
Figure 15. Model Illustrating Hypothesis Relating EDN1-Mediated Vasoconstriction to Drug Resistance and Reduced MVD.	75



## LIST OF ABBREVIATIONS

SCLC	Small Cell Lung Carcinoma
NSCLC	Non-Small Cell Lung Carcinoma
RTK	Receptor Tyrosine Kinase
EGFR	Epidermal Growth Factor Receptor
EGF	Epidermal Growth Factor
TGF- $\alpha$	Transforming Growth Factor- $\alpha$
MAPK	Mitogen Activated Protein Kinase
PI3K	Phosphatidyl Inositol 3' Kinase
STAT	Signal Transducer and Activator of Transcription
VEGF-A	Vascular Endothelial Growth Factor A
TKI	Tyrosine Kinase Inhibitor
EMT	Epithelial-to-Mesenchymal Transition
SCC	Squamous Cell Carcinoma
HGF	Hepatocyte Growth Factor
PGF	Progression Free Survival
NT	Non-Target
CDH1	Epithelial Cadherin (E-Cadherin)
IGF- 1R	Insulin-like Growth Factor-1 Receptor
ZEB1	Zinc Finger E-Box Binding Homeobox 1

ZEB2	Zinc Finger E-Box Binding Homeobox 2
bHLH	Basic Helix-Loop-Helix
TGF- $\beta$	Transforming Growth Factor- $\beta$
EDRF	Endothelium-Derived Relaxing Factor
EDN1	Endothelin-1
EDN2	Endothelin-2
EDN3	Endothelin-3
EDNRA	Endothelin Receptor A
EDNRB	Endothelin Receptor B
GPCR	Guanine Nucleotide-Binding Protein-Coupled Receptor
PKB	Protein Kinase B
VEGFR1	Vascular Endothelial Growth Factor Receptor 1
VEGFR2	Vascular Endothelial Growth Factor Receptor 2
PDE5	Phosphodiesterase Type 5
MVD	Microvessel Density
VEGF-A	Vascular Endothelial Growth Factor A
VEGF-B	Vascular Endothelial Growth Factor B
VEGF-C	Vascular Endothelial Growth Factor C
VEGF-D	Vascular Endothelial Growth Factor D
VPF	Vascular Permeability Factor
ECM	Extracellular Matrix
HIF-1 $\alpha$	Hypoxia-Inducible Factor 1 $\alpha$
PIGF	Placental Growth Factor

HUVEC	Human Umbilical Vein Endothelial Cell
DMEM	Dulbecco's Modified Eagle's Medium
FBS	Fetal Bovine Serum
RPMI	Roswell Park Memorial Institute
BCA	Bicinchoninic Acid Assay
EBM	Endothelial Basal Media
EGM	Endothelial Growth Media
OCT	Optimal Cutting Temperature
IHC	Immunohistochemical
TBS	Tris Buffered Saline
PFS	Progression Free Survival
$\Delta$ NT	Non-Target Knockdown shRNA
$\Delta$ EDN1	Endothelin-1 Knockdown shRNA
$\Delta$ CDH1	E-Cadherin Knockdown shRNA

## ABSTRACT

Angiogenesis in NSCLC has been identified as important therapeutic target in combination with EGFR TKIs. However, only small incremental advancements have been made for the use of angiogenesis inhibitors in NSCLC and it remains elusive why the inhibition of VEGF-mediated neovascularization is not therapeutically efficacious. I present experimental evidence that a subpopulation of NSCLC cells with EGFR TKI-induced EMT contributes toward the attenuation of the response to EGFR TKI therapy. One of the hallmarks of cancer is heterogeneity and I have previously demonstrated that tumor heterogeneity within NSCLC cell lines harboring EGFR kinase domain mutations gives rise to divergent resistance mechanisms in response to treatment. *In vivo* admix models are instructive in studying intratumoral heterogeneity and in elucidating therapeutic responses and tumor-host interactions. While NSCLC cells with acquired EGFR TKI resistance and EMT phenotype did not exhibit growth advantage *in vitro*, a 50% epithelial EGFR TKI sensitive and 50% mesenchymal EGFR TKI resistant admix provided significant growth advantage *in vivo* assessed by caliper measurement. This preliminary result led us to hypothesize that changes in angiogenic growth factor expression during the EMT process might lead to the *in vivo* growth advantage I observed. To test the hypothesis, I utilized the Luminex multiplex assay system to quantify secreted growth factors, cytokines, and chemokines important in angiogenesis. I have discovered that epithelial EGFR TKI sensitive cells secrete a significant amount of VEGF-A and cells with acquired/transient EGFR TKI resistance with an EMT phenotype secrete substantial amount of EDN1. Using an *in vitro* tube formation assay, I

showed that secreted VEGF-A and EDN1 in admix conditions work synergistically to promote endothelial cell differentiation. Furthermore, this synergistic effect can be attenuated by VEGFR2/EDNRA dual inhibition. Surprisingly, ectopic overexpression of EDN1 in EGFR-mutated HCC827 cells resulted in significant growth retardation *in vivo*. Informed by a literature search, I hypothesized that the presence of EDN1 in the tumor microenvironment contributes positively to EGFR TKI resistance, possibly through the vasoconstrictive property of EDN1. I observed that epithelial/mesenchymal admix tumors and ectopic overexpression of EDN1 in EGFR-mutated HCC827 cells conferred significantly more resistance to gefitinib *in vivo*. This result led us to hypothesize that EDN1 may reduce MVD in EGFR-mutated NSCLC tumors leading to poor EGFR TKI penetrance *in vivo*. I tested this through CD31 IHC staining and MVD calculation. I indirectly tested poor EGFR TKI penetrance by examining phosphorylated EGFR and found maintenance of the signal in admix and mesenchymal tumors. Taken together, I suggest that inhibition of the EDN1 signaling system may be an important component to a blood vascular-based approach to treatment of EGFR-mutation positive NSCLC.

## CHAPTER ONE

### INTRODUCTION

#### **Overview of Lung Cancer**

Cancer represents one of the largest causes of death within the United States, with an estimated one in four deaths attributed to cancer related disease. Among these, lung cancer represents the leading cause of cancer-related deaths with 222,500 new cases in 2017 alone and an estimated 155,870 cases resulting in the death of the patient in the same year[1]. Since the late 1980's, incidence of lung cancer has generally decreased although this decline has varied among the several histologically defined sub- types. While squamous, large and small cell lung carcinoma rates have declined during this period, the incidence of lung adenocarcinoma remains stable among male patients and has increased among women and shows large racial variances[2].

Lung cancer is histologically divided into two main sub-types; SCLC and NSCLC. SCLC typically originates in the lung bronchi and is a fast-growing cancer which commonly metastasizes early in development and represents approximately 10% of all lung cancer cases. NSCLC represents approximately 85-90% of all lung cancer cases and is divided into 3 sub-types. Squamous cell carcinoma generally originates within the center of the lung and is common among smoking patients. Large cell carcinoma can originate in any area of the lung and is characterized as a fast-growing cancer. Adenocarcinoma generally originates in the outer sections of the lung and is a broadly slow-growing cancer.

Additionally, adenocarcinoma is most commonly seen in smokers although it is the most common type of lung cancer among non- smokers as well[3].

Based on the metastatic status of the cancer, lung cancer is typically divided into four stages. Stage I is characterized by a small (<3cm) tumor which is localized to one lung. Stage II is characterized by a larger tumor (>5cm) which has spread to local lymph nodes. Stage III involves a tumor which has spread to distant lymph nodes. Stage IV represents the most advanced cases of lung cancer and involves a large tumor (>7cm) which has metastasized to both lungs, into pleural effusion or into a different tissue in the body[4]. Stage IV lung cancer is commonly referred to as advanced stage or metastatic lung cancer.

The staging diagnosis is used to determine the treatment regimen for the patient. Stage I and stage II lung cancers are most often treated with surgical resection of either the affected lobe of the lung or wedge resection. Depending on the risk factor of the resected tumor, adjuvant chemotherapy or radiation therapy may be prescribed. Resected tumors are commonly tested for the presence of cancer cells at the margins of the section. If positive margins are seen, another surgery or chemotherapy is commonly prescribed. Stage III is commonly treated with a combination of chemotherapy, radiation therapy and surgery. Stage IV lung cancers represent the most difficult to treat since the cancer has achieved a large tumor size and metastasized to distant parts of the body. This is also the stage at which most cases of lung cancer are diagnosed. These patients are often not eligible for surgery or chemotherapy[5]. Therefore, it is important to explore developmental therapeutics targeting the specific genetic abnormalities present in the tumor. Although these treatments are unlikely to result in life-long remission, any extension of life or increase in quality of life is quite valuable to the patient.

The discovery of the oncogenic drivers in lung cancers has led to targeted therapies which directly target the abnormal signaling pathways which lead to the propagation of lung cancer. These therapies have been shown to effectively treat advanced stage lung cancers with less risk of side effects compared to traditional chemotherapy. One common driver of lung cancer is the RTK EGFR. Mutations in the kinase domain of this receptor strongly predicts a poor prognosis and response to drugs which inhibit EGFR[6].

### **EGFR Kinase Domain Mutation in NSCLC**

EGFR is a membrane-bound surface RTK. RTKs have been shown to have critical roles in normal cell signaling and have also been implicated in the progression of many types of cancer[7]. RTKs are a part of the larger family of protein tyrosine kinases which includes receptor tyrosine kinases which possess a trans-membrane domain and non-receptor tyrosine kinases which lack trans-membrane domains[8].

EGFR is a member of the ErbB family of receptors. The ErbB family contains four related receptor tyrosine kinases: ErbB1 (EGFR), ErbB2 (HER2), ErbB3 (HER3) and ErbB4 (HER4). This family of receptors is known to be over-expressed in several cancers including NSCLC and breast cancer. EGFR has been consistently shown to be over-expressed in 40-80% of NSCLC patients depending on the histological classification of the disease[9]. EGFR has been shown to be activated by several ligands including EGF, TGF- $\alpha$ , amphiregulin, heparin-binding EGF, and betacellulin[10]. Binding of EGFR to its ligands results in the homo- or hetero-dimerization with other ERBB family receptors leading to internalization and auto-phosphorylation of the receptor by the tyrosine kinase domain. Phosphorylated EGFR serves as a scaffold for the binding of signal transduction proteins such as Grb2 which then leads to an intracellular signaling cascade involving



down-stream proteins such as Ras[11]. The MAPK, PI3K, the AKT pathway and the STAT pathway represent four major signaling cascades activated by EGFR activation[12]. These pathways are known to regulate gene expression, inhibition of apoptosis, angiogenesis and cellular proliferation leading to the development of malignancy[13]. Although it was originally believed that EGFR signaling was distinct from angiogenesis, a link between angiogenesis and EGFR signaling pathways has been described through the EGFR-dependent stimulation of VEGF-A, a major inducer of angiogenesis[14].

A common driver of NSCLC disease is activating kinase domain mutations in EGFR which occurs in 10-15% of Caucasian patients and 35% of Asian patients[15], KRAS which occurs in 40% of Caucasian patients and 10% of Asian patients[16], or ALK which occurs in 7-10% of all NSCLC patients[17]. These mutations cause the cell to become dependent on the mutated signaling pathway and renders the tumor exquisitely sensitive to inhibition of their respective mutated pathways, a phenomenon known as oncogene addiction. In oncogene addiction, pro-apoptotic signaling generally increases as a response to increased pro-survival signaling by the mutated oncogenic driver. The use of targeted inhibitors results in the removal of oncogenic driver signaling leading to cell death through up-regulated pro-apoptotic signaling. This phenomenon is known as oncogenic shock[18]. Activating EGFR mutations commonly occur within exons 18-21, which code for a portion of the kinase domain. Around 90% of EGFR exon 18-21 mutations consist of exon 19 deletions or exon 21 point mutations resulting in a constitutively active receptor[19]. The activating mutations commonly seen in EGFR are commonly localized to the p-loop, a set of residues which contributes to holding the receptor in the inactive state. In the wild-type receptor, the p-loop interacts with a c-helix regulatory domain to hold the

receptor in the inactive state. Point mutations such as the common L858R or G719S substitutions occur within this p-loop and disrupt interactions with the regulatory c-helix. This causes the receptor to adopt a conformation similar to the activated wild-type receptor. The increased sensitivity of EGFR with activating mutations such as L858R to EGFR TKIs has been attributed to increased van der Waals interactions between the drug and an aspartic acid residue in position 855. In the wild-type receptor, this residue is pointed away from the ATP binding cleft but in the context of a p-loop point mutation such as L858R, changes in receptor conformation result in ASP855 being rotated toward the ATP binding cleft resulting in stronger binding between the receptor and drug[20, 21]. In the more common case of EGFR exon 19 deletions (44% of all EGFR activating mutations)[22], residues 746-750 are absent. These residues localize to the regulatory c-helix domain. The deletion of these residues disrupts the interaction between the c-helix and p-loop leading to constitutive EGFR activity by forcing the receptor to adopt a conformation similar to the activated wild-type receptor. Like exon 21 point mutations, this type of mutation results in an increased affinity for EGFR TKIs and reduced affinity for ATP[23].

The first drugs to target this pathway were the receptor TKIs gefitinib and erlotinib[16]. These drugs are reversible ATP competitive inhibitors and NSCLC cells harboring EGFR kinase domain mutations are exquisitely sensitive to the drugs due to their oncogene addiction[15]. Furthermore, adverse side effects from the usage of EGFR TKIs has been shown to be minimal. In 2004, an evaluation of safety and efficacy of the EGFR TKI gefitinib was conducted among 31 Chinese advanced NSCLC patients which had progressed following systemic chemotherapy. It was found that gefitinib was well tolerated as

administered by a daily oral tablet (250mg) and adverse events were generally mild (grade 1 or 2) and reversible. The most frequent adverse effects in this study were diarrhea and acne form rash. The tumor response rate in this study was 35.5% and the median overall survival was 11.5 months[24]. Due to these results and other agreeing studies, gefitinib has been approved as a safe and effective treatment for advanced stage NSCLC with positive EGFR activating mutations.

Unfortunately, response to EGFR TKI is not universal. Primary resistance occurs through several avenues and acquired resistance can emerge due to secondary mutation (T790M) in EGFR[25], the up-regulation of the RTK MET[26], the transformation of NSCLC cells into a SCLC phenotype or through EMT[27].

### **Resistance to EGFR TKI Treatment**

Primary resistance to EGFR TKI treatment is commonly defined as tumor insensitivity during first-line administration of EGFR TKIs. Although the mechanisms behind EGFR TKI primary resistance are not well understood, mutations have been identified which lower the binding affinity of EGFR toward TKI molecules. The most frequent mutations which result in primary resistance are those represented by an exon 20 insertion. These mutations exist as roughly 1-10% of all EGFR mutations and represent mutations within the N-terminus of EGFR (M766 to C775) and most commonly, mutations concentrate within the C-helix (A767 to C775) region. This region is important for the manipulation of ATP by the kinase domain of EGFR into the correct orientation for catalysis.

Another important mutation implicated in primary EGFR TKI resistance is represented by the variant III in-frame deletion of exon 2-7 which code for the extracellular domain of

the receptor. Interestingly, this mutation prevents EGFR from binding to its ligands such as EGF. Although currently debated, it is thought that this mutation results in structural changes in EGFR which affect the conformation of the ATP-binding pocket, preventing EGFR TKI drug binding. This mutation is present in 5% of SCC and has been shown to affect TKI resistance *in vitro*[28].

Primary resistance may not only occur due to mutations in EGFR but also due to genetic alterations within EGFR down-stream signaling members. Treatment by EGFR TKIs results in the induction of the apoptosis signaling cascade leading to the death of the cell[29]. An important pro- apoptotic protein is the Bcl-2 family member, BIM. BIM functions by inhibiting anti-apoptotic Bcl-2 family proteins at the mitochondria or by activating the pro-apoptotic protein BAX[30]. Patients with BIM deletion mutations or low levels of BIM mRNA have been associated with a poor response to EGFR TKI treatment[31].

### **Acquired Resistance**

Treatment with EGFR TKIs generally elicits a strong response among NSCLC patients harboring EGFR activating mutations but drug resistance typically develops within 6-18 months of treatment[32]. This acquired resistance to EGFR TKIs greatly reduces patient progression-free survival in advanced stage NSCLC[33]. It is important to study the underlying genetic and expression level changes which occur during the acquisition of resistance in order to design treatments which can treat patients with acquired EGFR TKI resistance.

The most common route to acquired resistance is through the T790M mutation in exon 20 of EGFR. This mutation represents approximately 50% of all acquired resistance

cases[25]. This mutation occurs within the ATP-binding pocket of EGFR and results in an increased affinity for ATP and a decreased affinity for first-generation EGFR TKIs[25]. In 2005, a family with a germ line T790M mutation was shown to have a predisposition to lung cancer suggesting a possible link between the T790M mutation and tumor growth advantage in the absence of selection by EGFR TKI treatment[34]. This predisposition is most likely explained by the increased affinity of EGFR harboring T790M for ATP resulting in increased EGFR signaling. While the T790M mutation results in decreased affinity for first-generation EGFR TKIs such as gefitinib or erlotinib, patients harboring this mutation remain sensitive to next-generation irreversible EGFR inhibitors such as afatinib or dacomitinib[35]. Clinical trials have been performed with these drugs and adverse effects were generally limited to diarrhea and skin rash. While the development of these drugs were designed specifically for patients harboring the T790M mutation, the response to these drugs in phase II clinical trials was modest compared to first-generation EGFR TKIs[36]. Therefore, it has become clear that further research will be required to overcome acquired resistance due to the T790M mutation.

The transmembrane receptor tyrosine kinase MET has also been implicated in acquired resistance to EGFR TKI treatment. MET is a single-pass transmembrane tyrosine kinase receptor which is important in normal functions such as embryonic development and wound healing. The only known ligands for this receptor are HGF and its splice variants[37]. Abnormal MET amplification has been shown to correlate with a poor prognosis in several cancer types including lung, breast, kidney, liver and brain[38]. MET activation by HGF leads to phosphorylation of the tyrosine residues T1234, and T1235. These phosphorylated residues interact with several signal transduction proteins ultimately

feeding into the MAPK, PI3K and STAT signaling pathways leading to increased cell growth and survival. In NSCLC, MET amplification has been implicated in approximately 20% of EGFR TKI resistance cases[39] and therefore represents a major pathway of acquired resistance to EGFR TKI therapy. Because of this, several clinical trials have been performed with dual EGFR/MET inhibitors as a primary treatment of advanced stage NSCLC. In 2010, a phase II clinical trial exploring dual MET/EGFR inhibition using the MET inhibitor, ARQ197 and the EGFR TKI erlotinib was performed. PFS was seen to be enhanced within patients receiving dual inhibitor treatment and was particularly effective in patients with non-squamous histology, K-RAS mutation, and EGFR wild-type status. Adverse side effects were not seen to be significantly increased among patients receiving dual inhibitor treatment compared to single arm treatment and were limited to rash, fatigue, diarrhea and nausea[40]. Although an improvement in patient outcome was seen among those receiving dual MET/EGFR inhibitor therapy, escape from drug sensitivity was seen among a sub-population of patients implicating other resistance mechanisms as important in EGFR TKI insensitivity[40].

The ErbB family member HER2 has also been implicated in acquired resistance to EGFR TKI treatment. In 2012, Takezawa et al. reported HER2 amplification in 12% of tumors with acquired resistance to EGFR TKIs compared to only 1% of untreated lung adenocarcinomas[41]. Similar to MET amplification, HER2 amplification has been seen to activate the same down-stream signaling cascade as EGFR signaling involving the MAPK, PI3K and STAT pathways[42]. With this information, a clinical trial was reported by Janjigian et al in 2014 assessing dual therapy using the anti-EGFR antibody Cetuximab and the second generation EGFR TKI afatinib[43]. Afatinib has been shown to effectively inhibit

EGFR receptors harboring the T790M mutation as well as the HER2 receptor[44]. The study showed a similar response rate in patients harboring the T790M mutation compared to T790M negative tumors. The authors attributed the similar response rates between these two cohorts to HER2 amplification in T790M-negative responding patients and identify HER2 as an important target in Afatinib therapy[43]. Therefore, HER2 amplification has been identified as an important mechanism of acquired resistance in EGFR activating mutation positive NSCLC tumors[45].

As well as the previously discussed mechanisms, IGF-1R expression has also been shown to be associated with a poor prognosis in NSCLC patients treated with EGFR TKIs. Additionally, the expression of IGF-1R has been shown as a negative prognosis biomarker in NSCLC patients[46]. Through over-expression and knock out models, it has been shown that IGF-1R does not exhibit its prognostic effects through proliferative or survival signaling pathways such as the MAPK and AKT pathways respectively[47]. In light of this result, alternate pathways must be explored. Recently, Varkaris et al. showed a ligand-independent activation of the MET receptor through IGF-1R activation[48]. At this point in time, the most supported mechanism of EGFR TKI resistance mediated through IGF-1R amplification has been through trans-activation of other relevant receptors[49] and may explain why a direct link between IGF-1R expression and EGFR TKI resistance has not been shown.

Aside from genetic mutation, phenotypic-mediated acquired resistance has been shown in tumors which have developed acquired resistance to EGFR TKIs. One important mechanism has been identified as the histological conversion of NSCLC to SCLC. This conversion was first seen in 2006 in which an EGFR mutant positive adenocarcinoma

patient showed tumor response to EGFR TKI therapy for 18 months but following disease progression, a second biopsy showed a SCLC histology harboring the original EGFR activating mutation[50]. Following this observation, several other cases of NSCLC to SCLC transformation have been identified[51, 52]. It has long been understood that p53/RB1 loss has an important role in the tumorigenesis of SCLC and one study showed that all SCLC tumors tested showed either a mutation or loss of RB1 expression[53]. Furthermore, an analysis of repeat biopsy samples acquired from EGFR TKI treated NSCLC patients harboring a SCLC conversion showed a 100% rate of RB1[50] loss further implicating RB1 loss as an important event in SCLC conversion. Taken together, the conversion from a NSCLC histology to a SCLC histology has been supported as an important mechanism to acquired resistance to EGFR TKI treatment in a subset of NSCLC patients.

An additional important phenotype-mediated acquired resistance mechanism to EGFR TKIs has been shown in tumors harboring a sub-population of cancer cells expressing mesenchymal marker proteins such as CD44, N-Cadherin, and Vimentin[27, 54]. These marker proteins are well known to be up-regulated during EMT and have been associated with poor response to EGFR TKI therapy. The EMT process also commonly results in cancer cells with increased capabilities for invasion and metastasis as well as stem-like properties. It has been shown that the EMT process can be induced in NSCLC cell lines by chronic exposure to EGFR TKIs[55]. This process will occur *in vitro* over an approximately 6-month period[55]. This is also the time frame in which acquired EGFR TKI resistance occurs in NSCLC patients undergoing EGFR TKI treatment, supporting the view that EMT contributes to EGFR TKI acquired insensitivity[56]. In support of this



view, Cao et al. performed a statistical analysis in the CICAMS and TCGA dataset correlating EMT signature genes with a significantly worse overall survival[23]. Moreover, Uramoto et al. showed that nearly half (44%) of analyzed human EGFR TKI resistant NSCLC tumors show a down-regulation of epithelial markers coupled with the up-regulation of mesenchymal markers[57]. The localization of mesenchymal cells within the tumor has been shown to be concentrated within the invasive front of the tumor while cells which follow behind typically show epithelial traits and maintain extensive cell-cell adhesion properties[58, 59]. Within the tumor mass, it has been proposed that cells which maintain an epithelial phenotype secrete EMT-inducing factors to surrounding cells. These epithelial cells maintain a sub-population of mesenchymal cells spread heterogeneously throughout the tumor[60]. Taken together, these data suggest a link between a mesenchymal sub-population and EGFR TKI resistance in NSCLC.

### **EMT Overview**

Epithelial cells cover the body surface and form the lining of body cavities such as the digestive tract and lung alveoli. These surfaces typically contain minimal amounts of extracellular matrix and exhibit an apical to basal polarity. Conversely, mesenchymal cells make up several different cell types such as osteoblasts, adipocytes and fibroblasts. These cells are involved in producing the non-cellular stroma which gives support to other cell types. EMT is a process in which an epithelial cell loses its adherens junctions, polarity and reorganizes its cytoskeleton[56]. Several transcription factors have been identified as key players in this transition including SNAIL, ZEB1 and ZEB2 and bHLH factors[56]. Changes in the cytoskeletal complex proteins typically involves the repression of cytokeratin and the up-regulation of vimentin expression. These changes in protein

expression have been shown to be initiated by a combination of various pathways which respond to extracellular cues including TGF- $\beta$ [61]. Furthermore, expression of TGF- $\beta$  has been shown to be increased upon EGFR TKI treatment[55] providing a strong correlation between the induction of EMT and EGFR TKI treatment. When EMT occurs the cell becomes more stem-like and frequently demonstrates drug resistance, increased metastasis and invasiveness[62]. Cells which have undergone EMT typically show reduced expression of EGFR as well as its ligands and typically express other RTKs such as AXL[27]. Because of these changes in expression lead to EGFR TKI resistance, EMT has been identified as an important process in the development of drug resistance and the associated up-regulated receptors have been identified as targets in alternative therapies.

### **Endothelin-1 Overview**

Endothelial cells form a single-celled lining of the inner wall of the blood vessel. It was originally believed that these cells simply form a barrier separating blood from vascular smooth muscle cells. With the discovery of EDRF, a new avenue of vascular research was opened focusing on the signaling capability of the endothelium. Years later, a potent vasoconstriction-inducing peptide was isolated from bovine endothelial cell culture supernatant and was termed EDN1. Soon after this discovery, two other isoforms of endothelin were discovered and termed EDN2 and EDN3. The endothelins were originally thought to work systemically to affect blood pressure although it was later found that circulating endothelin levels are quite low and the peptide acts primarily as a local hormone. Beyond its effect on vasoconstriction it was found that endothelin can also act as a mitogen for endothelial cells and vascular smooth muscle cells[63]. Because of this result, endothelin has been explored as not only a vasoconstriction-inducing factor but also

as a factor which can induce the proliferation of endothelial and smooth muscle cells.

The endothelin signaling axis has been implicated not only in NSCLC[64] but in other cancers such as colorectal and kidney cancer and the expression of the ligand EDN1 and the EDNRA expression has been linked to poor survival outcomes and increased disease progression in these cancers[65, 66]. The endothelin signaling system consists of three different peptides, EDN1, EDN2, and EDN3 and their two receptors EDNRA and EDNRB which belong to a family of GPCRs. EDNRA shows similar affinities for EDN1 and ET-2 but a 100-fold reduction in affinity for ET-3. Conversely, EDNRB shows a similar affinity for EDN1, EDN2 and EDN3[67]. EDNRA, EDNRB and EDN1 have been shown to be commonly up-regulated in multiple cancer types[68, 69] and therefore I hypothesize that EDN1 is exerting an effect on NSCLC cells and endothelial cells through EDNRA or EDNRB. The activation of EDNRA has been shown to result in the activation of several pathways including the mitogen activated protein kinase (MAPK), the PI3K, and PKB pathways[70]. The activation of these pathways is known to increase the proliferation, cell growth, and survival[71]. The activation of the EDNRA receptor has also been linked to the activation of the non-receptor tyrosine kinase, SRC[72]. SRC has many targets within the cell and the activation of SRC can result in the activation of RTKs such as the VEGFR1[73], and EGFR[74]. These receptors canonically stimulate the MAPK, PI3K and PKB pathways increasing cell proliferation, growth and survival[75, 76]. Furthermore, the inhibition of SRC has been linked to increased E-cadherin expression and the inhibition of EMT[126]. Because of these previous observations, I identified the endothelin signaling axis as a worthwhile avenue to explore the pro-tumorigenic effect of the EMT phenotype.

### **EDN1 and Vasoconstriction**

Of the discovered endothelins, the effects of EDN1 have been most thoroughly characterized and seen to be the most active. The role of EDN1 in normal pulmonary function is to maintain basal vascular tone. In general, it is understood that the activation of the  $K_{ATP}$  channel inhibits pulmonary vasoconstriction. Through the EDNRA receptor on smooth muscle cells, EDN1 has been shown to inhibit the activation of the  $K_{ATP}$  channel leading to pulmonary vasoconstriction. Additionally, EDN1 has been shown to be up-regulated during hypoxic pulmonary vasoconstriction and causes a vasoconstrictive effect both *in vitro* and *in vivo*[77]. Following these observations, EDNRA blockade has been explored for controlling vasoconstriction in humans[78].

The progression of human pulmonary arterial hypertension is known to result from the occlusion or vasoconstriction of pulmonary vessels leading to progressive right ventricular failure[79]. Several clinical trials have been conducted examining the effect of EDNRA antagonists in a pulmonary arterial hypertension model. Recently, Galie et al. showed that the addition of the EDNRA antagonist Ambrisentan to standard tadalafil-monotherapy resulted in a significantly lower risk of clinical-failure events (50%) compared to tadalafil or Ambrisentan monotherapy[80]. Tadalafil functions by inducing nitric-oxide release in endothelial cells through PDE5 inhibition leading to vasodilation[81]. The increased efficacy seen in the Galie trial was attributed to the additive effect of inducing vasodilation with tadalafil and inhibiting vasodilation with Ambrisentan[80].

While EDN1 signaling has been thoroughly explored in cardiovascular disease[80] and various cancer types[69, 84, 86], evidence for its role in NSCLC remains limited.

Boldrini et al. showed that expression of EDN1 was related to a poor prognosis in NSCLC patients[64] although the mechanism behind this remains unexplored. EDN1 signaling has previously been shown to have a pro-angiogenic effect on cultured HUVEC cells and has been shown to enhance the pro-angiogenic effect of VEGF *in vitro*[82, 83]. It would therefore be expected that EDN1 expression *in vivo* would correlate with greater angiogenesis and therefore tumor growth. This has proven to be the case in several tumor types including ovarian carcinoma[69] and chondrosarcoma[84]. Surprisingly, anti-neovascularization exerted by EDN1 has also been reported in other cancer types such as castration-resistant prostate cancer[85] and some melanomas[86]. The decreased tumor growth in these cancers were attributed to the vasoconstrictive properties of EDN1 preventing sufficient blood flow to the tumor. Furthermore, it has been shown that retarded tumor growth in castration-resistant prostate cancer over-expressing EDN1 can be abrogated by treatment with vasodilators further implicating EDN1-mediated vasoconstriction in obstructing tumor growth[85]. It is therefore an aim of this study to explore whether EDN1 shows a pro-angiogenic or anti-angiogenic effect on tumor growth in NSCLC. Commonly, tumor neo-angiogenesis is evaluated by calculation of MVD within the tumor. I will utilize this technique to evaluate tumor neo-angiogenesis in a NSCLC model.

### **VEGF Signaling Overview**

The VEGFs are the principal regulators of blood vessel growth and function in adulthood. These signaling peptides consist of 5 members: VEGF-A, VEGF-B, VEGF-C, VEGF-D, and PlGF. These members exist primarily as homodimers although a heterodimer between VEGF-A and PlGF has been reported[87]. VEGF-A was originally described by Senger et al. in 1983 and was originally designated as VPF[88]. The function of VEGF

family proteins is further expanded through alternative splicing. For example, VEGF-A is naturally found in 4 isoforms, VEGF<sup>121</sup>, VEGF<sup>145</sup>, VEGF<sup>165</sup>, and VEGF<sup>189</sup>. These isoforms show differential ability to bind ECM components such as heparin sulfate and determine the level of VEGF-A retention at the cell surface or ECM[89]. The expression of VEGF-A is regulated by HIF-1 $\alpha$ , leading to increased expression in hypoxic environments[90].

VEGF-A primarily interacts with the receptor VEGFR2. VEGFR2 is a RTK family protein with an extracellular ligand binding domain and an intracellular tyrosine kinase domain connected by a single transmembrane domain. Like other RTKs, VEGF-A binding to VEGFR2 induces homo- or hetero-dimerization leading to auto-phosphorylation of the intracellular domain, allowing the phosphorylated protein complex to act as a scaffold for the binding of down-stream signaling members[91]. VEGFR2 plays an essential role in angiogenesis in both normal development and tumorigenesis. Shalaby et al. showed that VEGFR2<sup>-/-</sup> mice die at E8.5 due to impaired hematopoietic and endothelial cell development[92]. Several inhibitors of VEGFR2 have been tested in clinical trials with the aim of inhibiting blood vessel development in the context of cancer-related disease. A phase II clinical trial was conducted with the VEGFR2 inhibitor, ramucirumab. 140 patients with recurrent or advanced stage NSCLC were given ramucirumab as an adjuvant treatment with traditional chemotherapy. Hypertension was reported as the primary adverse effect. The median progression free survival was recorded as 6.5 months in patients receiving adjuvant ramucirumab compared to 4.3 months in patients receiving chemotherapy alone[93]. While modest improvements in patient prognosis was common across these clinical trials, the promise of VEGFR inhibitor therapy has largely failed to produce significant improvements in NSCLC patients.

Given that angiogenesis is a hallmark of several types of progressive tumors, VEGF signaling has been implicated as a potential therapeutic target. Overexpression of the VEGFs has been found in most human cancers including NSCLC. The expression of VEGFs in NSCLC has been linked to increased tumor recurrence, metastasis and death. The angiogenic phenotype associated with VEGF expression is considered a hallmark of malignancy in which increased tumor neo-angiogenesis provides a pathway to metastasis and increased tumor growth rate[94]. Because of this, the VEGF signaling pathway has been examined in NSCLC disease progression. To date, two antiangiogenic agents, bevacizumab and ramucirumab have been approved for the treatment of advanced or metastatic NSCLC as adjuvant therapy to standard first-line chemotherapy[95]. These monoclonal antibodies target VEGF or its receptor VEGFR2 respectively. Small molecule inhibitors of VEGFR2 have also been explored in targeting angiogenesis in NSCLC although these drugs to date have largely failed to improve patient outcome compared to first-line chemotherapy. The multi-target inhibitor, nintedanib, in combination with the chemotherapy agent docetaxel, is the exception to this rule. Nintedanib targets not only VEGF, but also PDGF and FGF signaling pathways and effectively reduces tumor neo-angiogenesis and improves overall survival in patients with advanced or metastatic NSCLC[96]. This result has generated interest in targeting VEGF signaling with other targeted therapy such as EGFR TKIs[97].

### **EGFR TKI Plus VEGFR2 Inhibition in the Clinic**

Because tumor neo-angiogenesis is strongly mediated by VEGF-A/VEGFR2 and EGFR signaling strongly mediates tumorigenesis and disease progression[98-101], several clinical trials have been performed exploring the benefit of dual EGFR/VEGFR2 inhibition

in advanced stage NSCLC patients. The benefit of this treatment was seen to vary between studies. A phase II clinical trial was performed with the dual EGFR/VEGFR2 inhibitor vandetanib[102]. The aim of the study was to examine if dual EGFR/VEGFR2 inhibition could increase the rate of pleurodesis in advanced stage NSCLC patients. The production of pleural effusion has been identified as a marker of advanced stage NSCLC and a common treatment is the insertion of a pleural catheter for the draining of the pleural cavity. VEGF has also been implicated as an important signaling molecule in the production of pleural effusion. Because of this, VEGF signaling inhibition was examined as a potential way to target pleural effusion production. While the administered daily oral dose of 300mg vandetanib was well tolerated among patients, the treatment did not significantly decrease the time to pleurodesis[103].

A phase II clinical trial was reported in NSCLC patients which have progressed after responding to treatment with either gefitinib or erlotinib using the dual EGFR/VEGFR2 inhibitor, XL647. Patients received a daily oral dose of 300mg XL647 throughout the course of the study. A 3% response rate was seen in this study with only one patient in the trial showing a significant response to the treatment. Patients with a T790M mutation showed a significantly worse progression-free survival rate and the one patient which showed a response lacked a T790M mutation. The responding patient eventually progressed after 8 months of XL647 treatment. Since the 3% response rate did not meet the pre-specified threshold for recommended further study, XL647 was deemed unfit for patients which have progressed following gefitinib or erlotinib treatment[104].

Another phase II clinical trial was reported comparing the response to the EGFR TKI erlotinib given with placebo or with the VEGFR2 inhibitor sunitinib in advanced stage



NSCLC patients. Patients admitted into the study were those that had progressed after receiving platinum-based chemotherapy. Patients received either 37.5 mg/day sunitinib plus 150mg/day erlotinib or placebo plus erlotinib. In the 132 randomly assigned patients, the median PFS was 2.8 months in patients receiving the combination therapy compared to 2.0 months in those receiving erlotinib plus placebo and the overall survival was 8.2 months compared to 7.6 months. The combination treatment was generally well-tolerated although common adverse events such as diarrhea, rash and fatigue was seen at a greater frequency among patients receiving the combination treatment. The study concluded that the combination sunitinib/erlotinib therapy did not significantly increase the PFS compared to erlotinib alone[105].

To date, no clinical trials have been conducted examining the benefit of VEGFR2/EDNRA dual inhibition therapy. It is therefore important to explore how the VEGF and EDN1 signaling pathways interact during NSCLC disease progression and drug treatment.

## CHAPTER TWO

### MATERIALS AND METHODS

#### **Cell Lines and Cell Culture**

HCC4006 cells were obtained from ATCC.org (ATCC CRL-2871). HCC4006 harbors a mutation (L747 - E749 deletion, A750P) in the EGFR tyrosine kinase domain which prevents the regulation of EGFR activation. The cell line was established from a 50+ year old Caucasian male with an adenocarcinoma through the collection of pleural effusion. Cells show a population doubling time of 41 hours cultured in RPMI-1640 medium (ATCC 30-2001) supplemented with 10% FBS.

HCC4006 Ge-R cells with a mesenchymal phenotype were produced from epithelial HCC4006 cells by former members of the Shimamura lab by exposing HCC4006 cell to increasing concentrations of the EGFR TKI gefitinib over a 6 month period to a final concentration of 10 $\mu$ mol/L resulting in a polyclonal EGFR TKI resistant cell line. EGFR TKI resistance was confirmed by measuring cell viability after allowing cells to grow in gefitinib-free media for 7 days followed by gefitinib treatment. Cells were then cultured without drug and resistance to gefitinib was measured periodically[55]. Cells presented a mesenchymal phenotype as shown by Western blot of common mesenchymal markers[56].

HCC827 cells were obtained from ATCC.org (ATCC CRL-2868). HCC827 possesses a mutation (E746 – A750 deletion) in the EGFR tyrosine kinase domain which

prevents the regulation of EGFR activation. The cell line was isolated from the lung of a 39 year old caucasian female with an adenocarcinoma. Cells show a population doubling time of 28 hours cultured in RPMI-1640 medium (ATCC 30-2001) supplemented with 5% FBS.

ER23 cells were produced in a similar manner as HCC4006 Ge-R cells by previous members of the Shimamura lab. HCC827 cells were exposed to increasing concentrations of the EGFR TKI erlotinib up to a final concentration of 10 $\mu$ mol/L. Clones were isolated and were able to proliferate normally in the presence of 10 $\mu$ mol/L erlotinib. EGFR TKI resistance was confirmed by measuring cell viability after allowing cells to grow in erlotinib-free media for 7 days followed by erlotinib treatment. Cells were then cultured without drug and resistance to erlotinib was measured periodically[55]. Cells presented a mesenchymal phenotype as shown by Western blot of common mesenchymal markers[56].

The 293LTV cell line was established from primary embryonic human kidney and transformed with human adenovirus type 5 DNA. The genes encoded by the E1 region of the adenovirus construct are expressed in these cells and allow for high protein production. This cell line also expresses the SV40 large T antigen and Neomycin resistance genes allowing for stable high-volume production of lentiviral particles[106]. 293LTV cells were routinely cultured in 10% FBS DMEM supplemented with 1000 $\mu$ g/mL ABAM and 1000 $\mu$ g/mL G418.

HUVEC were obtained from Lonza (Lonza Group, CC-2935). HUVEC cells are primary cells derived from a single donor from the resected endothelium of umbilical cord veins. HUVEC cells were expanded in EGM media (Lonza Group, CC-3024, CC-3124) and stored in liquid nitrogen. Cells were passaged by aspirating growth media and

rinsing cells with Lonza HEPES buffered saline solution (Lonza Group, CC-5022). Trypsin/EDTA (Lonza Group, CC-5012) was introduced to the culture flask and allowed to sit at 37°C for 3-5min. After cells have detached, trypsin was neutralized with Trypsin Neutralizing Solution (TNS, Lonza Group, CC-5002). Multiple frozen aliquots of early passage (passage  $\leq 2$ ) HUVEC cells were prepared following trypsinization by freezing in 80% EGM media, 10% DMSO, and 10% FBS and stored in liquid nitrogen.

### **Luminex Multiplex Assay**

The Luminex human angiogenesis/growth factor magnetic bead panel 1 kit (Millipore Sigma, HAGP1MAG-12K) was used to perform immunoassay analysis on conditioned media prepared as previously described. In a 96-well plate, wells are rinsed with assay buffer and 25 $\mu$ L of standards or conditioned media was added to each well along with 25 $\mu$ L of assay buffer. 25 $\mu$ L of mixed beads were added to each well and allowed to incubate at 2-8°C overnight (16-20 hours) with agitation on a plate shaker. With the plate on a magnetic base (Millipore Sigma, #40-285), well contents are removed by decanting followed by 3 cycles of washing using 200 $\mu$ L of wash buffer in each well. 25 $\mu$ L of detection antibodies were then added to each well and incubated with agitation for 1 hour at room temperature. 25 $\mu$ L streptavidin-phycoerythrin was then added to each well and allowed to bind for 30 minutes at room temperature. Well contents were then washed 3 times as previously described and 100 $\mu$ L sheath fluid was added to each well. The plate was then analyzed on the Luminex FM3D running xPONENT® for FlexMAP™ 3D version 4.0.846.0 SP1. Statistical significance was calculated using a one way ANOVA test with a *post hoc* Student's t-test. A heatmap was produced from the resulting data using the Morpheus web-based tool from Broad Institute. Results were log<sub>2</sub> transformed and

differences in expression were displayed for each analyte independently.

### **Cell Counting**

All cell counting was performed using the Countess automated cell counter (Thermo Fisher Scientific, 10227). Detached cells were mixed with trypan blue at a 1:1 ratio and 10 $\mu$ L was pipetted to a Countess cell counting chamber slide (Thermo Fisher Scientific, C10228). Live cell count was used for seeding calculations.

### **Lentiviral Production and Transduction**

293LTV cells were thawed from liquid nitrogen storage and seeded onto a Nunc T-75 flask (Cat # 156499) in DMEM containing 10% FBS, 1000 $\mu$ g/mL G418, and 1000 $\mu$ g/mL ABAM. 48 hours prior to transfection, media was changed to antibiotic-free DMEM containing 10% FBS. On the day of transfection, the following reagents were combined in a sterile microtube: 4 $\mu$ g pLKO plasmid (target or control), 4 $\mu$ g  $\Delta$ R8.2 plasmid, 0.5 $\mu$ g VSV-G plasmid. Final volume was brought to 176 $\mu$ L with Opti-MEM and 24 $\mu$ L TransIT-LT1 was added and gently pipetted to mix bringing the final volume to 200 $\mu$ L. Mixture was incubated at room temperature for 20-30 minutes. 293LTV cells were trypsinized and  $1 \times 10^6$  cells were seeded onto 60mm Corning BioCoat Collagen coated plates. The mixture from the previous step was added drop-wise onto 293LTV cells and gently rocked to mix. Plates were allowed to incubate at 37° C overnight. Media was replaced with 3mL 10% FBS RPMI containing 0.58% BSA (20g/100mL +Ca<sup>2+</sup>/+Mg<sup>2+</sup> PBS) and plates were allowed to incubate at 37° C for 72 hours. Cell culture supernatant was collected and plates were flash frozen with LN<sub>2</sub>, allowed to thaw and cell debris and any remaining viral particles were added to the collected supernatant. Supernatant was centrifuged at 400xg for 3 minutes to remove cell debris. Supernatant was passed through a

0.45 $\mu$ M pore SFCA membrane (Nalgene, 723-2545). Viral supernatant was stored at 4° C and used for transduction within a week of the production. 24 hours prior to transduction, target cells were seeded at 8 $\times$ 10<sup>5</sup> cells/plate in a 60mm plate to achieve 70-80% confluency at the time of transduction including an extra plate for mock transduction. Virus containing supernatant was mixed at a 1:1 ratio with appropriate target cell culture media and target cell media was replaced with this mixture. Polybrene (Santa Cruz Biotechnology, SC-134220) was added directly to the plate at a final concentration of 5 $\mu$ g/mL for HCC4006 cells and HCC4006 derived cells or 10 $\mu$ g/mL for HCC827 cells and HCC827 derived cells. Media was replaced with the target cell media/virus containing supernatant every 24 hours until 3 rounds of transduction was achieved. Following transduction, virus containing media was removed and plates were washed twice with +Ca/+Mg DPBS and plates were incubated at 37° C for 24 hours in proper culture media. After 24 hours, media was changed with proper cell culture media and proper selection agent concentration was increased until cells which underwent mock transduction died. The selection agent used for HCC827 EDN1 over-expression models was blasticidin and the concentration was increased to a final concentration of 5 $\mu$ g/mL. The selection agent used for HCC4006 Ge-R shEDN1 knockdown model was puromycin increased to a final concentration of 5 $\mu$ g/mL. Transduction was considered complete when all mock transduction cells died and final selection agent concentration was achieved.

### shRNA Sequences Used

Target	RNAi consortium number	sequence	Remarks
EDN1	TRCN0000003847	5' – GCAGTTAGTGAGAGGAAGAAA – 3'	
Non-Target	N/A	5' – GCGCGATAGCGCTAATAATTT – 3'	Sigma SHC-002

**Table 1: List of shRNA sequences used in study.** shRNA knockdown and viral transduction and infection were performed as previously reported[55].

### Conditioned Media Preparation

HCC4006, Ge-R, HCC827, and ER23 cells were seeded onto 6-well plates at  $3 \times 10^5$  total cells/well as a pure culture or admix. 24H after seeding, media was replaced with 1.5ml of the proper culturing media based on cell type. Cells were allowed to grow at 37° C for 48 hours. Conditioned media was collected after 48h and centrifuged at 400g for 10 minutes to remove cellular debris. Cell culture supernatant was collected and flash frozen in liquid nitrogen and stored in liquid nitrogen until assayed. Cells were lysed using 1x Cell Lysis Buffer (Cell Signaling Technology, 9803S). Cell lysates were analyzed for total protein concentration by BCA (Thermo Fisher Scientific, 23225) and calculated values were used to normalize measured cell culture supernatant target protein concentrations.

### *In vitro* Angiogenesis

An *in vitro* tube formation assay was performed according to manufacturer's recommendations. Briefly, ibidi  $\mu$ -slide angiogenesis plate (ibidi, 81501) was coated with 10  $\mu$ L of reduced growth factor Matrigel (Corning, 356231) and allowed to solidify for 30 minutes at 37°C with 5% CO<sub>2</sub>. During this time, HUVEC cells were harvested. Cells were

counted and 50  $\mu\text{L}$  of cell suspension containing 7500 cells was added to each well containing Matrigel matrix. For conditioned media assays, HUVEC cells were suspended in the respective conditioned media such that 50  $\mu\text{L}$  of suspension contained 7500 cells and added to each well containing Matrigel matrix. The slides were then incubated at 37°C with 5%  $\text{CO}_2$  for 8 hours. Following incubation, Calcein AM (Thermo Fisher Scientific, C1430) was added directly to each well to a final concentration of 1 $\mu\text{M}$ . Slide was allowed to incubate at 37°C with 5%  $\text{CO}_2$  for 10 minutes. Tube formation was captured by taking fluorescent images with an Evos FL Cell Imaging System (Thermo Fisher Scientific, AMF4300) with the GFP channel. Negative controls for all tube formation were performed in EBM (Lonza Group, CC-3121) which contains proper salt and pH levels for endothelial cells but lacks any pro-angiogenic growth factors. Positive controls in all tube formation assays were performed in complete EGM (Lonza Group, CC-3024) which contains the pro-angiogenic growth factors hEGF, VEGF-A, R3-IGF-1, hFGF- $\beta$ , Heparin, and FBS at manufacturer recommended concentrations.

### **Image Analysis**

Tube formation images were analyzed using the ImageJ Angiogenesis Analyzer plugin provided as free software from the Gilles Carpentier Research Group[107]. The parameters measured include total tubule length, mesh area and number of nodes.

### **Western Blot Analysis**

Protein concentrations were determined by the Pierce BCA Protein Analysis Kit (Thermo Fisher Scientific, 23225). Non-specific binding was blocked with 5% nonfat milk and incubated with primary antibodies proteins of interest, E-Cadherin (Cell Signaling Technology, 3195), N-Cadherin (Cell Signaling Technology, 13116), CD44 (Cell Signaling



Technology, 3578), actin (Cell Signaling Technology, 8457) and EDNRA (Novus, NB600-836). The membranes were then washed in PBS plus 0.1% Tween-20 and incubated with HRP-conjugated goat anti-rabbit antibody (Cell Signaling Technology, 7074S). The membrane was then developed with ECL reagent (Pierce, 32106) and exposed on CL-Xposure film (Thermo Scientific, 34089).

### **Murine Xenograft**

All animal studies were done in accordance with IACUC guidelines under the IACUC application “Testing Therapeutic Compounds in NSCLC” (LU # 207437). Approximately  $5 \times 10^6$  total cells were injected sub-cutaneously into both right and left flanks of mice. The mice were treated (oral gavage) with gefitinib (50mg/kg) daily. Tumor dimensions were measured via external caliper measurement thrice weekly and tumor volume was calculated ( $TV = (\text{width})^2 \times \text{length} / 2$ ).

### **IHC Sample Preparation**

Murine xenograft tumors were flash frozen in OCT compound (Tissue-Tek, 4583) and stored at  $-80^\circ\text{C}$  until sectioning. Sections were prepared using a Cryostar NX50 OP cryostat (MICROM International GmbH) to prepare sections of  $5\mu\text{M}$  thickness. Sections were mounted on Superfrost™ Plus Gold slides (Thermo Fisher Scientific, FT4981GLPLUS). Slides were returned to  $-80^\circ\text{C}$  and stored until staining.

### **Immunohistochemical Staining**

IHC staining was performed following the recommended protocol provided by Cell Signaling Technologies for frozen tissues. Briefly,  $5\mu\text{M}$  thick sections were fixed for 15 minutes in 3% formaldehyde at room temperature. Slides were washed in wash buffer (1X TBS) twice for 5 minutes each followed by 10 minute incubation at room temperature in 3%

H<sub>2</sub>O<sub>2</sub> diluted in methanol. Slides were washed twice for 5 minutes in wash buffer followed by incubation in blocking solution (1X TBS/0.3% Triton-X 100/5% normal goat serum). Blocking solution was removed and immediately replaced by primary antibody specific to the protein of interest at 1:50 dilution in blocking solution and allowed to incubate at 4°C overnight. Antibodies used included those targeting total EGFR (Cell Signaling Technology, 4267), E-Cadherin (Cell Signaling Technology, 3195), CD44 (Cell Signaling Technology, 3578) and phosphorylated EGFR (Cell Signaling Technology, 2237). Antibody was removed and slides were washed in wash buffer 3 times for 5 minutes each. Biotinylated secondary antibody was added to each slide diluted 1:100 in blocking solution and allowed to incubate for 30 minutes. ABC reagent (Vectastain, PK-6100) was prepared according to manufacturer's specifications and allowed to stand at room temperature for 30 minutes before use. Slides were washed in wash buffer 3 times for 5 minutes each followed by 30 minute incubation in ABC reagent at room temperature. ABC reagent was removed and slides washed in wash buffer for 3 times for 5 minutes each. DAB substrate was prepared according to manufacturer's recommendation and added to each slide. Slides were allowed to develop for 2 minutes before being submersed in dH<sub>2</sub>O. Slides were counterstained with Hematoxylin per manufacturer's recommendations. Slides were washed in dH<sub>2</sub>O twice for 5 minute each. Slides were incubated in 95% ethanol twice for 10 seconds each. Slides were then incubated in 100% ethanol twice for 10 seconds each then repeated in xylene twice for 10 seconds each. Coverslips were mounted using Permount Mounting Medium (Thermo Fisher Scientific, SP15-500) and slides were allowed to dry overnight prior to imaging. Representative images were collected in 2 untreated tumors and 4 treated tumors for each condition.

### **Microvessel Density Determination**

MVD was determined by the “hot spot” method to count endothelial cell-lined blood vessels[85, 108-110]. Briefly, areas of highest microvessel density were determined to calculate the average of 3 fields/section in two tumors/condition, Field=0.16mm<sup>2</sup> at 200x. CD31 was used as a marker for endothelial cells because it has been shown to be the best marker for blood vasculature in benign and malignant tumors[111]. Since CD31 is also expressed on platelets, macrophages, neutrophils and monocytes, I exclude any single cells staining positive for CD31. Any CD31<sup>+</sup> cell clusters, clearly separated from adjacent microvessels, tumor tissue, or other tissue elements were considered as a single countable microvessel[108]. Images were randomized prior to manual counting in order to reduce bias. Fields with MVD closest to the average was displayed as representative images. Significance was determined by one-way ANOVA with a *post hoc* student's T test for significance.

## CHAPTER THREE

### RESULTS

#### **Induction of EMT in EGFR Mutation-Positive NSCLC Cell Lines**

I began by ensuring the epithelial or mesenchymal status of the cell lines to be used in our study. I found that the expression of the canonical epithelial cell marker E-Cadherin was down-regulated in HCC4006Ge-R mesenchymal cells compared to epithelial HCC4006 cells, whereas canonical mesenchymal cell markers N-Cadherin and CD44 were up-regulated (Figure 1A). Similarly, E-Cadherin expression was down-regulated in mesenchymal ER23 while N-Cadherin and CD44 were up-regulated (Figure 1B). Additionally, E-Cadherin depletion using lentiviral shRNA efficiently down-regulated E-cadherin and resulted in an up-regulation of N-Cadherin and CD44 (Figure 1C).

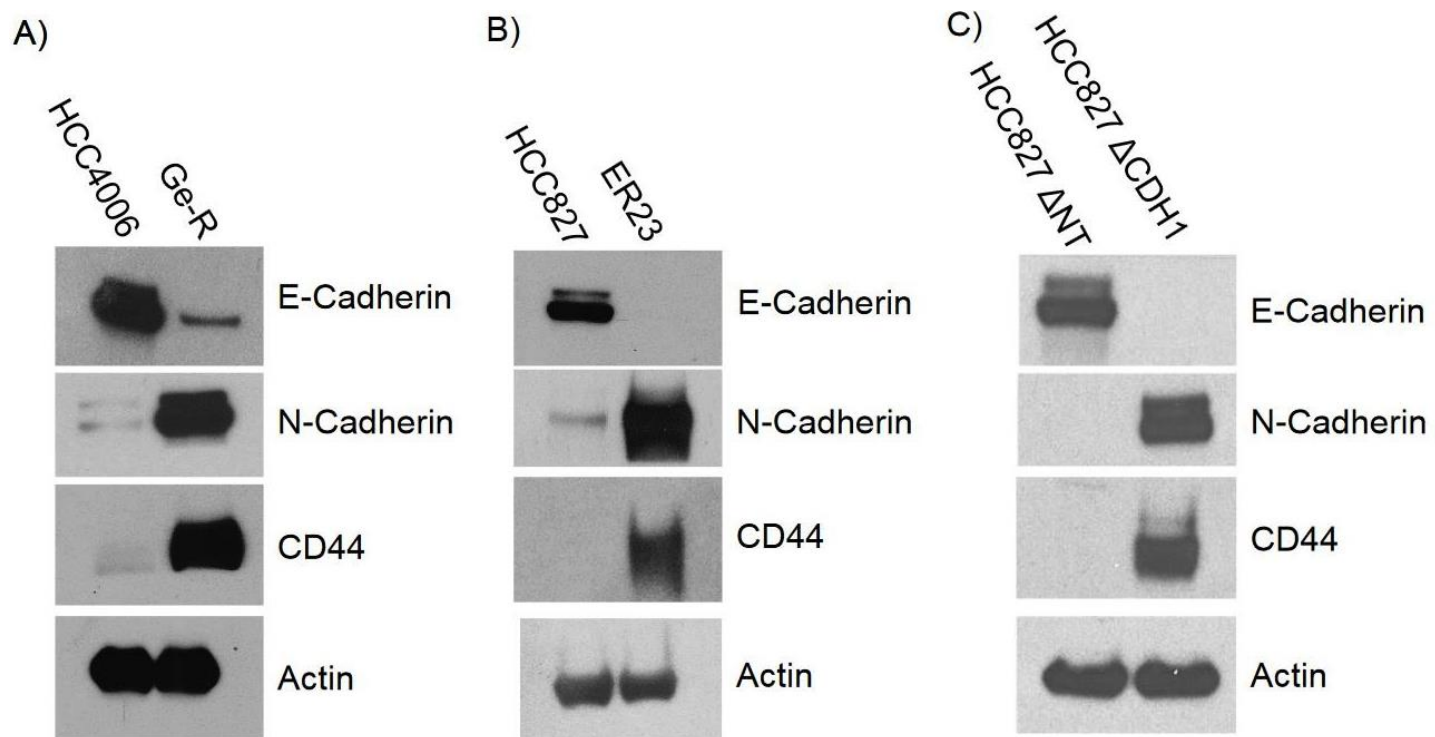


**Figure 1. Induction of EMT in EGFR Mutation-Positive NSCLC Cell Lines.** A) Epithelial HCC4006 to mesenchymal HCC4006Ge-R comparing epithelial marker E-Cadherin to mesenchymal markers N-Cadherin and CD44. B) Epithelial HCC827 to mesenchymal ER23 comparing epithelial marker E-Cadherin to mesenchymal markers N-Cadherin and CD44. C) Epithelial HCC827  $\Delta$ NT to mesenchymal HCC827  $\Delta$ CDH1 comparing epithelial marker E-Cadherin to mesenchymal markers N-Cadherin and CD44.

**Admix of Epithelial HCC827 and Mesenchymal ER23 Cell Types Confers a Growth Advantage *In Vivo* but No Growth Advantage is Seen in Epithelial and Mesenchymal Admix *In Vitro* in Multiple Cell Lines**

Soucheray et. al. showed that chronic EGFR inhibition in EGFR mutated NSCLC cells promoted acquired EGFR TKI resistance with a mesenchymal phenotype[55]. To develop novel therapeutics against the EGFR TKI resistant mesenchymal NSCLC cells, our laboratory attempted developing xenograft models of the mesenchymal cells. However, the growth of the mesenchymal NSCLC cells was significantly impaired *in vivo*. Together with our collaborators, I have found that the mesenchymal NSCLC cells need to be mixed with epithelial cells for optimal growth *in vivo*. Therefore, I wanted to study why epithelial and mesenchymal cell populations need to be mixed for the optimal *in vivo* growth. To this end, a subcutaneous xenograft was performed, in which epithelial HCC827 or mesenchymal ER23 cells were injected as a pure culture or in a 50/50 admix sub- cutaneously in an immunologically deficient murine model. I observed that epithelial HCC827 cells successfully established a tumor in all injections. As I have previously seen, mesenchymal ER23 cells only established tumors in 80% of injections, and produced tumors of very limited volume (Fig.2A). Notably, a 50/50 epithelial/mesenchymal admix successfully established tumors in all injections and exhibited a greater tumor volume at the termination of the experiment compared to epithelial tumors ( $p < 0.001$ ) or mesenchymal tumors ( $p < 0.0001$ ). Based on this result, I hypothesized that epithelial and mesenchymal cells are programmed to contribute to each other for optimal tumor growth. To test the hypothesis, I have mixed epithelial HCC827 cells and mesenchymal ER23 cells in a 50/50 admix co- culture *in vitro*. While epithelial

HCC827 cells initially grow faster than mesenchymal ER23 cells, no significant difference in proliferation was observed at the end of a 6 day growth period *in vitro*. The 50/50 admix conditions produced no significant advantage in cell proliferation compared to HCC827 or ER23 pure cultures at the end of a 6 day growth period (Figure 2B). To ensure that the *in vitro* result is not cell lineage specific, I repeated the same *in vitro* experiment using epithelial HCC4006, mesenchymal Ge-R or a 50/50, 70/30 or 30/70 admix. I observed that all admix conditions failed to produce a significant growth advantage compared to HCC4006 cells or Ge-R cells alone *in vitro* (Figure 2C).

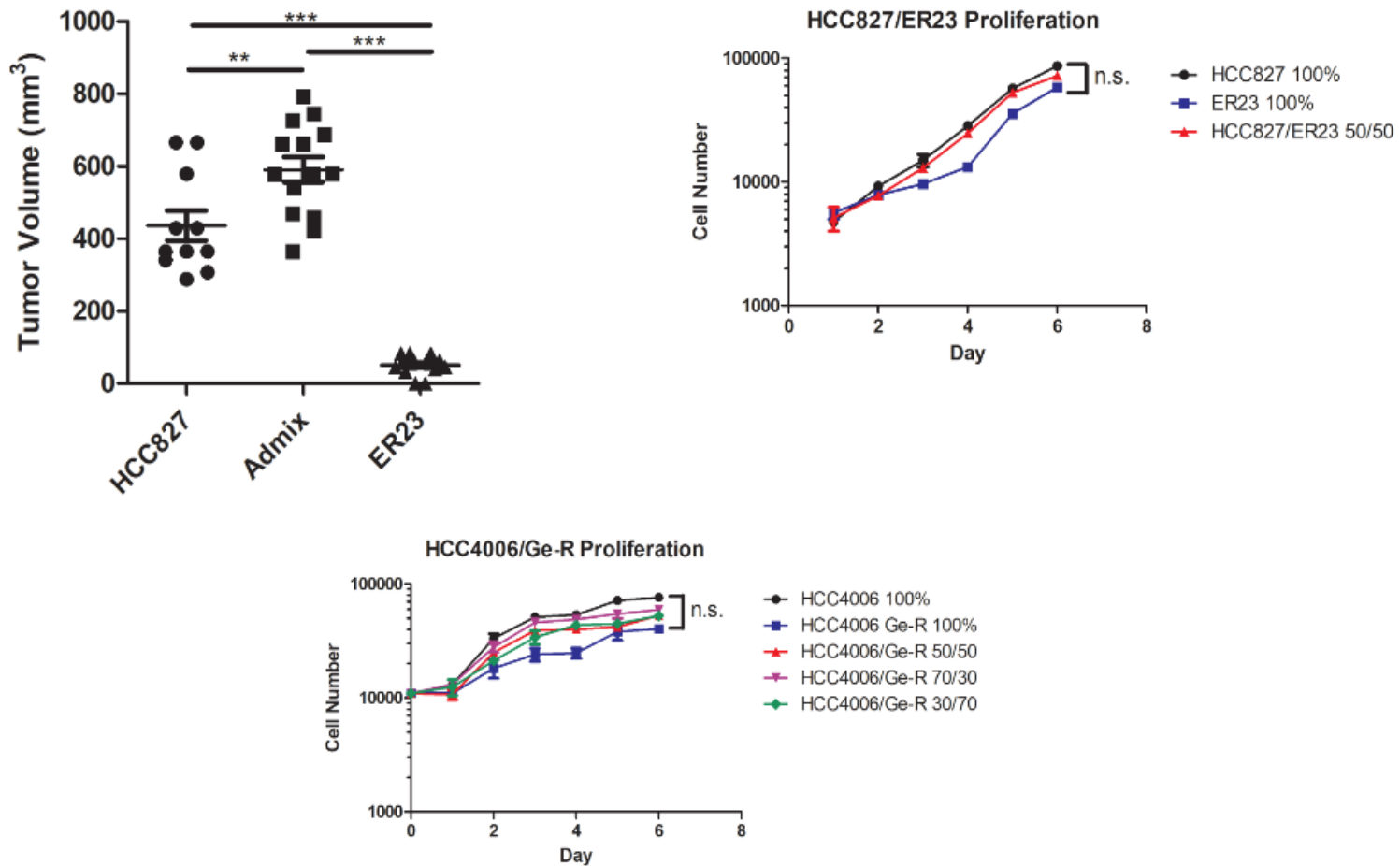


**Figure 2. Admix of Epithelial HCC827 and Mesenchymal ER23 Cell Types Confer a Growth Advantage *In Vivo* but No Growth Advantage is Seen in Epithelial and Mesenchymal Admix *In Vitro* in Multiple Cell Lines.** A) Subcutaneous xenograft of a 50/50 admix of epithelial HCC827 and mesenchymal ER23 cells demonstrate a growth advantage *in vivo* compared to pure epithelial ( $p < 0.001$ ) or mesenchymal xenografts ( $p < 0.0001$ ). B) 2-D co-culture of epithelial HCC827 and mesenchymal ER23 cells do not result in a growth advantage *in vitro*. Significance was determined by two-way ANOVA with a post hoc student's t-test. C) 2-D co-culture of epithelial HCC4006 and mesenchymal HCC4006 Ge-R cells do not result in a growth advantage *in vitro*. Significance was determined by two-way ANOVA with a post hoc student's t-test.



### **HCC827/ER23 50/50 Admix at Time of Implantation Results in an Epithelial Dominated Tumor at 24 Days**

E-Cadherin has been identified as a reliable marker of epithelial cells[112] while CD44 has been identified as a reliable marker of mesenchymal cells[54]. Since our murine xenograft models of admix conditions were implanted in a 50/50 ratio, and I showed that epithelial and mesenchymal cells display no significant difference in proliferation rates *in vitro* (Figure 2B,C) I hypothesized both epithelial and mesenchymal cells would continue to maintain a 50/50 ratio within admix xenografts. To test this hypothesis, I performed IHC staining for E-Cadherin and CD44 on frozen sections prepared from the xenograft tumors. I found high levels of E-Cadherin expression in epithelial HCC827 tumors and high levels of CD44 in mesenchymal ER23 tumors. I found more cells with E-Cadherin expression than cells with CD44 expression in the admix tumors. The CD44-positive mesenchymal cells were distributed throughout the admix tumor at a low frequency (Figure 3).

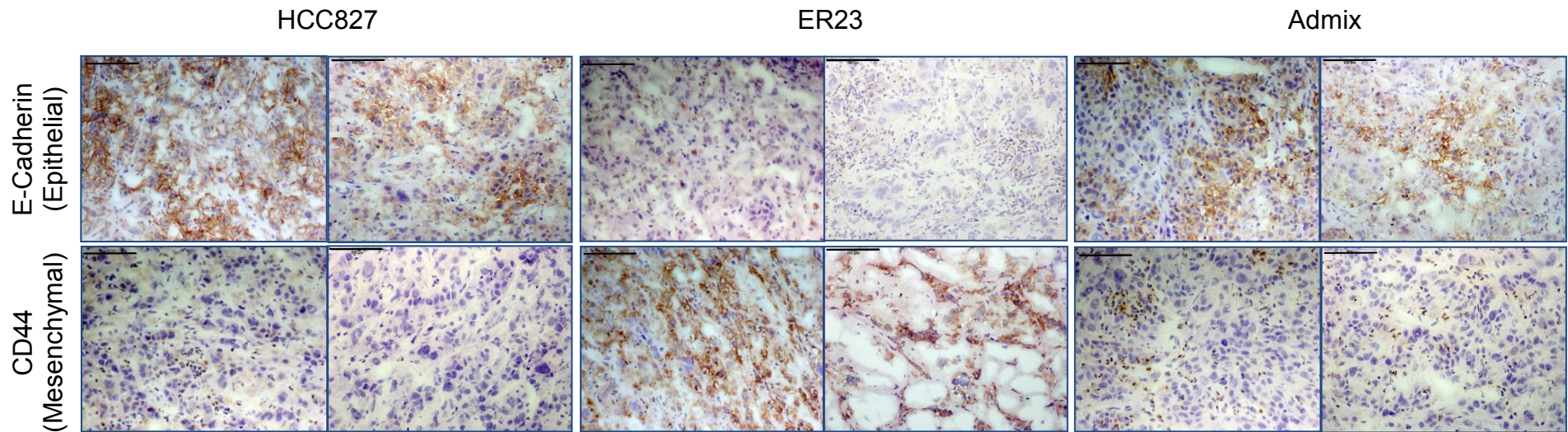


**Figure 3. HCC827/ER23 50/50 Admix at Time of Implantation Results in an Epithelial Dominated Tumor at 24 Days**

Representative images from murine sub-cutaneous xenografts established by epithelial HCC827 cells, mesenchymal ER23 cells or a 50/50 admix stained for epithelial marker E-Cadherin or mesenchymal marker CD44. All micrographs are taken at 20x magnification. Scale bars represent 100 $\mu$ m.

### **The EMT Process Results in Differential Expression of Several Pro-Angiogenic and Growth Factors**

Since the increased tumorigenicity of epithelial and mesenchymal admix cells were observed only *in vivo*, I sought to determine if tumor-host interaction might be the causal factor for the observed growth advantage. I hypothesized that a change in gene expression during EMT may be establishing a signaling pathway between the tumor and host vasculature. To assess whether the EMT process results in a change in expression in factors known to influence blood vasculature, I performed a Luminex multiplex assay analyzing the concentrations of secreted factors by epithelial or mesenchymal cells into the media in an *in vitro* culture over a 48 hour growth period. I assessed the concentration of VEGF-A, EDN1, FGF-2, VEGF-C, VEGF-D, Angiopoietin-2, FGF-1, HGF, PLGF and endoglin. I compared epithelial HCC4006, HCC827, and HCC827 shNT to mesenchymal HCC4006Ge-R, ER23, HCC4006 O-R, and HCC827 shCDH1. I observed that all epithelial and mesenchymal cell lines tested secreted similar concentrations of VEGF-C, VEGF-D, FGF-1, HGF, PLGF, and endoglin. I discovered that VEGF-A secretion was lower in all mesenchymal cell lines tested compared to epithelial cells. Furthermore, I observed that EDN1 secretion was higher in all mesenchymal cell lines tested compared to epithelial cells (Figure 4). While Angiopoietin-2 was significantly up-regulated in HCC827 when mesenchymal phenotype was induced, the same increase was not seen in HCC4006 with a mesenchymal phenotype. FGF-2 secretion was high in HCC4006Ge-R or HCC4006O-R compared to epithelial HCC4006 although this result was not observed in HCC827 cells (Figure 4). I therefore focused on the secreted concentration of VEGF-A and EDN1.

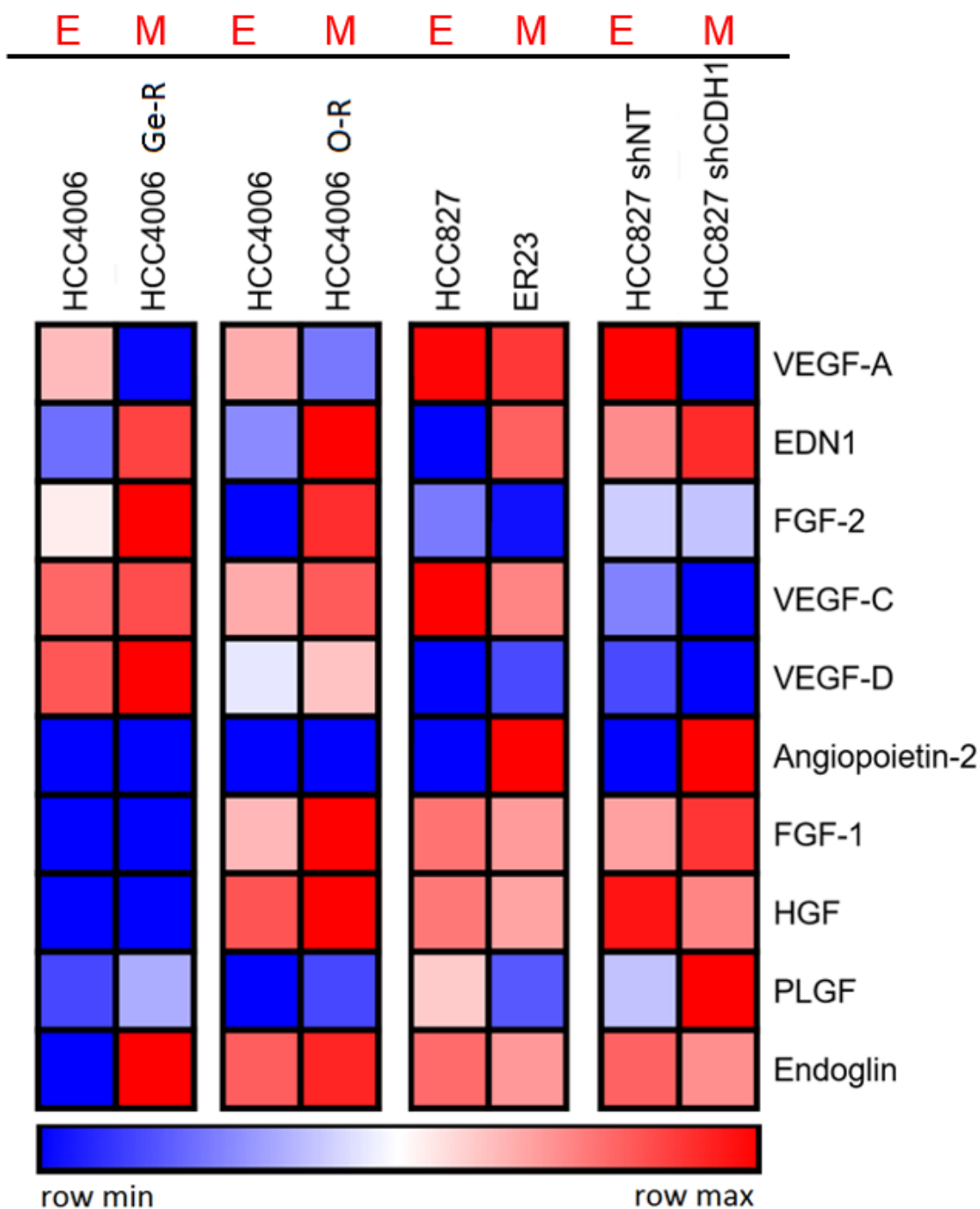


**Figure 4. EMT Process Results in Differential Expression of Several Pro-Angiogenic and Growth Factors.** Luminex multiplex angiogenesis/growth factor multiplex assay analysis comparing HCC4006/HCC4006 Ge-R, HCC827/ER23, HCC4006/HCC4006 O-R, and HCC827 shNT/HCC827 shCDH1. Cell culture supernatant was collected and analyzed for secreted concentrations of VEGF-A, VEGF-C, VEGF-D, EDN1, FGF-1, FGF-2, angiopoietin-2, HGF, PLGF and endoglin. All epithelial cell lines have been labeled with an E while all mesenchymal cell lines were labeled with an M.

## **Induction of EMT or EGFR Inhibition Results in a Significant Increase in EDN1**

### **Secretion and Decrease in VEGF-A Secretion**

I evaluated our Luminex Multiplex assay results quantitatively using a one-way ANOVA analysis with a *post hoc* student's T test for significance. I found that in comparing HCC4006 and HCC4006Ge-R there was a significant reduction in VEGF-A secretion ( $p < 0.001$ ) coupled with a significant increase in EDN1 secretion ( $p < 0.001$ ) during a 48 hour growth period. Furthermore, I observed no significant reduction in VEGF-A secretion in a 50/50 epithelial/mesenchymal admix compared to epithelial alone coupled with a significant decrease in EDN1 concentration (Figure 5A). This may be due to EDN1 being secreted by mesenchymal HCC4006Ge-R cells and taken up by epithelial HCC4006 cells. I sought to replicate this result in other cell lines. I saw a significant increase in EDN1 secretion ( $p < 0.001$ ) coupled with a significant decrease in VEGF-A secretion ( $p < 0.001$ ) in mesenchymal HCC4006O-R compared to epithelial HCC4006 cells (Figure 5B). I also observed a significant increase in EDN1 secretion ( $p < 0.001$ ) coupled with a significant increase in EDN1 secretion ( $p < 0.001$ ) when comparing mesenchymal ER23 or HCC827 shCDH1 compared to epithelial HCC827 cells (Figure 5C,D). I also observed a non-significant reduction in VEGF-A secretion when HCC827 cells were grown in a 50/50 admix with ER23 cells while EDN1 expression was predictably found to be at ~%50 of that of a pure mesenchymal ER23 cell culture. Because EDN1 concentrations were not depleted in our 50/50 admix condition, we used HCC827/ER23 cell lines for all *in vivo* studies. It remained unclear whether this change from VEGF-A to EDN1 secretion represented an event in the EMT process or a consequence of EGFR inhibition. To analyze this, I exposed epithelial HCC4006 to 100nM gefitinib treatment for

72 hours. I observed that short-term gefitinib was sufficient to induce a significant up-regulation of EDN1 secretion coupled with a significant down-regulation of VEGF-A (Figure 5E).

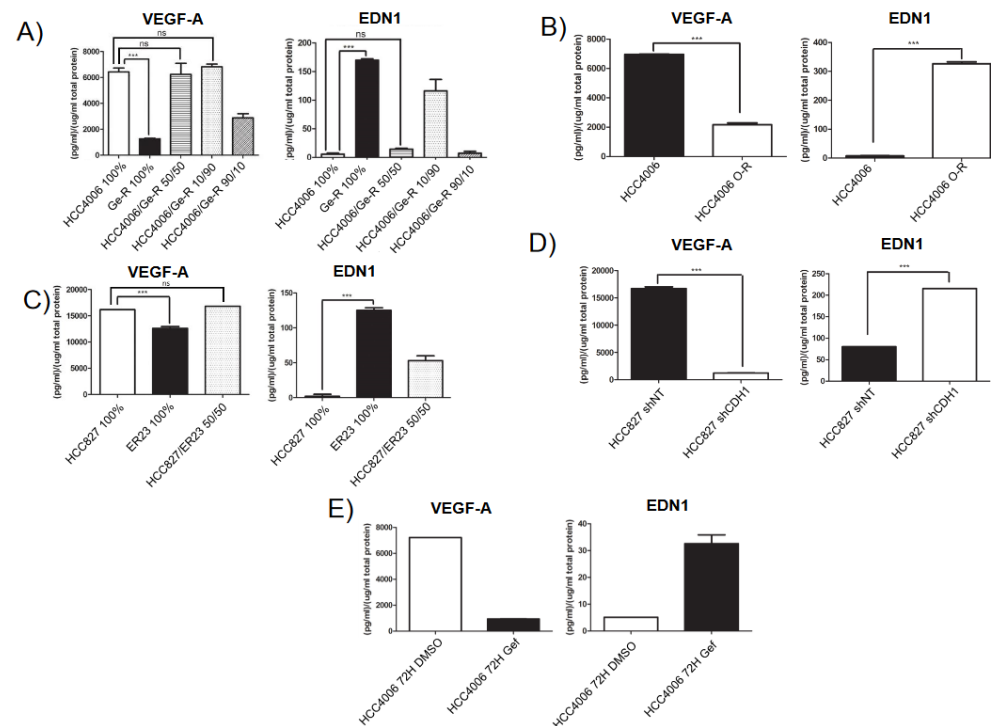


**Figure 5: Induction of EMT or EGFR Inhibition Results in a Significant Increase in EDN1 Secretion and Decrease in VEGF-A Secretion.** A) Epithelial HCC4006 showed robust levels of VEGF-A secretion and relatively low levels of EDN1 whereas mesenchymal HCC4006 Ge-R cells secreted significantly greater concentrations of EDN1 and significantly lower concentrations of VEGF-A ( $p < 0.0001$ ). No significant change in VEGF-A secretion was seen under 50/50 or 10/90 epithelial and mesenchymal co-culture conditions. B) Epithelial HCC4006 and mesenchymal HCC4006 O-R cell lines exhibit a significant loss of VEGF-A secretion coupled with a significant gain in EDN1 secretion ( $p < 0.0001$ ). C) Epithelial HCC827 and mesenchymal ER23 cell lines exhibit a significant loss of VEGF-A secretion coupled with a significant gain in EDN1 secretion ( $p < 0.0001$ ). D) Epithelial HCC827 shNT and mesenchymal HCC827 shCDH1 cell lines exhibit a significant loss of VEGF-A secretion coupled with a significant gain in EDN1 secretion ( $p < 0.0001$ ). E) 72 hour EGFR TKI treatment (100nM gefitinib) was sufficient to cause the loss of VEGF-A secretion and gain of EDN1 secretion in epithelial HCC4006 cells. Significance was determined by one way ANOVA analysis with post hoc student T-test.

**Epithelial/Mesenchymal Admix Conditioned Media Confers Greater Differentiation Potential in Cultured HUVEC Endothelial Cells Compared to Epithelial or Mesenchymal Pure Culture Conditioned Media**

It has been previously shown that *in vitro* tube formation is enhanced under both 10nmol/L EDN1 and 1ng/ml VEGF-A when performed with HUVEC cells. These factors demonstrated a synergistic effect leading to greater angiogenic potential when used in combination compared to either agent alone[83]. Since I have already seen notable concentrations of VEGF-A and EDN1 in epithelial and mesenchymal cell culture supernatant respectively, I hypothesized that conditioned media produced from admix conditions would contain significant levels of both VEGF-A and EDN1. If true, admix conditioned media would offer greater angiogenic potential in a tube formation assay compared to epithelial or mesenchymal cells grown alone. In an 8 hour tube formation assay, the condition media from HCC4006 and HCC4006Ge-R cells grown in a 50/50 admix promoted greater tube formation potential compared to supernatants from HCC4006 or HCC4006Ge-R cells (Figure 6A). Images were captured with an Evos FL Cell Imaging System (AMD, AMF4300) in the GFP channel. Images were analyzed using the ImageJ Angiogenesis Analyzer plugin provided as free software from the Gilles Carpentier Research Group[107]. A significant increase in the number of nodes ( $p<0.01$ ), total tubule length ( $p<0.01$ ) and mesh area ( $p<0.001$ ) was seen in HCC4006 and Ge-R cells grown in a 50/50 admix when compared to negative control EBM or HCC4006 or Ge-R cells grown in pure culture (Figure 6B).



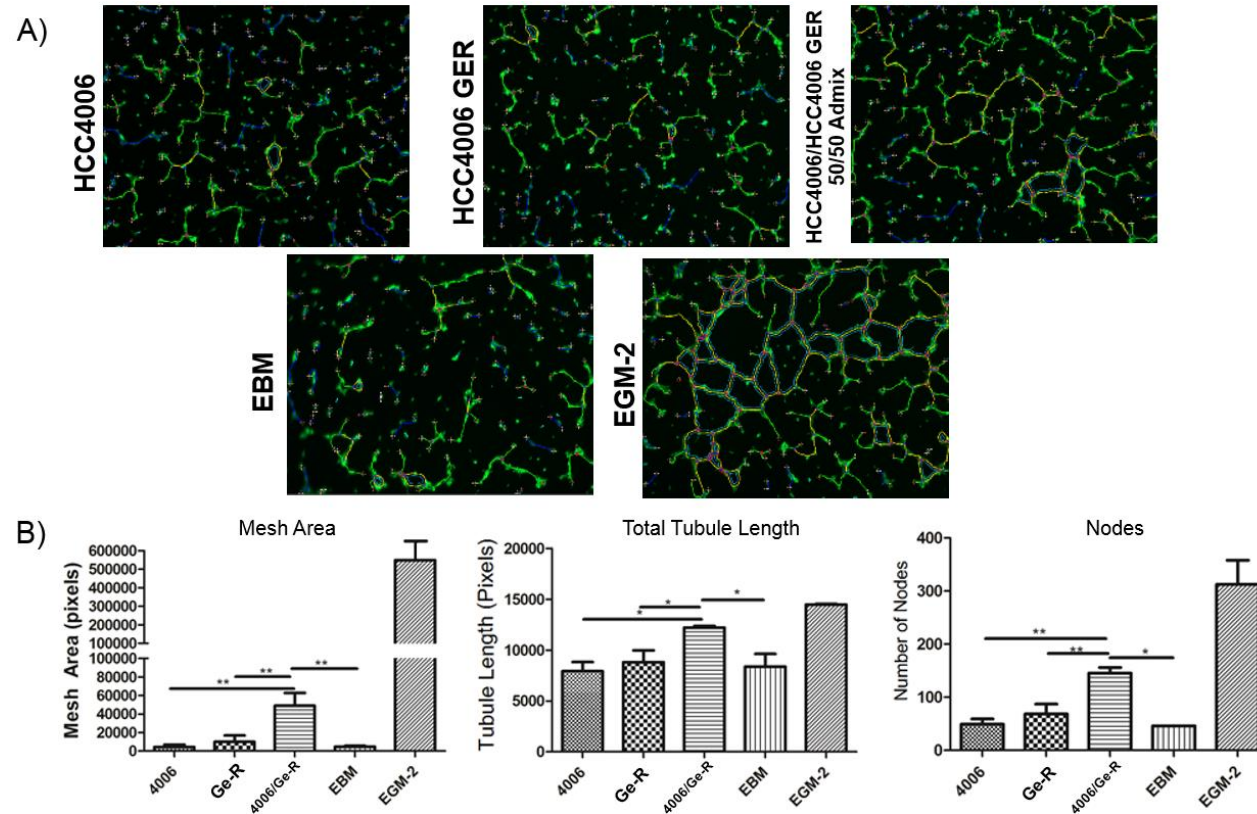


**Figure 6. Epithelial/Mesenchymal Admix Conditioned Media Confers Greater Differentiation Potential in Cultured HUVEC Cells Compared to Epithelial or Mesenchymal Pure Culture Conditions.** A) Qualitative comparison of conditioned media produced from epithelial HCC4006 cells, mesenchymal HCC4006 Ge-R cells, and HCC4006/HCC4006 Ge-R cells grown in 50/50 admix. Tube formation in basal media (EBM) and fully supplemented growth media (EGM-2) has been included as negative and positive controls respectively. Images are representative of 3 repeat experiments. Traces in green represent total tube length; red points represent nodes, blue traces represent mesh areas. B) ImageJ angiogenesis quantification of commonly analyzed tube formation parameters including mesh area ( $p < 0.001$ ), total tubule length ( $p < 0.01$ ) and number of nodes ( $p < 0.01$ ). Significance determined by one-way ANOVA with post hoc student's t-test. Error bars represent standard error between repeat samples.

To test if the result that increased tube formation in supernatant from the admix cells is due primarily to the presence of VEGF-A and EDN1, I performed a tube formation assay in growth factor reduced EBM with either 10nM VEGF-A, 10nM EDN1 or a combination of 10nM VEGF-A and 10nM EDN1 (Figure 7A). These concentrations were calculated from the concentrations of VEGF-A and EDN1 as measured by Luminex analysis (Figure 5). I found that while all conditions failed to produce a significant increase in tube formation above basal levels, a clear trend toward enhanced tube formation was present in the combination treatment compared to either single target treatment (Figure 7B).

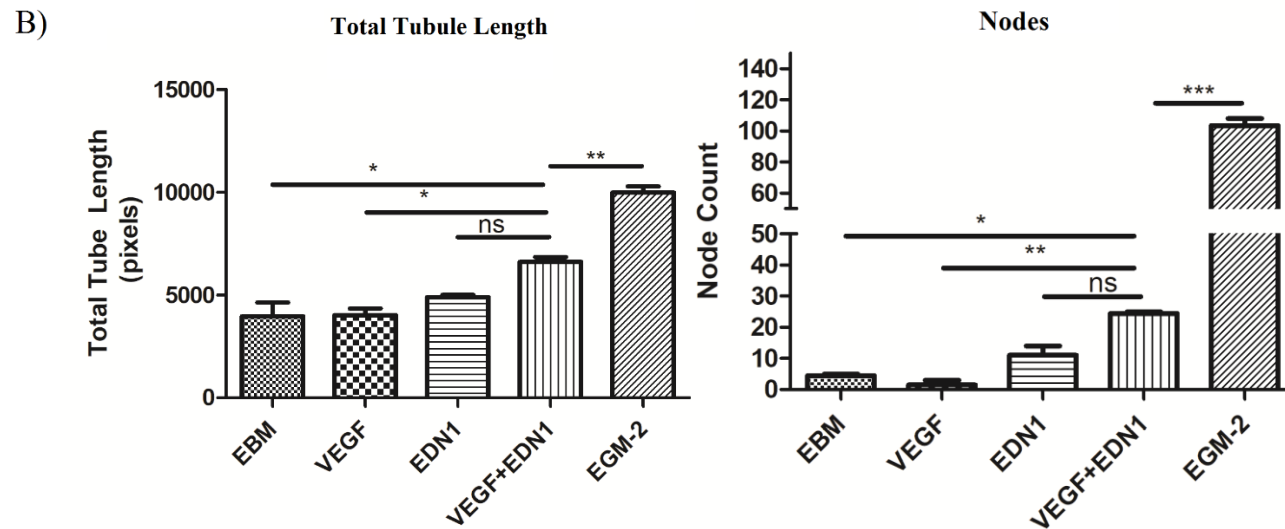
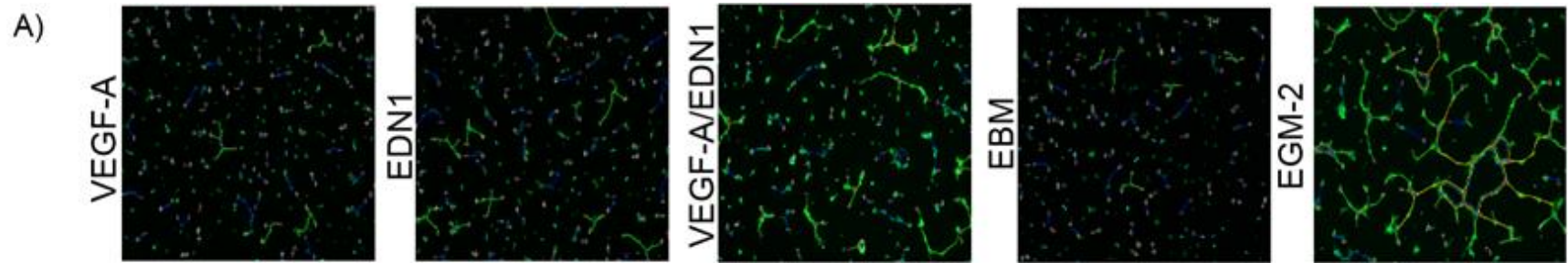


**Figure 7. *In Vitro* Angiogenesis Analyzed by Tube Formation Assay.** A) Qualitative comparison of tube formation in basal EBM media supplemented with 10ng/mL VEGF-A, 10nM EDN1 or a combination of both factors. Tube formation in basal media EMB and fully supplemented EGM-2 has been included as negative and positive controls respectively. Images are representative of 3 repeat experiments. B) ImageJ angiogenesis quantification of commonly analyzed tube formation parameters including, total tubule length and number of nodes. Significance determined by one-way ANOVA with post hoc student's t-test. Error bars represent standard error between repeat samples.

### **Sunitinib/Zibotentan Combination Therapy Effectively Inhibits Tube Formation *In Vitro***

To further test if the increased tube formation in the conditioned media from the admix cells are due to the effects of VEGF-A and END1, I utilized chemical inhibitors of VEGFR2 and EDNRA, sunitinib and Zibotentan respectively, to investigate if inhibition of VEGFR2 and EDNRA could suppress tube formation by the condition media. While sunitinib is known to also inhibit PDGFRs and other VEGFRs, its main target is VEGFR2. Zibotentan was chosen because it is a specific inhibitor to EDNRA. Representative images from tube formation in untreated admix conditions, low-dose 10nM sunitinib treatment, low-dose 100nM Zibotentan treatment, and dual drug treatment were obtained (Figure 8A). Upon quantification, I observed that low dose (10nM) sunitinib did not produce a significant reduction in tube formation in conditioned media produced from admix conditions. Likewise, low dose (100nM) Zibotentan did not produce a significant reduction in tube formation in conditioned media produced from admix conditions. The combination of 10nM sunitinib and 100nM Zibotentan significantly inhibited tube formation ( $p < 0.01$ ) in admix conditioned media (Figure 8B). I therefore showed that the combination treatment targeting both VEGFR and EDNRA as an effective inhibitor of angiogenesis *in vitro*.

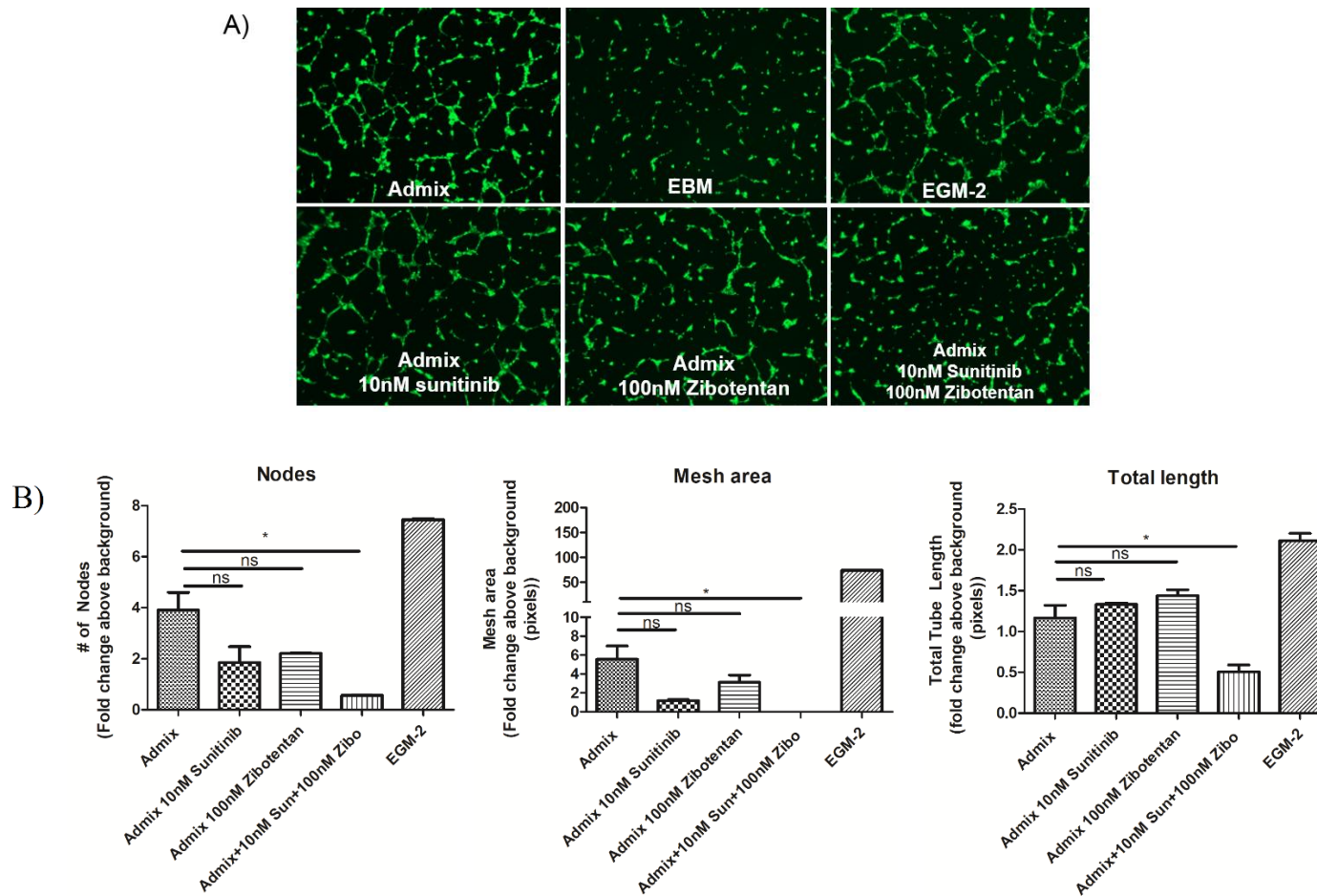


**Figure 8. *In Vitro* Inhibition of Angiogenesis Analyzed by Tube Formation Assay.** A) Qualitative comparison of tube formation in conditioned media produced from a 50/50 admix of epithelial HCC4006 and mesenchymal GER cells treated with 10nM Sunitinib, 100nM Zibotentan, or a combination of the two factors, respectively. Images are representative of 3 repeat experiments. B) ImageJ angiogenesis quantification of commonly analyzed tube formation parameters including number of nodes, total tubule length and total mesh area. Significance determined by one-way ANOVA with post hoc student's t-test. Error bars represent standard error between repeat samples.

**The Expression of EDNRA and Phosphorylated VEGFR2 in HUVEC Cells is Increased Under 8H Stimulation by Admix Conditioned Media and Sunitinib Abrogates VEGFR Phosphorylation**

Since VEGF-A has been shown to primarily exhibit its pro-angiogenic effect through the VEGFR2 receptor, I consider VEGFR2 phosphorylation as a marker of VEGF-A activity[91]. While VEGF-A has been shown to strongly bind to VEGFR1, the receptor has been shown to have a weak effect on angiogenesis[113]. I therefore focused our studies on VEGFR2 signaling. To test whether I am effectively inhibiting VEGFR2 through low dose 10nM sunitinib treatment, I examined VEGFR2 signaling under stimulation by conditioned media produced from epithelial HCC4006 cells and mesenchymal HCC4006GE-R cells grown under 50/50 admix conditions (Figure 9). I found that while total VEGFR2 was comparable under all conditions tested, phosphorylated VEGFR2 was up-regulated under stimulation by conditioned media produced under admix conditions or by complete EGM which contains no VEGF-A or EDN1. Phosphorylated VEGFR2 was abrogated by low dose 10nM sunitinib treatment when added to either admix conditioned media or complete EGM. I observed that EDNRA levels are decreased under unstimulated 8h EBM conditions while EDNRA levels are comparable when stimulated by conditioned media or complete EGM in the presence or absence of sunitinib treatment (Figure 9). EDNRA, total VEGFR2 and phosphorylated VEGFR2 expression was normalized against a vinculin loading control.

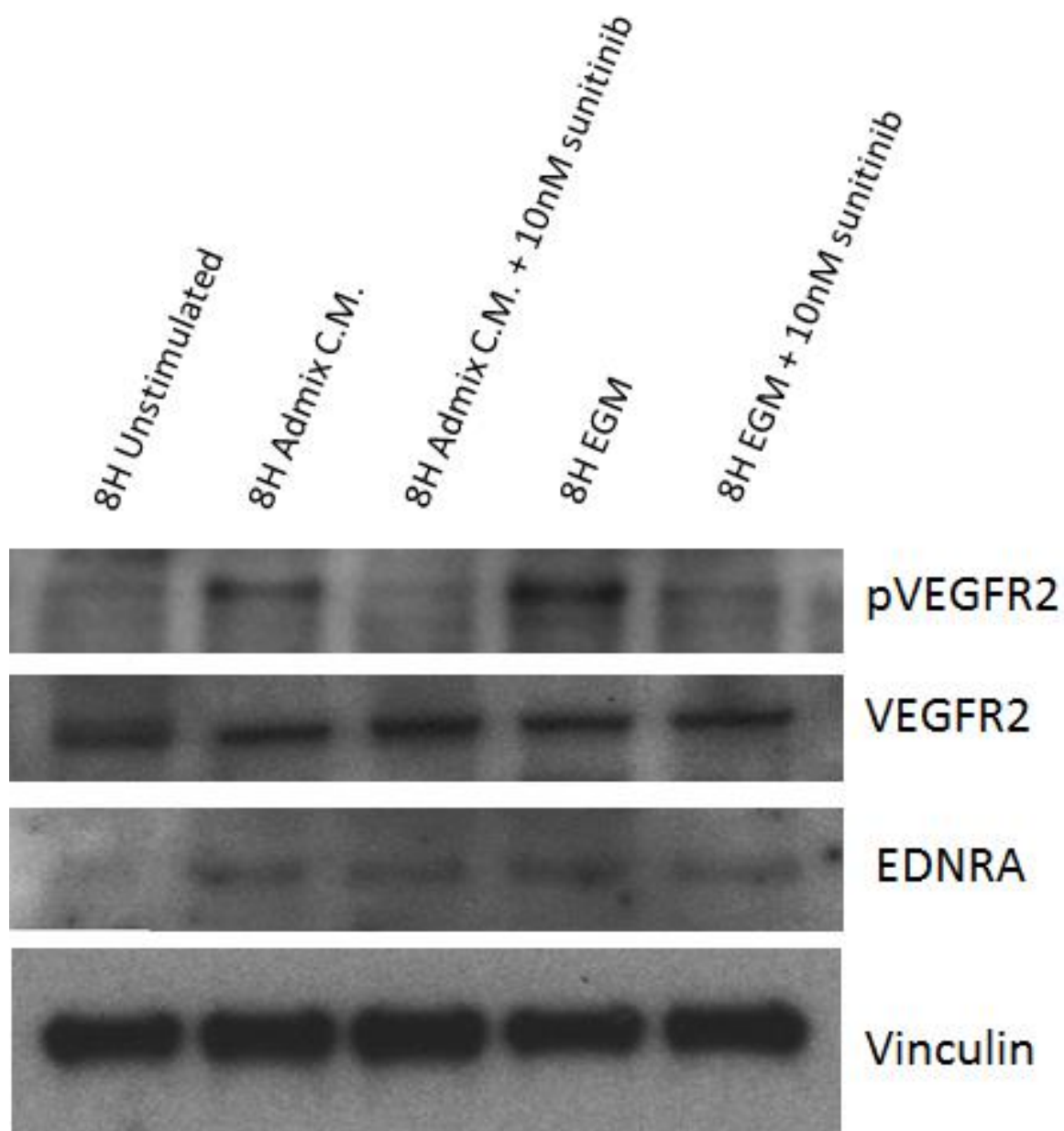


**Figure 9. HUVEC Cells Express EDNRA and Phosphorylated VEGFR2 is Up-Regulated Under 8H Stimulation by Admix Conditioned Media While Being Effectively Abrogated by 10nM Sunitinib Treatment.** Western blot comparing expression of EDNRA, VEGFR2, and pVEGFR2 under unstimulated conditions (8H basal EBM media) or stimulation with admix conditioned media or complete growth media (EGM) with or without 10nM sunitinib.

**NSCLC Cells Lines with an EDN1 Over-Expression or Knock-Down Phenotype maintain VEGF-A Secretion *In Vitro* and EDN1 Secretion was Associated With Significantly Lower Tumor Growth**

I sought to analyze the effect of EDN1 on the tumor microenvironment *in vivo*, therefore, I generated a HCC827 cell line which ectopically expresses EDN1 using a pLX lentiviral expression vector (HCC827 EDN1). I used HCC827 cells transduced with a pLX vector lentivirus coding for flag-V5 as a control (HCC827 Flag/V5). Upon antibiotic marker selection, I ensured constitutive EDN1 secretion in the supernatant from HCC827 pLX EDN1 cells using Luminex assay. Additionally, the secretion of VEGF-A was maintained in these cells (Figure 10A). Interestingly, when I performed a sub-cutaneous xenograft experiment comparing the growth of HCC827 Flag/V5 to HCC827 EDN1, I observed that HCC827 Flag/V5 cells showed a growth advantage compared to HCC827 EDN1 as analyzed by caliper measurement (Figure 10B). To test if secretory EDN1 attenuates *in vivo* tumor growth, I generated HCC4006Ge-R cells with either an EDN1 or non-target knockdown. The depletion of EDN1 was confirmed in supernatants from the engineered cells using the Luminex assay (Figure 10C). Interestingly, EDN1 knockdown in Ge-R cells resulted in a significant increase in VEGF-A secretion compared to non-target knockdown (Figure 10C). To further test the role of EDN1 on tumor growth rate, tumors grown with Ge-R shEDN1 in admix with epithelial HCC4006 cells were shown to possess a growth advantage *in vivo* compared to Ge-R shNT cells in admix with epithelial HCC4006 cells (Figure 10D). Taken together, these data suggest that EDN1 is not important in explaining why admix conditions produce a growth advantage *in vivo*.



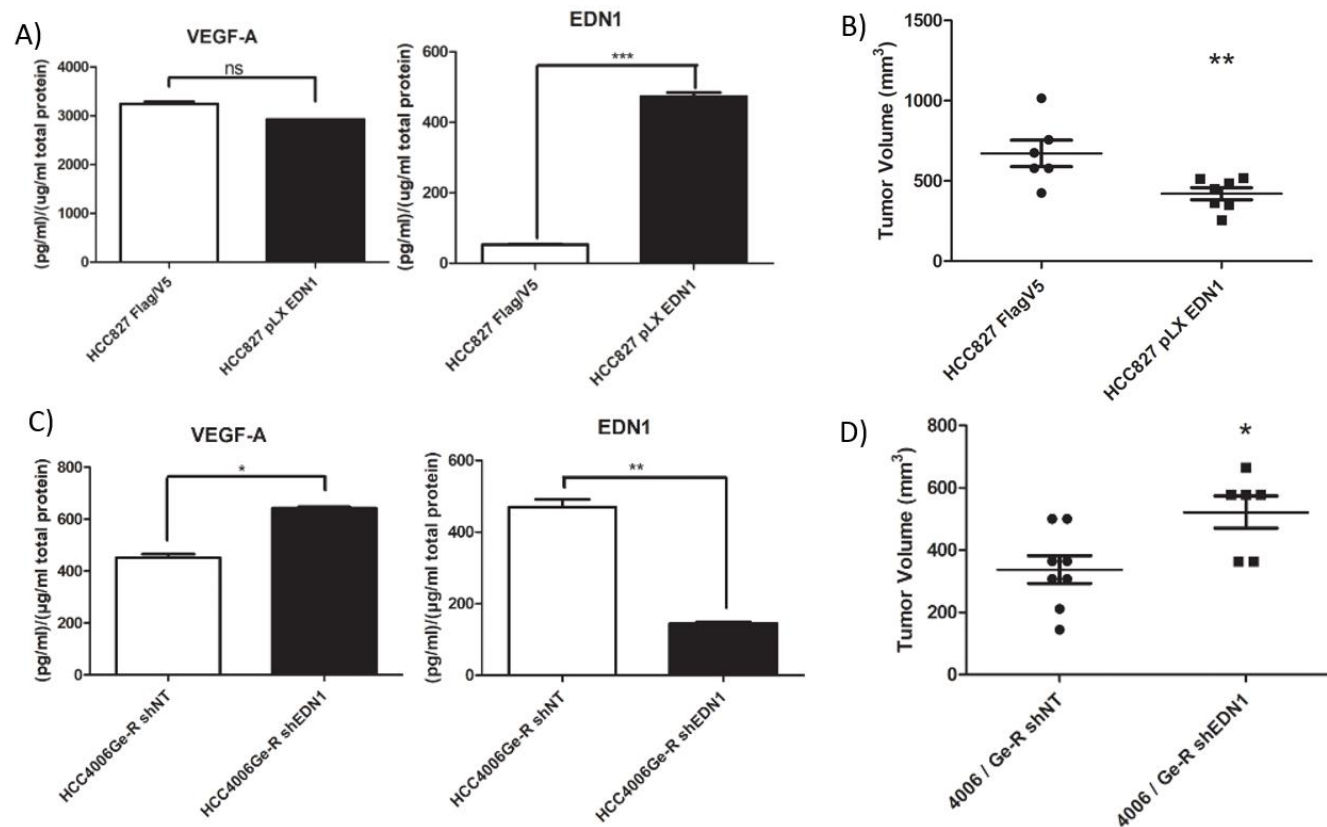


**Figure 10: NSCLC Cells Lines Harboring EGFR Kinase Domain Mutations Maintain VEGF-A Secretion *In Vitro* When EDN1 is Either Over-Expressed or Knocked Down and Result in a Slower or Faster Growing Tumor Respectively *In Vivo*. All Error Bars Represent Standard Error of Mean Between Repeat Conditions. A) VEGF-A (ns) and EDN1 ( $p < 0.001$ ) secretion as measured by a Luminex multiplex assay analyzing conditioned media produced over 48h in HCC827 Flag/V5 or pLX EDN1. B) HCC827 pLX EDN1 significantly inhibits tumor growth compared to HCC827 pLX Flag/V5 tumors ( $p = 0.0069$ ). C) VEGF-A ( $p < 0.01$ ) and EDN1 ( $p < 0.001$ ) secretion as measured by a Luminex multiplex assay analyzing conditioned media produced over 48h in Ge-R shNT or Ge-R shEDN1. D) Ge-R shEDN1 grown in admix with HCC4006 significantly potentiates tumor growth compared to Ge-R shNT ( $p = 0.0186$ )**

### **EDN1 Expressing Tumors Show Significantly Greater EGFR TKI Resistance *In Vivo***

I observed that EDN1 expression did not correlate with a growth advantage *in vivo*, although it is known that EDN1 expression is a known negative prognostic marker in NSCLC. I therefore sought to test whether EDN1 expression could positively affect EGFR TKI resistance. I tested gefitinib sensitivity in epithelial HCC827 and gefitinib resistance in mesenchymal ER23 cells *in vitro* by MTS assay (Figure 11A). I subjected HCC827, ER23, and the admix xenograft tumors to a 6-day course of gefitinib (50mg/kg daily) treatment. Tumor volume was calculated using external caliper measurement and upon completion of the drug treatment, tumor volume was measured via caliper following tumor excision. Percent residual tumor was calculated by comparing tumor volume before and after the gefitinib treatment. I found that both pure mesenchymal and admix tumors show significantly higher residual tumor volume following gefitinib treatment compared to epithelial tumors ( $p < 0.0001$ ) (Figure 11B). I also treated HCC827 Flag/V5 and HCC827 pLX EDN1 tumors with gefitinib for 6 days and measured tumor volume after excision from the mouse. I found that while EDN1 over-expression resulted in a slower growing tumor (Figure 10B), the resulting tumor was more resistant to gefitinib treatment as shown by a significantly greater residual tumor volume ( $p = 0.0353$ ) after 6 days of gefitinib treatment (Figure 11D). Taken together, these data suggest that EDN1 expression contributes to drug resistance *in vivo*.

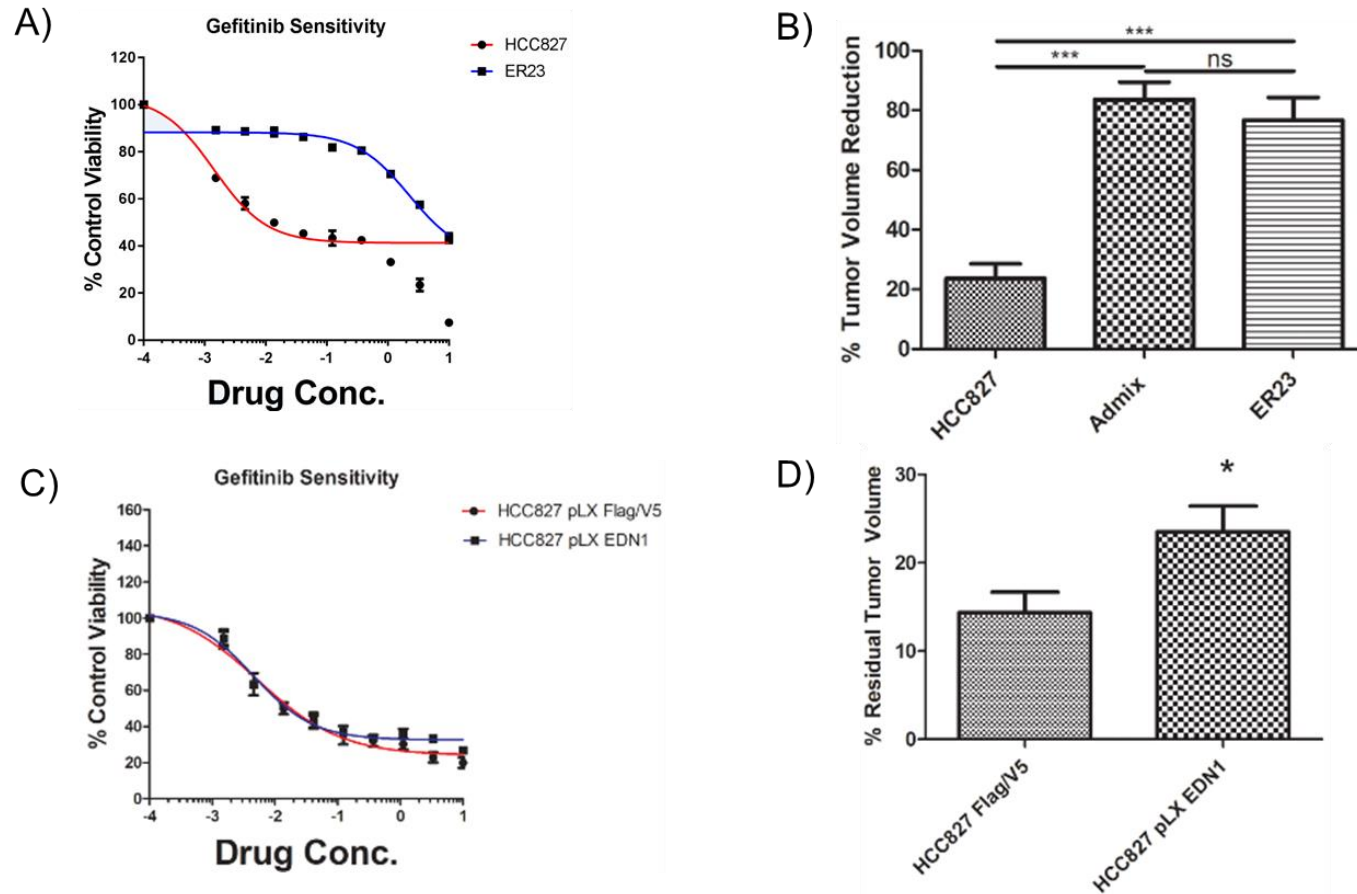


**Figure 11. Mesenchymal or Epithelial/Mesenchymal Admix Tumors and Tumors Overexpressing EDN1 Result in Significantly Greater EGFR TKI Resistance *In Vivo*. Error Bars Represent Standard Error Between Means for All Figures.** A) Sensitivity to gefitinib treatment as measured by MTS assay comparing HCC827 to ER23. B) Subcutaneous xenograft of mesenchymal ER23 and 50/50 admix of HCC827 and ER23 demonstrates significant drug resistance *in vivo* compared to pure epithelial xenografts ( $p < 0.0001$ ). C) Sensitivity to gefitinib treatment as measured by MTS assay comparing HCC827 pLX Flag/V5 to HCC827 pLX EDN1. D) Percent tumor volume change following 6-day gefitinib treatment (50mg/kg daily) ( $p = 0.0353$ ).

## **The Presence of EDN1 Secreting Cells in Admix Tumors or an Over-Expression Model Promotes Significantly Reduced Microvessel Density**

Because I observed significant drug resistance in tumors with an EDN1 secreting mesenchymal sub-population *in vivo* but not *in vitro*, I performed a literature search to identify tumor-host interactions involving EDN1 contributing to drug resistance. It has been previously shown that a lower MVD correlates with drug resistance in NSCLC[125]. I hypothesized that epithelial/mesenchymal admix conditions and mesenchymal xenografts would result in a tumor with lower MVD compared to epithelial tumors due to the vasoconstrictive properties of EDN1. By constricting local vessels, EDN1 may be limiting nutrient availability to the epithelial sub-population of the tumor. This effect would lower available VEGF-A secretion by epithelial cells and lead to lower MVD. Upon drug treatment, a diminished MVD may be leading to poor drug perfusion and an increase in apparent drug resistance *in vivo*. To explore this, I performed sub-cutaneous xenografts using epithelial HCC827, mesenchymal ER23 or a 50/50 admix. I prepared frozen sections from the resulting tumors and performed IHC staining for CD31. I chose to use CD31 as a marker for endothelial cells because it has been shown to be the best marker for blood vasculature in benign and malignant tumors[111]. Since CD31 is also expressed on platelets, macrophages, neutrophils and monocytes, I exclude any single cells staining positive for CD31. I considered any CD31<sup>+</sup> cell cluster, clearly separated from adjacent microvessels, tumor tissue, or other tissue elements as a single countable microvessel[108]. I found a significant decrease in MVD in mesenchymal ER23 or HCC827/ER23 50/50 admix tumors compared to epithelial HCC827 tumors ( $p < 0.0001$ ) (Figure 12A). I then sought to isolate the effect of EDN1 expression through an EDN1 knockdown model. I

performed sub-cutaneous xenografts using epithelial HCC4006 cells grown alone or in a 50/50 admix with mesenchymal Ge-R cells with either an EDN1 knockdown or a non-target knockdown (Figure 12B). Tumors produced from HCC4006 cells grown in admix with EDN1 secreting HCC4006Ge-R shNT cells (Figure 10C) show a significant decrease in MVD compared to HCC4006 ( $p < 0.001$ ). This effect was abrogated by lentiviral shRNA knockdown of EDN1 (Figure 12B). It is important to note that most areas of high vessel density were identified around the edges of the tumor section. This is most likely due to the short growth time of these tumors relative to their analog within a patient. Blood vasculature growth typically begins at the margins of a tumor and proceeds inward[124]. If a longer growth time was permissible, I would expect areas of high blood vessel density to be present within the tumor body as well as margins.

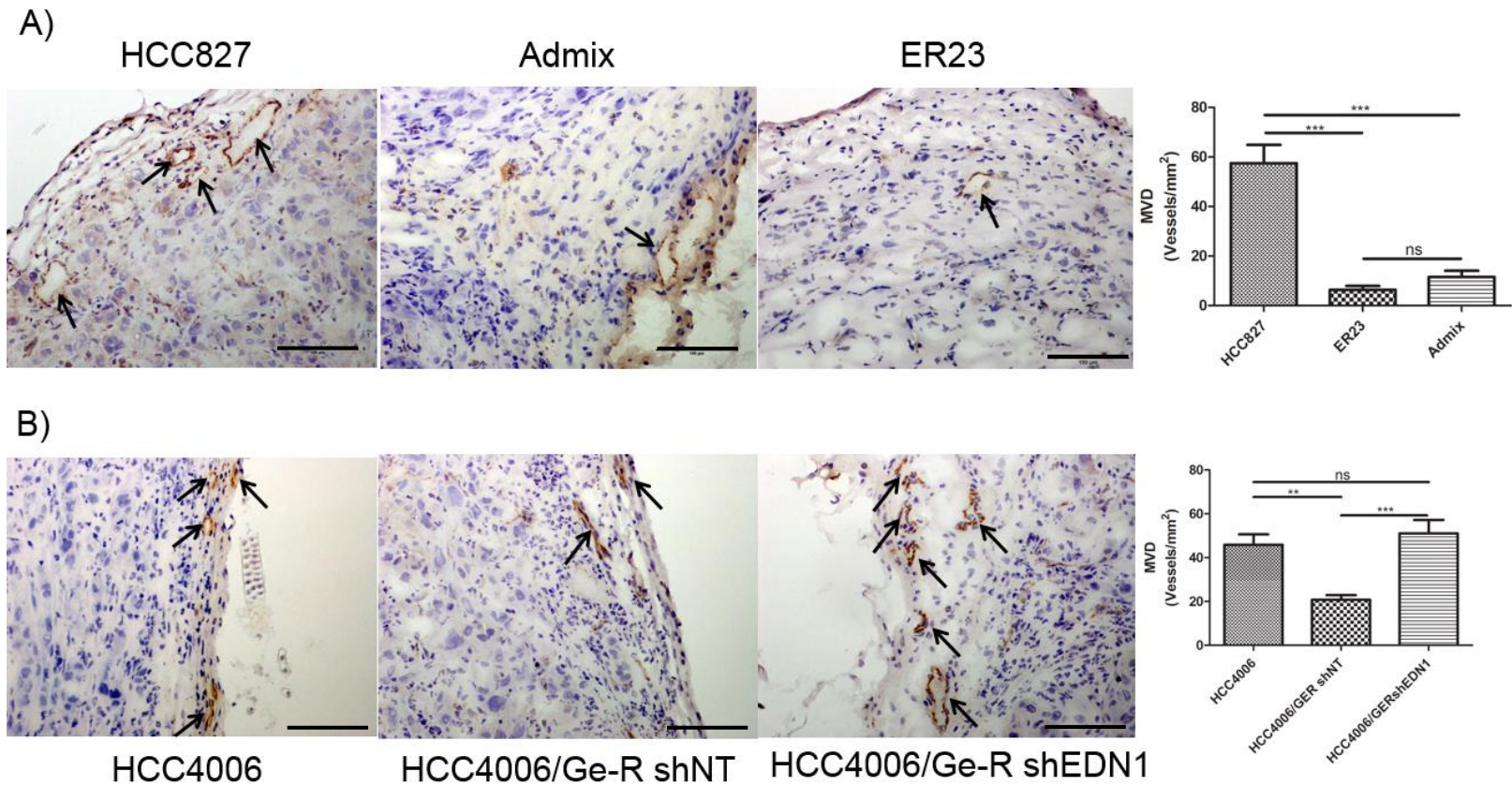


**Figure 12. Epithelial/Mesenchymal Admix Conditions Results in Significantly Lower Blood Vessel Density Which Can be Abrogated Through Knockdown of EDN1 in Mesenchymal Cells. Significance was Determined by One-Way ANOVA With a *Post Hoc* Student's T-Test. Scale Bars Represent 100 $\mu$ m. Error Bars Represent Standard Error Between Means.**

A) Representative images from tumors produced from epithelial HCC827, and mesenchymal ER23 cells grown alone or in a 50/50. Images taken at 20x magnification. MVD was calculated by the "hot spot" method as previously described. B) Representative images from tumors produced from epithelial HCC4006, and HCC4006 cells grown in admix with mesenchymal Ge-R cells with a non-target or EDN1 shRNA knockdown. Images taken at 20x magnification. MVD was calculated by the "hot spot" method as previously described.

### **Phosphorylated EGFR is Maintained in Gefitinib Treated Mesenchymal and Admix Tumors**

Phosphorylated EGFR has been accepted as a reliable pharmacodynamics marker for EGFR TKIs. Consequently, I could assess the bioavailability of EGFR TKIs in the tumor by measuring the level of pEGFR[114]. I found that epithelial/mesenchymal admix xenograft tumors are significantly more resistant to EGFR TKIs than epithelial xenograft tumors (Figure 11B). I first wanted to assess if EGFR TKIs were effectively delivered to admix xenografts by measuring p-EGFR by IHC staining. To produce representative images, 2 tumors from untreated conditions and 4 tumors from treated conditions were examined. I performed IHC staining for phosphorylated EGFR on tumor sections prepared from epithelial HCC827, mesenchymal ER23 or admix tumors. I found that phosphorylated EGFR was effectively reduced by gefitinib treatment in epithelial HCC827 tumors while phosphorylated EGFR was maintained in mesenchymal ER23 and admix tumors (Figure 13). I also examined total EGFR expression by IHC staining in the same set of samples. I found that total EGFR expression was comparable across all untreated conditions. Among gefitinib treated tumors, epithelial HCC827 tumors show a disruption of solid structure and a down-regulation of EGFR while mesenchymal ER23 tumors and admix tumors display a maintenance of total EGFR expression (Figure 14). The disruption of a densely packed tumor cell structure and the adoption of a spongiform morphology has been associated with sensitivity to EGFR TKI treatment in a NSCLC model[122].



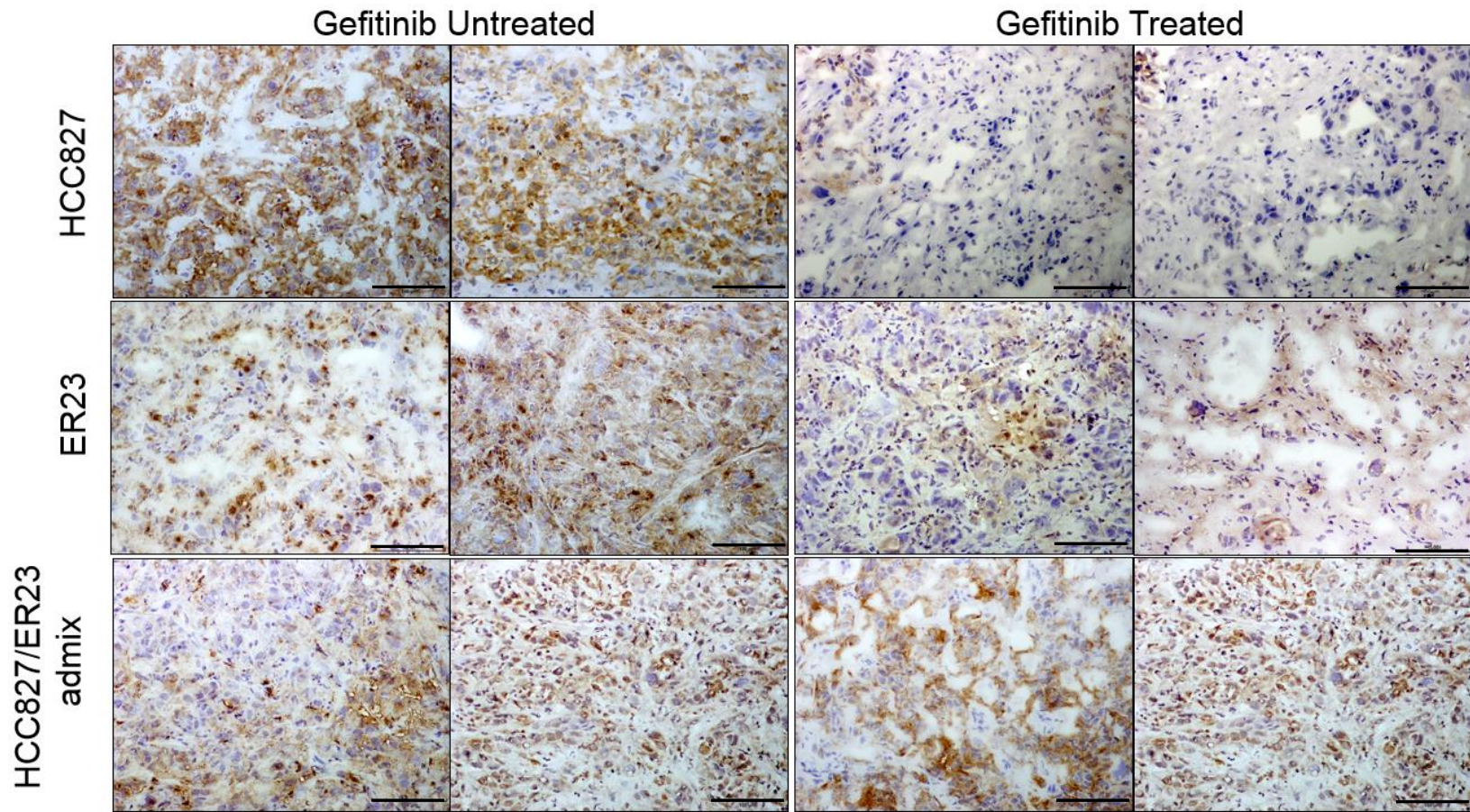


**Figure 13. Phosphorylated EGFR is Maintained in Gefitinib Treated Mesenchymal and Admix Conditions.** Representative images from murine sub-cutaneous xenografts established by epithelial HCC827 cells, mesenchymal ER23 cells or a 50/50 admix stained for phosphorylated EGFR. All micrographs are taken at 20x magnification. Scale bars represent 100 $\mu$ m.



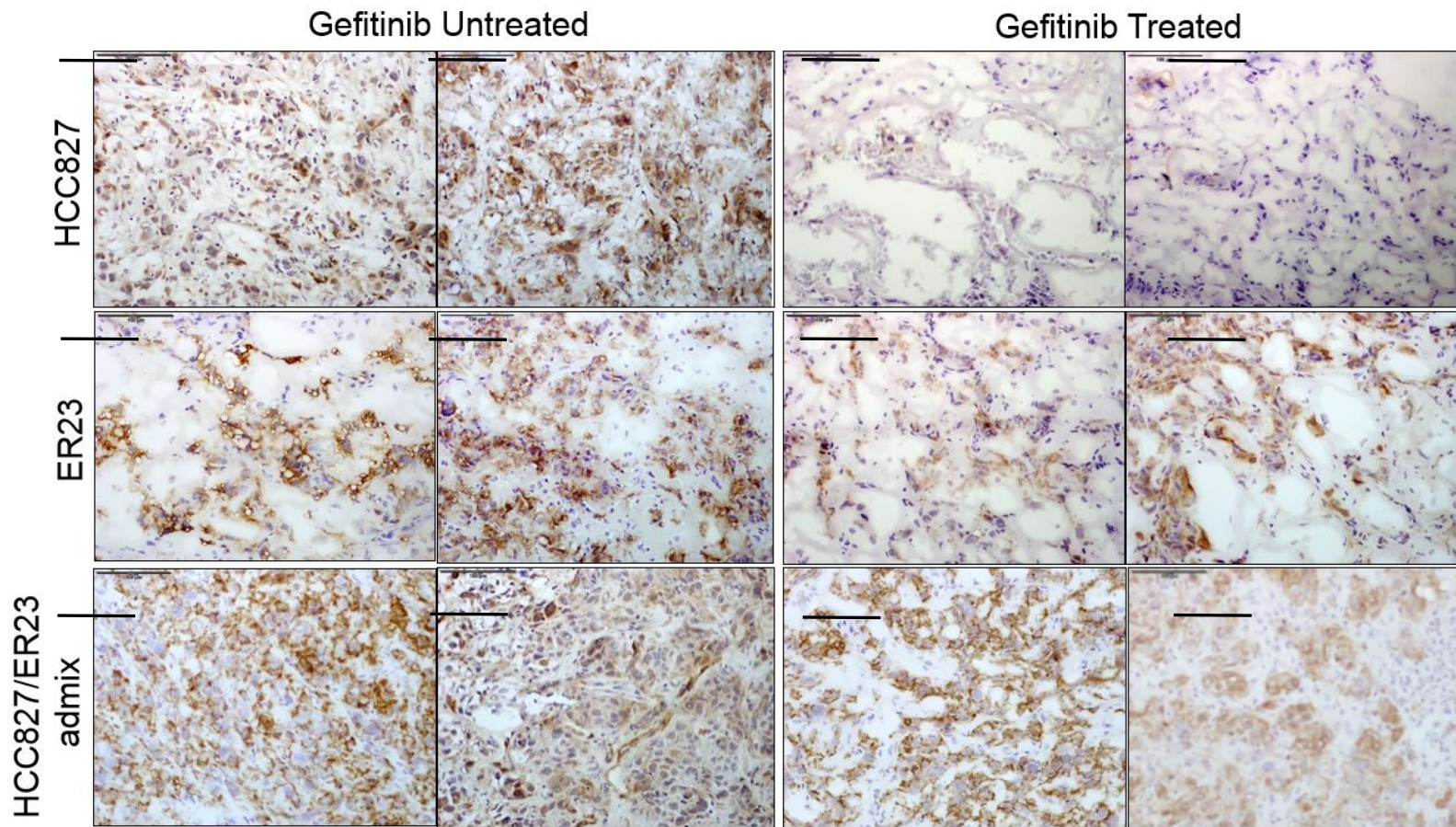


**Figure 14: Total EGFR is Comparable in Untreated Conditions While Total EGFR is Maintained in Gefitinib Treated Mesenchymal ER23 and Admix Tumors.** Representative images from murine sub-cutaneous xenografts established by epithelial HCC827 cells, mesenchymal ER23 cells or a 50/50 admix stained for total EGFR. All micrographs are taken at 20x magnification. Scale bars represent 500µm and 100µm respectively

## CHAPTER FOUR

### DISCUSSION

Activating EGFR mutations in NSCLC patients allow for the use of therapies targeting EGFR signaling. While EGFR TKI therapy is initially efficacious in most EGFR mutation positive NSCLC patients, the disease eventually progresses after the emergence of acquired resistance and limits the efficacy of this therapy[25]. In an attempt to circumvent the limitations of EGFR TKI therapy, several clinical trials were performed attempting to limit the effect of tumor neo-angiogenesis in NSCLC. These trials focused on the inhibition of VEGFR2 signaling to prevent neo-angiogenesis, a prerequisite for the tumor colonization upon metastasis. Unfortunately, the treatment combining VEGFR2 inhibitors with standard chemotherapy or EGFR TKIs show little to no survival advantage over therapeutic regimens which do not include VEGFR2 inhibition[93, 103-105]. This result is surprising due to the documented importance of tumor neo-angiogenesis in tumor growth and disease progression as well as the documented VEGFR2 expression in NSCLC tumors. Since patients showing resistance to EGFR TKI therapy also commonly present a heterogeneous tumor, I sought to explore whether tumor heterogeneity could explain why VEGFR2-based therapies failed in the clinic. In order to study this question, we must understand the dynamics of how tumor heterogeneity emerges in the patient.

It has been proposed that most spontaneous tumors originate from a single

cell[115]. While there has since been evidence to support this model[116], limitations in tumor biopsy sampling protocols do not allow for the exclusion of a multicellular origin in some human tumor types. Regardless of mechanism of origin, it is generally accepted that tumor heterogeneity increases over time and in response to drug treatment in human patients. Indeed, at time of diagnosis, the majority of tumors display heterogeneity in regards to several morphological and physiological characteristics. These differential characteristics often manifest in cell surface receptor expression, proliferative capacity and angiogenic potential.

The induction of an EMT phenotype has been studied in at least two major ways. The first involves exposing epithelial cells to increasing concentrations of EGFR TKIs over a period of time[55]. The second involves the depletion of epithelial markers such as E-Cadherin by lentiviral shRNA transduction[117]. The advantage of studying EGFR TKI resistance by EMT in cells chronically exposed to increasing doses of EGFR TKIs is that it represents the direct *in vitro* analog of the EMT phenotype which emerges in patients undergoing EGFR TKI therapy. However, off- target effects of drug treatment may result in changes in expression independent of the EMT process. Induction of EMT by lentiviral shRNA knockdown of E-Cadherin eliminates the possibility of EMT- independent changes in expression, however the mechanism of induction is artificial and not seen in patients. It is therefore imperative to study EMT mediated EGFR TKI resistance by using a multitude of cell lines created through both processes. In order to study EMT-mediated EGFR TKI resistance in NSCLC cells, I utilized cells with a mesenchymal phenotype produced from chronic exposure to EGFR TKI treatment or through lentiviral knockdown of the epithelial marker E-Cadherin. I validated the use of lentiviral knockdown and chronic drug treatment

for the generation of NSCLC cell lines displaying a mesenchymal phenotype. The mesenchymal properties of these cell lines form the basis of our study on EMT-mediated tumor heterogeneity.

I initially set out to determine how epithelial and mesenchymal lung cancer cells interact *in vivo*. To this end, I performed a sub-cutaneous xenograft in a murine model with epithelial HCC827, mesenchymal ER23 cells, or a 50/50 admix. I found that admix conditions produce tumors with greater volume compared to either epithelial or mesenchymal cells alone. In order to determine if this effect was due to signaling between epithelial and mesenchymal cells, I performed an *in vitro* growth assay using epithelial cells, mesenchymal cells or multiple admix conditions and measured cell count over a 6 day period. I found that while admix conditions produced a growth advantage *in vivo* (Figure 2A), this effect was not present *in vitro* (Figure 2B,C). If an interaction between epithelial cells and mesenchymal cells could explain the growth advantage seen under admix conditions *in vivo* I would expect this result to be replicated *in vitro*. Since I did not see this, it suggests that the growth advantage seen *in vivo* may be due to tumor-host microenvironment interaction.

One major way in which tumors are known to interact with the host is through the blood vasculature. During excision of our xenograft tumors, it was observed that admix tumors seemed to have greater blood vasculature compared to epithelial or mesenchymal. I hypothesized that the interaction between admix tumors and the host vasculature may explain why admix conditions confer a growth advantage *in vivo* but not *in vitro*. To determine if EMT affected the expression of angiogenesis-related growth factors, I performed a Luminex multiplex assay for 10 factors known to influence blood vasculature.

By performing this assay on supernatants from epithelial, mesenchymal or admix cell culture, I can measure the amount of each secreted factor. I focused on the effect of EMT on the secretion of VEGF-A and EDN1 since these showed differential secretion in all cell lines tested when comparing epithelial to mesenchymal cells. I found that during the EMT process, the secretion of VEGF-A was significantly reduced while the secretion of EDN1 was significantly up-regulated (Figure 5A-D). Interestingly, in 50/50 HCC4006/HCC4006Ge-R admix conditions I found that VEGF-A secretion was comparable to that of epithelial HCC4006 alone. While I expected to see an approximately 50% reduction in EDN1 secretion due to half of the number of mesenchymal HCC4006Ge-R cells seeded in the 50/50 admix compared to HCC4006Ge-R pure culture, I found a significantly lower EDN1 concentration in the 50/50 admix. It is possible that in HCC4006 cell lines, EDN1 secreted by mesenchymal cells is taken up by epithelial cells leading to increased VEGF-A secretion. This result was not replicated in a comparison between epithelial HCC827 and mesenchymal ER23 cell lines. In these cell lines, a 50/50 admix produced VEGF-A concentrations similar to epithelial cells alone and EDN1 concentrations approximately 50% of that of mesenchymal cells alone. Based on this result we used HCC827 and ER23 cell lines for our admix *in vivo* studies.

It was unclear whether this change in secretion was an early or late event in the EMT process, therefore I measured factors secreted by epithelial HCC4006 cells treated with short-term (72 hours) 100nM gefitinib treatment. I found that 72 hours of gefitinib treatment was sufficient to produce the switch from primarily VEGF-A secretion to primarily EDN1 secretion (Figure 5E). I therefore conclude that the switch from VEGF-A secretion to EDN1 secretion represents either an early effect of the EMT process or a direct

consequence of EGFR inhibition. These events may be linked considering short-term EGFR inhibition has been shown to induce TGF- $\beta$  expression which can result in EMT[55]. I believe that EGFR TKI treatment primes the cell for the switch from VEGF-A secretion to EDN1 secretion during the EMT process. This change in expression may result in greater tumor neo-angiogenesis providing a possible explanation of why admix tumors show a growth advantage *in vivo*.

Using *in vitro* tube formation assay, I determined the effect of VEGF-A and EDN1 on endothelial cell differentiation. By depositing endothelial HUVEC cells onto a reduced-growth factor Matrigel coated plate, I exposed endothelial cells to conditioned media produced from epithelial, mesenchymal or admix cell cultures. By measuring the formation of tube structures I can measure the ability of conditioned media to induce differentiation in endothelial cells. I found that conditioned media produced from admix culture conditions induced greater tube structure compared to epithelial or mesenchymal cells alone (Figure 6A). By utilizing the ImageJ angiogenesis analyzer plugin[107], I objectively quantified several parameters useful for assessing the differentiation of endothelial cells. I focus on total tubule length, node count, and mesh area. The total tubule length measurement is an indicator of overall differentiation level. The node count parameter is analogous to the sprouting step of *in vivo* angiogenesis in which endothelial cells differentiate to establish an outgrowth from an established blood vessel. Mesh area is analogous to the ability for newly established blood vessels to join with already established blood vessel structures *in vivo* and therefore represents the highest-order organization of blood vasculature structure. I found that conditioned media from admix culture conditions showed a significant increase in total tubule length, node count, and mesh area. I therefore conclude that admix conditions

induces greater endothelial cell differentiation compared to epithelial or mesenchymal pure culture conditions *in vitro* (Figure 6B).

To test if the presence of both VEGF-A and EDN1 could explain the increased endothelial cell differentiation seen in our conditioned media experiment *in vitro*, I performed the tube formation assay using exogenous recombinant VEGF-A and EDN1 (Figure 7A). I found that the addition of both of these factors was sufficient to produce a trend toward a greater tube formation morphology compared to either factor alone or basal media conditions. Our ImageJ quantification of this experiment lacks mesh area due to the overall lower tube formation compared to the conditioned media experiment. The addition of both factors did not produce a significant increase in total tube length and node count although a clear trend is present (Figure 7B). I rationalize this by acknowledging the diverse population of unknown growth factors that may be present in conditioned media. While VEGF- A and EDN1 secretion is an important component to this population, it likely does not represent the only EMT-mediated change in growth factor secretion important in blood vasculature regulation. Indeed I observed an up-regulation of several other angiogenesis-related growth factors in our cell lines such as FGF-2 or angiopoietin-2 upon the EMT process (Figure 4). While these factors were only shown be up-regulated in HCC4006 and HCC827 cell lines respectively, it is possible these factors individually contribute to endothelial cell differentiation. Additionally, I recognize that our conditioned media preparation is somewhat of a black box in which unmeasured factors may be contributing to VEGF-A/EDN1-mediated endothelial cell differentiation.

I then sought to test whether the VEGF-A/EDN1 signaling systems were targetable by drugs known in the field to inhibit the involved receptors for these factors. To this end, I

utilized the VEGFR2 inhibitor sunitinib and the EDNRA specific inhibitor Zibotentan. Sunitinib is a potent multi-target inhibitor sold under the trade name Sutent by Pfizer Inc. It was first approved for use in renal cell carcinoma and imatinib-resistant gastrointestinal stromal tumors on January 26, 2006. Sunitinib is able to inhibit all receptors for platelet-derived growth factor and all VEGF species receptors. Sunitinib has also been shown to inhibit the receptor tyrosine kinase CD117 (c-KIT)[105]. Zibotentan is an EDNRA specific inhibitor developed by AstraZeneca for use in the treatment of prostate cancer. The drug failed a phase III clinical trial for prostate cancer and has since been discontinued after failing to show any survival benefit to patients[118]. I chose to use Zibotentan due to its EDNRA-specific activity and the efficacy of the drug for inhibiting EDNRA signaling *in vitro*. Because a sufficiently high concentration of either of these drugs can effectively inhibit tube formation by conditioned media, I must establish low-dose concentrations of each drug in order to examine the benefit of dual therapy. I found that 10nM sunitinib and 100nM Zibotentan failed to significantly inhibit tube formation induced by admix cell culture conditioned media when used alone. In contrast, the combination treatment at these concentrations significantly abrogated tube formation as measured by ImageJ quantification of node count, total tubule length and mesh area (Figure 8). These results suggest that the dual treatment of sunitinib/Zibotentan sufficient to abrogate the additive effect these growth factors have on endothelial cell differentiation. In order to test if our low dose 10nM sunitinib treatment was effectively able to abrogate VEGF-A mediated signaling, I examined the effect of stimulation by conditioned media produced from admix culture conditions on HUVEC cells. I exposed HUVEC cells to admix conditioned media for 8 hours and complete EGM media either alone or with 10nM sunitinib. I found that



admixed conditioned media effectively up-regulated phosphorylated VEGFR2 as expected. Furthermore, the addition of 10nM sunitinib was sufficient to down-regulate phosphorylated VEGFR in admixed conditioned media or EGM conditions. These results suggest 10nM sunitinib is an effective concentration for the inhibition of VEGFR2 in HUVEC cells (Figure 9). This result supports our dual VEGFR2/EDNRA inhibition tube formation assay. Since I am able to effectively reduce phosphorylated VEGFR2 by 10nM sunitinib treatment, tube formation seen under single target sunitinib treatment must be due to other growth factors present in admixed conditioned media; possibly EDN1. This result highlights the importance of multiple signaling pathways in the induction of a tube formation morphology *in vitro*. I also examined EDNRA expression and found that EDNRA is down-regulated after 8 hours in basal EBM media unstimulated conditions. EDNRA expression was seen to be comparable among stimulated conditions with or without sunitinib treatment. Since EDNRA activation opens the L-type  $\text{Ca}^{2+}$  channel resulting in the influx of  $\text{Ca}^{2+}$  to the cytosol, the quantification of intracellular  $\text{Ca}^{2+}$  concentration using flow cytometry is commonly accepted as an assay to assess EDNRA activation by the EDN1 stimulation[119]. In order to exclude other  $\text{Ca}^{2+}$  channel activators present in conditioned media, I will need to perform the assay to evaluate if recombinant EDN1 would activate EDNRA in vascular endothelial cells and if the activation can be abrogated by 100nM Zibotentan treatment.

In order to study the specific effects of EDN1 in the tumor microenvironment *in vivo*, I produced epithelial HCC827 cell lines ectopically expressing EDN1 or Flag/V5 control. I confirmed VEGF-A secretion was maintained by Luminex analysis (Figure 10A). To our surprise, tumors grown from HCC827 EDN1 over-expressing cells showed a

significant growth retardation compared to HCC827 Flag/V5 cells (Figure 10B). This result forced us to reconsider the effect of EDN1 in the tumor microenvironment. I have shown that EDN1 secretion is up-regulated in cells with a mesenchymal phenotype, and it is well known that tumors harboring a mesenchymal sub-population are significantly more resistant to EGFR TKI treatment[57]. I therefore hypothesized that EDN1 secretion in the tumor microenvironment may be contributing to drug resistance. While EDN1 secretion has been linked to increased MVD in several tumor types including ovarian carcinoma[69] and chondrosarcoma[84], the opposite has been found in castration-resistant prostate cancer[85] and some melanomas[86]. The decreased tumor growth in these cancers were attributed to the vasoconstrictive properties of EDN1 preventing sufficient blood flow to the tumor. If this is also true in a NSCLC model, it would explain why EDN1 over-expressing tumors show significant growth retardation. Upon drug treatment, the decreased MVD would become beneficial to the tumor by limiting drug perfusion within the tumor. I hypothesized that the vasoconstrictive property of EDN1 was contributing to EGFR TKI resistance in our NSCLC model.

Therefore, I returned to our epithelial HCC827, mesenchymal ER23 and admix condition xenograft model. Upon 6-day gefitinib treatment, I observed significantly greater residual tumor volume in admix and mesenchymal tumors compared to epithelial (Figure 11B). I hypothesize that EDN1 is limiting blood supply to the tumor therefore limiting the growth of the epithelial component of admix tumors. Since epithelial cells are the main contributor to VEGF-A secretion, EDN1 could exert an anti-angiogenic effect on admix tumors. Additionally, upon EGFR TKI treatment, epithelial cells switch from VEGF-A secretion to EDN1 secretion (Figure 5E). I believe this also occurs within admix tumors but

the presence of constitutively EDN1 secreting mesenchymal cells may prime the tumor to competently constrict the relevant vasculature to prevent drug perfusion.

To test if EGFR TKI resistance was due to EDN1 secretion, I subjected our HCC827 EDN1 over-expression xenografts to a 6-day gefitinib treatment and measured residual tumor volume by caliper measurement. HCC827 EDN1 expressing tumors were allowed to reach the same volume as Flag/V5 control prior to treatment. I found that HCC827 EDN1 over-expressing tumors showed significantly greater residual tumor volume compared to HCC827 Flag/V5 following gefitinib treatment (Figure 11D). As expected, EDN1 over-expressing cells showed no significant increase in gefitinib resistance *in vitro* (Figure 11C). This further implicated the host vasculature in EDN1-mediated EGFR TKI resistance. If EDN1 was acting to decrease MVD in our NSCLC model, I would expect a lower MVD in admix tumors. Indeed I observed that MVD was significantly reduced in admix and mesenchymal tumors compared to epithelial (Figure 12A). In order to determine if this effect was due to EDN1 secretion, I established mesenchymal HCC4006Ge-R cell lines expressing a shRNA knockdown of *EDN1* or non-target control. A murine xenograft was performed and CD31 staining was conducted on the resulting tumors. I found that EDN1-competent HCC4006Ge-R shNT cells grown in admix with epithelial HCC4006 cells show significantly lower blood vessel density compared to HCC4006 alone. This effect can be abrogated through the knockdown of EDN1 in mesenchymal HCC4006Ge-R cells grown in admix with HCC4006 cells (Figure 12B). This result further supports the hypothesis that EDN1 secretion within the tumor microenvironment is contributing to MVD depression. If this were true, I would expect gefitinib penetrance to be decreased in tumors with an EDN1-secreting component.

To indirectly assess the penetrance of EGFR TKIs in epithelial, mesenchymal and admix tumors, I measured total EGFR expression as well as the phosphorylation of EGFR in these tumors by IHC staining. I found that EGFR is expressed at comparable levels in untreated epithelial, mesenchymal or admix tumors. Epithelial tumors treated with gefitinib showed wide-scale destruction of tumor structure as well as a down regulation of EGFR expression. Conversely, mesenchymal and admix tumors showed a maintenance of EGFR expression upon gefitinib treatment (Figure 14). The phosphorylation of EGFR serves as a pharmacodynamics marker of EGFR activity and the effectiveness of inhibition by EGFR TKIs[114]. Therefore, I performed IHC staining for phosphorylated EGFR in untreated and treated epithelial, mesenchymal or admix tumors to indirectly assess the penetrance of EGFR TKIs in the tumors. I observed that gefitinib treatment abrogated the phosphorylated EGFR signal in epithelial tumors suggesting the availability of gefitinib was sufficient to inhibit EGFR activity. Interestingly, both mesenchymal and admix tumors maintained phosphorylated EGFR following gefitinib treatment (Figure 13). Since both mesenchymal and epithelial cells harbor mutated EGFR that is constitutively active and exquisitely sensitive to EGFR TKIs, an insufficient amount of EGFR inhibitor may be available in these tumors to fully suppress the EGFR phosphorylation. Surprisingly, I found that admix tumors are epithelial phenotype dominated (Figure 3). Since tumors grown from epithelial cells alone show exquisite sensitivity to EGFR TKIs, I conclude that the drug is not thoroughly penetrating these tumors. In order to test if poor EGFR TKI penetrance in the tumors is caused by the presence of EDN1, tumor samples need to be tested for intratumoral gefitinib concentration using mass spectrometry. To this end I have sent tumor chip samples to our collaborators for mass spectrometry analysis. I expect to find a

significantly decreased concentration of gefitinib in mesenchymal and admix conditions compared to epithelial as well as decreased gefitinib concentrations in EDN1 over-expressing tumors compared to Flag/V5 controls. I exclude the possibility of gefitinib-mediated EMT in drug treated tumors due to the short time period in which the drug treatment took place. In the clinic, EMT normally arises from EGFR TKI treatment over a period of ~6 months. Since our drug treatment period was limited to 6 days, this excludes the possibility that drug resistance could be explainable by gefitinib-mediated EMT.

I believe the growth advantage of admix conditions to not be explainable by the presence of EDN1 secreting cells within admix conditions. Indeed, tumors grown from HCC827 EDN1 over-expressing cells showed a significant growth retardation compared to HCC827 Flag/V5 cells (Figure 10B). I believe I did not capture the growth advantage of admix conditions *in vitro* because of the normoxic conditions used. Factors secreted by mesenchymal cells may show differential effects in the relatively hypoxic conditions present *in vivo*. Marek et al. described an autocrine feedback loop between epithelial and mesenchymal NSCLC cell lines involving the FGF-2 signaling pathway[120]. I also observed an up-regulation of FGF-2 in our mesenchymal HCC4006Ge-R cells compared to epithelial HCC4006 cells (Figure 4). Additionally, FGF-2 expression is well known to be up-regulated under hypoxic conditions[121]. I speculate that under hypoxic conditions, I may have observed a growth advantage *in vitro* in admix conditions compared to epithelial or mesenchymal pure cultures.

The *in vitro* tube formation assay inherently excludes the effect of vasoconstriction due to the lack of the smooth muscle that normally sheaths mature blood vessels *in vivo*. Therefore, the assay isolates the pro-differentiation capabilities of VEGF-A and EDN1 on

endothelial cells. In light of this realization, it makes sense that our *in vitro* results did not support our *in vivo* results. If only considering our *in vitro* results, I would propose that EDNRA inhibition may be an important addition to VEGFR2 inhibition-based treatment regimens due to the pro-angiogenic nature of EDN1 contributing to increased MVD in the tumor. Given that VEGFR2 inhibition in NSCLC clinical trials has been largely ineffective, I would pose that the switch between VEGF-A secretion to EDN1 secretion during EMT or EGFR TKI treatment (Figure 5A-E) represents an escape mechanism to VEGFR2 inhibition. In light of our *in vivo* results, I recommend EDNRA inhibition as an effective addition to a blood vascular-based approach to NSCLC treatment not to inhibit angiogenesis but to increase MVD leading to increased EGFR TKI tumor penetrance (Figure 12,14).

It has been previously shown that EDN1 can have differential effects on the blood vasculature depending on the tissue in which the tumor arose[69, 84-86]. It has been posed by previous researchers that EDN1 concentrations typically secreted by tumor cells may not be sufficient alone to overcome the vasoconstrictive effect of EDN1 and cause a pro-angiogenic effect. Therefore, the contribution of surrounding normal tissue to increasing EDN1 concentration cannot be ignored. It may be that in tissues which normally secrete high levels of EDN1, tumor cells secreting EDN1 have a pro-angiogenic effect whereas in tissues which are normally EDN1 poor, secretion of EDN1 has an anti-angiogenic effect. Therefore, a limitation of this study is that it is limited to sub-cutaneous xenograft models. The blood vasculature in the subcutaneous space is limited compared to that of the lung. Additionally the expression of EDN1 in the lung is known to be higher than that of the sub-cutaneous space. In order to properly study the effect of EDN1 on the tumor vasculature in

the native environment of the lung, I propose performing an intrapulmonary injection of epithelial, mesenchymal and admix tumor cell lines. I hypothesize that in a tissue of high native EDN1 expression, the effect of EDN1 may be pro- angiogenic.

I conclude by hypothesizing a model incorporating the vasoconstrictive properties of EDN1 into our observed MVD depression in EDN1-secreting tumors. I believe that in a purely epithelial tumor, the secretion of VEGF-A competently induces tumor neo-angiogenesis leading to tumor growth while maintaining vasodilation in the blood vasculature. Upon gefitinib treatment, the dilated properties of the tumor blood vasculature allow for the drug to fully penetrate the tumor allowing for maximal efficacy and significant tumor reduction. Although I have shown that short-term gefitinib treatment is sufficient to induce EDN1 secretion in epithelial cells, I hypothesize that this event does not occur fast enough to prevent significant tumor reduction. In a tumor completely composed of mesenchymal cells, the lack of VEGF-A secretion prevents tumor neo-angiogenesis while the secretion of EDN1 causes existing blood vasculature to become constricted. Together, this leads to a relatively small tumor unable to grow above a certain threshold. Upon gefitinib treatment, the limited and vasoconstricted blood vasculature results in poor drug penetrance leading to the observed drug resistance. In 50/50 admix conditions, the presence of EDN1 in the tumor microenvironment leads to vasoconstriction above basal levels while the presence of VEGF-A allows for enough tumor neo-angiogenesis to result in overall tumor growth. Upon gefitinib treatment, the presence of EDN1-secreting mesenchymal cells cause the protection of the epithelial cell component allowing the epithelial cells enough time to switch from VEGF-A secretion to EDN1 secretion. This high level of EDN1 secretion is then sufficient to induce additional vasoconstriction in the tumor blood vasculature further

preventing drug penetrance and leading to the observed drug resistance.

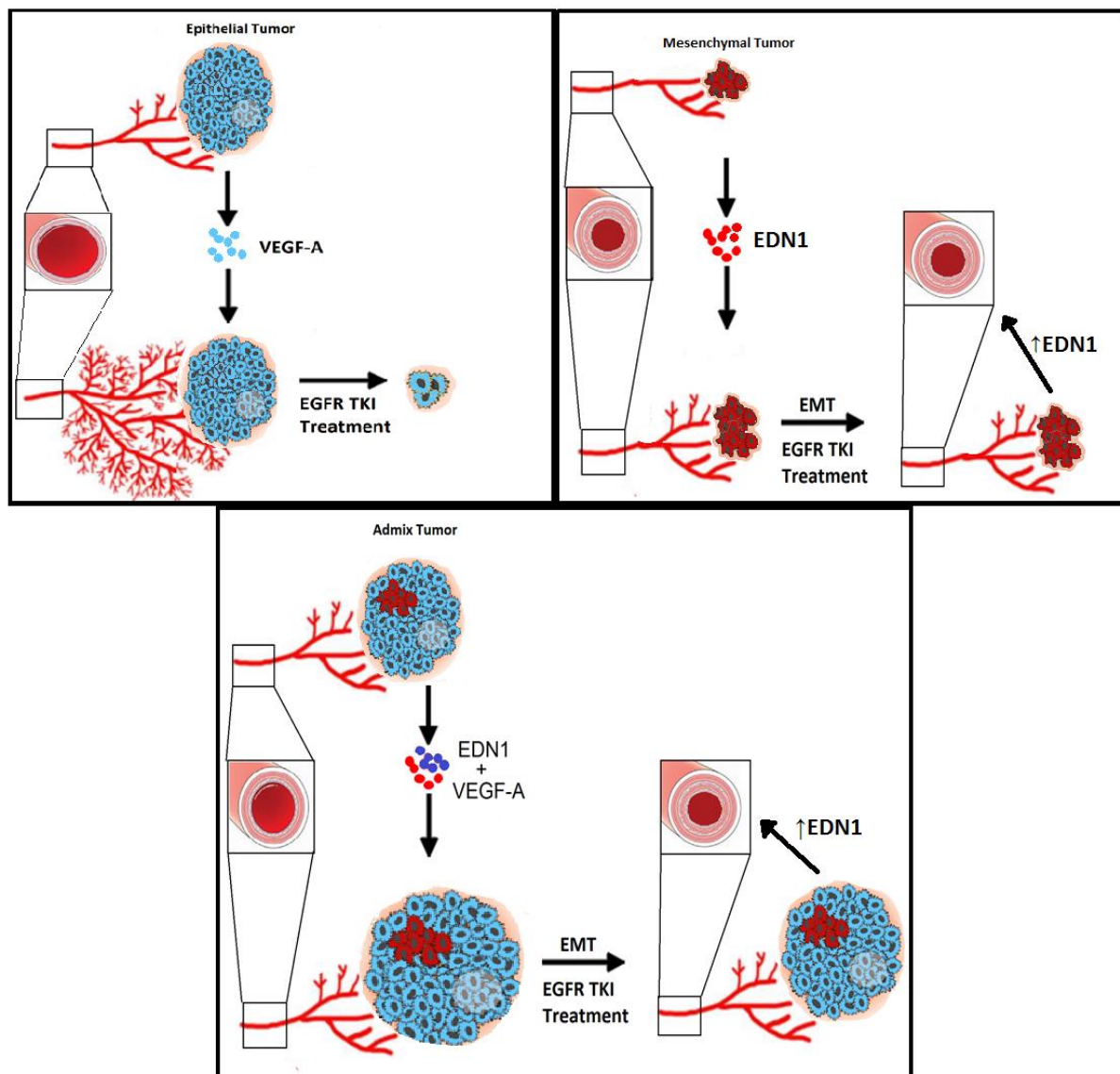


**Figure 15. Model Illustrating Hypothesis Relating EDN1-Mediated Vasoconstriction to Drug Resistance and Reduced MVD**

In summary, angiogenesis in NSCLC has been identified as important therapeutic target in combination with EGFR TKIs. However, only small incremental advancements have been made for the use of angiogenesis inhibitors in NSCLC and it remains elusive why the



inhibition of VEGF-mediated neovascularization is not therapeutically efficacious. I present experimental evidence that a subpopulation of NSCLC cells with EGFR TKI-induced EMT contributes toward the attenuation of the response to EGFR TKI therapy. One of the hallmarks of cancer is heterogeneity and I have previously demonstrated that tumor heterogeneity within NSCLC cells lines harboring EGFR kinase domain mutations gives rise to divergent resistance mechanisms in response to treatment. *In vivo* admix models are instructive in studying intratumoral heterogeneity and in elucidating therapeutic responses and tumor-host interactions. While NSCLC cells with acquired EGFR TKI resistance and EMT phenotype did not exhibit growth advantage *in vitro*, a 50% epithelial EGFR TKI sensitive and 50% mesenchymal EGFR TKI resistant admix provided significant growth advantage *in vivo* assessed by caliper measurement. This preliminary result led us to hypothesize that changes in angiogenic growth factor expression during the EMT process might lead to the *in vivo* growth advantage I observed. To test the hypothesis, I utilized the Luminex multiplex assay system to quantify secreted growth factors, cytokines, and chemokines important in angiogenesis. I have discovered that epithelial EGFR TKI sensitive cells secrete a significant amount of VEGF-A and cells with acquired/transient EGFR TKI resistance with an EMT phenotype secrete substantial amount of EDN1. Using an *in vitro* tube formation assay, I showed that secreted VEGF-A and EDN1 in admix conditions work synergistically to promote endothelial cell differentiation. Furthermore, this synergistic effect can be attenuated by VEGFR2/EDNRA dual inhibition. Surprisingly, ectopic overexpression of EDN1 in EGFR- mutated HCC827 cells resulted in significant growth retardation *in vivo*. Informed by a literature search, I hypothesized that the presence of EDN1 in the tumor microenvironment contributes positively to EGFR TKI resistance, possibly through the

vasoconstrictive property of EDN1. I observed that epithelial/mesenchymal admix tumors and ectopic overexpression of EDN1 in EGFR-mutated HCC827 cells conferred significantly more resistance to gefitinib *in vivo*. This result led us to hypothesize that the vasoconstrictive properties of EDN1 may reduce MVD in EGFR-mutated NSCLC tumors leading to poor EGFR TKI penetrance *in vivo*. I tested this through CD31 IHC staining and MVD calculation. I tested poor EGFR TKI penetrance indirectly by examining phosphorylated EGFR and found maintenance of the signal in admix and mesenchymal tumors. Taken together, I suggest that inhibition of the EDN1 signaling system may be an important component to a blood vascular-based approach to treatment of EGFR-mutation positive NSCLC when given as an adjuvant therapy to EGFR TKI treatment.

## REFERENCE LIST

1. Siegel, R.L., K.D. Miller, and A. Jemal, *Cancer Statistics, 2017*. CA Cancer J Clin, 2017. **67**(1): p. 7-30.
2. Meza, R., Meernik, C., Jeon, J., and Cote, M., *Lung cancer incidence trends by gender, race and histology in the United States, 1973-2010*. PLoS One, 2015. **10**(3): p. e0121323.
3. Pietrangelo, A., *Non-Small Cell Lung Cancer vs. Small Cell: Types, Stages, Symptoms, and Treatment*. Healthline Media, 2015.
4. Chheang, S. and K. Brown, *Lung cancer staging: clinical and radiologic perspectives*. Semin Intervent Radiol, 2013. **30**(2): p. 99-113.
5. Alberg, A.J., M.V. Brock, and J.M. Samet, *Epidemiology of lung cancer: looking to the future*. J Clin Oncol, 2005. **23**(14): p. 3175-85.
6. Katzel, J.A., M.P. Fanucchi, and Z. Li, *Recent advances of novel targeted therapy in non-small cell lung cancer*. J Hematol Oncol, 2009. **2**: p. 2.
7. Zwick, E., J. Bange, and A. Ullrich, *Receptor tyrosine kinase signalling as a target for cancer intervention strategies*. Endocr Relat Cancer, 2001. **8**(3): p. 161-73.
8. Hubbard, S.R. and J.H. Till, *Protein tyrosine kinase structure and function*. Annu Rev Biochem, 2000. **69**: p. 373-98.
9. Fujino, S., Enokibori, T., Tezuka, N., Asada, Y., Inoue, S., and Mori, A., *A comparison of epidermal growth factor receptor levels and other prognostic parameters in non-small cell lung cancer*. Eur J Cancer, 1996. **32A**(12): p. 2070-4.
10. Salomon, D.S., Brandt, R., Ciardiello, F. and Normanno, N., *Epidermal growth factor-related peptides and their receptors in human malignancies*. Crit Rev Oncol Hematol, 1995. **19**(3): p. 183-232.
11. Franklin, W.A., Veve, R., Hirsch, F.R., Helfrich, B.A., and Bunn, P.A. Jr., *Epidermal growth factor receptor family in lung cancer and premalignancy*. Semin Oncol, 2002. **29**(1 Suppl 4): p. 3-14.

12. Alroy, I. and Y. Yarden, *The ErbB signaling network in embryogenesis and oncogenesis: signal diversification through combinatorial ligand-receptor interactions*. FEBS Lett, 1997. **410**(1): p. 83-6.
13. Chan, T.O., S.E. Rittenhouse, and P.N. Tsichlis, *AKT/PKB and other D3 phosphoinositide- regulated kinases: kinase activation by phosphoinositide-dependent phosphorylation*. Annu Rev Biochem, 1999. **68**: p. 965-1014.
14. Petit, A.M., Rak, J., Hung, M.C., Rockwell, P., Goldstein, N., Fendly, B., Kerbel, R.S., *Neutralizing antibodies against epidermal growth factor and ErbB-2/neu receptor tyrosine kinases down-regulate vascular endothelial growth factor production by tumor cells in vitro and in vivo: angiogenic implications for signal transduction therapy of solid tumors*. Am J Pathol, 1997. **151**(6): p. 1523-30.
15. Lynch, T.J., Bell, D., Raffaella, S., Gurubhagavatula, S., Okimoto, R., Brannigan, B., Harris, P., Haserlat, S., Supko, J., Haluska, F., Louis, D., Christiani, D., *Activating mutations in the epidermal growth factor receptor underlying responsiveness of non-small-cell lung cancer to gefitinib*. N Engl J Med, 2004. **350**(21): p. 2129-39.
16. Jackman, D.M., Miller, V.A., Cioffredi, L.A., Yeap, B.Y., Janne, P.A., Riely, G.J, Ruiz, M.G., Giaccone, G., Sequist, L.V., Johnson, B.E., *Impact of epidermal growth factor receptor and KRAS mutations on clinical outcomes in previously untreated non-small cell lung cancer patients: results of an online tumor registry of clinical trials*. Clin Cancer Res, 2009. **15**(16): p. 5267-73.
17. Pillai, R.N. and S.S. Ramalingam, *The biology and clinical features of non-small cell lung cancers with EML4-ALK translocation*. Curr Oncol Rep, 2012. **14**(2): p. 105-10.
18. Sharma, S.V., Gajowniczek, P., Way, I.P., Lee, D.Y., Jiang, J., Yuza, Y., Classon, M., Haber, D.A., Settleman, J., *A common signaling cascade may underlie addiction to the Src, BCR-ABL, and EGF receptor oncogenes*. Cancer Cell, 2006. **10**(5): p. 425-35.
19. Ladanyi, M. and W. Pao, *Lung adenocarcinoma: guiding EGFR-targeted therapy and beyond*. Mod Pathol, 2008. **21 Suppl 2**: p. S16-22.
20. Yun, C.H., Boggon, T.J., Li, Y., Woo, M.S., Greulich, H., Meyerson, M., Eck, M.J., *Structures of lung cancer-derived EGFR mutants and inhibitor complexes: mechanism of activation and insights into differential inhibitor sensitivity*. Cancer Cell, 2007. **11**(3): p. 217-27.

21. Kumar, A., Petri, E.T., Halmos, B., Boggon, T.J., *Structure and clinical relevance of the epidermal growth factor receptor in human cancer*. J Clin Oncol, 2008. **26**(10): p. 1742-51.
22. Foster, S.A., Whalen, D. M., Ozen, A., Wongchenko, M. J., Yin, J., Yen, I., Schaefer, G., Mayfield, J. D., Chmielecki, J., Stephens, P. J., Albacker, L. A., Yan, Y., Song, K., Hatzivassiliou, G., Eigenbrot, C., Yu, C., Shaw, A. S., Manning, G., Skelton, N. J., Hymowitz, S. G. and Malek, S., *Activation Mechanism of Oncogenic Deletion Mutations in BRAF, EGFR, and HER2*. Cancer Cell, 2016. **29**(4): p. 477-493.
23. Cao, B., Feng, L., Lu, D., Liu, Y., Liu, Y., Guo, S., Han, N., Liu, X., Mao, Y., He, J., Cheng, S., Gao, Y. and Zhang, K., *Prognostic value of molecular events from negative surgical margin of non- small-cell lung cancer*. Oncotarget, 2017. **8**(32): p. 53642-53653.
24. Mu, X.L., Li, L. Y., Zhang, X. T., Wang, S. L. and Wang, M. Z., *Evaluation of safety and efficacy of gefitinib ('iressa', zd1839) as monotherapy in a series of Chinese patients with advanced non-small-cell lung cancer: experience from a compassionate-use programme*. BMC Cancer, 2004. **4**: p. 51.
25. Yun, C.H., Mengwasser, K. E., Toms, A. V., Woo, M. S., Greulich, H., Wong, K. K., Meyerson, M. and Eck, M. J., *The T790M mutation in EGFR kinase causes drug resistance by increasing the affinity for ATP*. Proc Natl Acad Sci U S A, 2008. **105**(6): p. 2070-5.
26. Engelman, J.A., Zejnullahu, K., Mitsudomi, T., Song, Y., Hyland, C., Park, J. O., Lindeman, N., Gale, C. M., Zhao, X., Christensen, J., Kosaka, T., Holmes, A. J., Rogers, A. M., Cappuzzo, F., Mok, T., Lee, C., Johnson, B. E., Cantley, L. C. and Janne, P. A., *MET amplification leads to gefitinib resistance in lung cancer by activating ERBB3 signaling*. Science, 2007. **316**(5827): p. 1039-43.
27. Thomson, S., Buck, E., Petti, F., Griffin, G., Brown, E., Ramnarine, N., Iwata, K. K., Gibson, N. and Haley, J. D., *Epithelial to mesenchymal transition is a determinant of sensitivity of non- small-cell lung carcinoma cell lines and xenografts to epidermal growth factor receptor inhibition*. Cancer Res, 2005. **65**(20): p. 9455-62.
28. Duan, J., Wang, Z., Bai, H., An, T., Zhuo, M., Wu, M., Wang, Y., Yang, L. and Wang, J., *Epidermal growth factor receptor variant III mutation in Chinese patients with squamous cell cancer of the lung*. Thorac Cancer, 2015. **6**(3): p. 319-26.
29. Deng, J., Shimamura, T., Perera, S., Carlson, N. E., Cai, D., Shapiro, G. I., Wong, K. K. and Letai, A., *Proapoptotic BH3-only BCL-2 family protein BIM*

- connects death signaling from epidermal growth factor receptor inhibition to the mitochondrion. Cancer Res, 2007. 67(24): p. 11867-75.*
30. Harada, H. and S. Grant, *Targeting the regulatory machinery of BIM for cancer therapy. Crit Rev Eukaryot Gene Expr, 2012. 22(2): p. 117-29.*
  31. Faber, A.C., Corcoran, R. B., Ebi, H., Sequist, L. V., Waltman, B. A., Chung, E., Incio, J., Digumarthy, S. R., Pollack, S. F., Song, Y., Muzikansky, A., Lifshits, E., Roberge, S., Coffman, E. J., Benes, C. H., Gomez, H. L., Baselga, J., Arteaga, C. L., Rivera, M. N., Dias-Santagata, D., Jain, R. K. and Engelman, J. A., *BIM expression in treatment-naive cancers predicts responsiveness to kinase inhibitors. Cancer Discov, 2011. 1(4): p. 352-65.*
  32. Sharma, S.V., Bell, D. W., Settleman, J. and Haber, D. A., *Epidermal growth factor receptor mutations in lung cancer. Nat Rev Cancer, 2007. 7(3): p. 169-81.*
  33. Kim, H., Yun, T., Lee, Y. J., Han, J. Y., Kim, H. T. and Lee, G. K., *Post-progression survival in patients with non-small cell lung cancer with clinically acquired resistance to gefitinib. J Korean Med Sci, 2013. 28(11): p. 1595-602.*
  34. Bell, D.W., Gore, I., Okimoto, R. A., Godin-Heymann, N., Sordella, R., Mulloy, R., Sharma, S. V., Brannigan, B. W., Mohapatra, G., Settleman, J. and Haber, D. A., *Inherited susceptibility to lung cancer may be associated with the T790M drug resistance mutation in EGFR. Nat Genet, 2005. 37(12): p. 1315-6.*
  35. Maione, P., Rossi, A., Bareschino, M., Sacco, P. C., Schettino, C., Casaluce, F., Sgambato, A. and Gridelli, C., *Irreversible EGFR inhibitors in the treatment of advanced NSCLC. Curr Pharm Des, 2014. 20(24): p. 3894-900.*
  36. Landi, L. and F. Cappuzzo, *Irreversible EGFR-TKIs: dreaming perfection. Transl LungCancer Res, 2013. 2(1): p. 40-9.*
  37. Johnson, M., Koukoulis, G., Kochhar, K., Kubo, C., Nakamura, T. and Iyer, A., *Selective tumorigenesis in non-parenchymal liver epithelial cell lines by hepatocyte growth factor transfection. Cancer Lett, 1995. 96(1): p. 37-48.*
  38. Kochhar, K.S., Johnson, M. E., Volpert, O. and Iyer, A. P., *Evidence for autocrine basis of transformation in NIH-3T3 cells transfected with met/HGF receptor gene. Growth Factors, 1995. 12(4): p. 303-13.*

39. Balak, M.N., Gong, Y., Riely, G. J., Somwar, R., Li, A. R., Zakowski, M. F., Chiang, A., Yang, G., Ouerfelli, O., Kris, M. G., Ladanyi, M., Miller, V. A. and Pao, W., *Novel D761Y and common secondary T790M mutations in epidermal growth factor receptor-mutant lung adenocarcinomas with acquired resistance to kinase inhibitors*. Clin Cancer Res, 2006. **12**(21): p. 6494-501.
40. Schiller, J.H., Akerley, W.L., Brugger, W., Ferrari, D., Garmey, E.G., Gerber, D.E., Orlov, S.V., Ramlau, R., Pawel, J., Sequist, L.V., *Results from ARQ 197-209: A global randomized placebo-controlled phase II clinical trial of erlotinib plus ARQ 197 versus erlotinib plus placebo in previously treated EGFR inhibitor-naive patients with locally advanced or metastatic non-small cell lung cancer (NSCLC)*. Journal of Clinical Oncology, 2010. **28**(18).
41. Takezawa, K., Pirazzoli, V., Arcila, M. E., Nebhan, C. A., Song, X., de Stanchina, E., Ohashi, K., Janjigian, Y. Y., Spitzler, P. J., Melnick, M. A., Riely, G. J., Kris, M. G., Miller, V. A., Ladanyi, M., Politi, K. and Pao, W., *HER2 amplification: a potential mechanism of acquired resistance to EGFR inhibition in EGFR-mutant lung cancers that lack the second-site EGFR T790M mutation*. Cancer Discov, 2012. **2**(10): p. 922-33.
42. Scrima, M., Marino, F., Oliveira, D., Marinaro, C., Mantia, E., Rocco, G., De Marco, C., Malanga, D., De Rosa, N., Rizzuto, A., Botti, G., Franco, R., Zoppoli, P., Viglietto, G., *Aberrant Signaling through the HER2-ERK1/2 Pathway is Predictive of Reduced Disease-Free and Overall Survival in Early Stage Non-Small Cell Lung Cancer (NSCLC) Patients*. J Cancer, 2017. **8**(2): p. 227-239.
43. Janjigian, Y.Y., Smit, E. F., Groen, H. J., Horn, L., Gettinger, S., Camidge, D. R., Riely, G. J., Wang, B., Fu, Y., Chand, V. K., Miller, V. A. and Pao, W., *Dual inhibition of EGFR with afatinib and cetuximab in kinase inhibitor-resistant EGFR-mutant lung cancer with and without T790M mutations*. Cancer Discov, 2014. **4**(9): p. 1036-45.
44. Miyazaki, K., Sato, S., Kodama, T., Satoh, H. and Hizawa, N., *Acquired T790M resistance to afatinib in EGFR mutated lung adenocarcinoma*. Tuberk Toraks, 2016. **64**(4): p. 317-318.
45. Cappuzzo, F., Gregorc, V., Rossi, E., Cancellieri, A., Magrini, E., Paties, C. T., Ceresoli, G., Lombardo, L., Bartolini, S., Calandri, C., de Rosa, M., Villa, E. and Crino, L., *Gefitinib in pretreated non-small-cell lung cancer (NSCLC): analysis of efficacy and correlation with HER2 and epidermal growth factor receptor expression in locally advanced or metastatic NSCLC*. J Clin Oncol, 2003. **21**(14): p. 2658-63.

46. Yeo, C.D., Park, K. H., Park, C. K., Lee, S. H., Kim, S. J., Yoon, H. K., Lee, Y. S., Lee, E. J., Lee, K. Y. and Kim, T. J., *Expression of insulin-like growth factor 1 receptor (IGF-1R) predicts poor responses to epidermal growth factor receptor (EGFR) tyrosine kinase inhibitors in non-small cell lung cancer patients harboring activating EGFR mutations*. Lung Cancer, 2015. **87**(3): p. 311-7.
47. Peled, N., Wynes, M. W., Ikeda, N., Ohira, T., Yoshida, K., Qian, J., Ilouze, M., Brenner, R., Kato, Y., Mascoux, C. and Hirsch, F. R., *Insulin-like growth factor-1 receptor (IGF-1R) as a biomarker for resistance to the tyrosine kinase inhibitor gefitinib in non-small cell lung cancer*. Cell Oncol (Dordr), 2013. **36**(4): p. 277-88.
48. Varkaris, A., Gaur, S., Parikh, N. U., Song, J. H., Dayyani, F., Jin, J. K., Logothetis, C. J. and Gallick, G. E., *Ligand-independent activation of MET through IGF-1/IGF-1R signaling*. Int J Cancer, 2013. **133**(7): p. 1536-46.
49. Akekawatchai, C., Holland, J. D., Kochetkova, M., Wallace, J. C. and McColl, S. R., *Transactivation of CXCR4 by the insulin-like growth factor-1 receptor (IGF-1R) in human MDA-MB-231 breast cancer epithelial cells*. J Biol Chem, 2005. **280**(48): p. 39701-8.
50. Oser, M.G., Niederst, M. J., Sequist, L. V. and Engelman, J. A., *Transformation from non-small-cell lung cancer to small-cell lung cancer: molecular drivers and cells of origin*. Lancet Oncol, 2015. **16**(4): p. e165-72.
51. Sequist, L.V., Waltman, B. A., Dias-Santagata, D., Digumarthy, S., Turke, A. B., Fidias, P., Bergethon, K., Shaw, A. T., Gettinger, S., Cosper, A. K., Akhavanfard, S., Heist, R. S., Temel, J., Christensen, J. G., Wain, J. C., Lynch, T. J., Vernovsky, K., Mark, E. J., Lanuti, M., Iafrate, A. J., Mino-Kenudson, M. and Engelman, J. A., *Genotypic and histological evolution of lung cancers acquiring resistance to EGFR inhibitors*. Sci Transl Med, 2011. **3**(75): p. 75ra26.
52. Yu, H.A., Arcila, M. E., Rekhtman, N., Sima, C. S., Zakowski, M. F., Pao, W., Kris, M. G., Miller, V. A., Ladanyi, M. and Riely, G. J., *Analysis of tumor specimens at the time of acquired resistance to EGFR-TKI therapy in 155 patients with EGFR-mutant lung cancers*. Clin Cancer Res, 2013. **19**(8): p. 2240-7.



53. Peifer, M., Fernandez-Cuesta, L., Sos, M. L., George, J., Seidel, D., Kasper, L. H., Plenker, D., Leenders, F., Sun, R., Zander, T., Menon, R., Koker, M., Dahmen, I., Muller, C., Di Cerbo, V., Schildhaus, H. U., Altmuller, J., Baessmann, I., Becker, C., de Wilde, B., Vandesompele, J., Bohm, D., Ansen, S., Gabler, F., Wilkening, I., Heynck, S., Heuckmann, J. M., Lu, X., Carter, S. L., Cibulskis, K., Banerji, S., Getz, G., Park, K. S., Rauh, D., Grutter, C., Fischer, M., Pasqualucci, L., Wright, G., Wainer, Z., Russell, P., Petersen, I., Chen, Y., Stoelben, E., Ludwig, C., Schnabel, P., Hoffmann, H., Muley, T., Brockmann, M., Engel-Riedel, W., Muscarella, L. A., Fazio, V. M., Groen, H., Timens, W., Sietsma, H., Thunnissen, E., Smit, E., Heideman, D. A., Snijders, P. J., Cappuzzo, F., Ligorio, C., Damiani, S., Field, J., Solberg, S., Brustugun, O. T., Lund-Iversen, M., Sanger, J., Clement, J. H., Soltermann, A., Moch, H., Weder, W., Solomon, B., Soria, J. C., Validire, P., Besse, B., Brambilla, E., Brambilla, C., Lantuejoul, S., Lorimier, P., Schneider, P. M., Hallek, M., Pao, W., Meyerson, M., Sage, J., Shendure, J., Schneider, R., Buttner, R., Wolf, J., Nurnberg, P., Perner, S., Heukamp, L. C., Brindle, P. K., Haas, S. and Thomas, R. K., *Integrative genome analyses identify key somatic driver mutations of small-cell lung cancer*. Nat Genet, 2012. **44**(10): p. 1104-10.
54. Luo, Z., Wu, R. R., Lv, L., Li, P., Zhang, L. Y., Hao, Q. L. and Li, W., *Prognostic value of CD44 expression in non-small cell lung cancer: a systematic review*. Int J Clin Exp Pathol, 2014. **7**(7): p. 3632-46.
55. Soucheray, M., Capelletti, M., Pulido, I., Kuang, Y., Paweletz, C. P., Becker, J. H., Kikuchi, E., Xu, C., Patel, T. B., Al-Shahrour, F., Carretero, J., Wong, K. K., Janne, P. A., Shapiro, G. I. and Shimamura, T., *Intratumoral Heterogeneity in EGFR-Mutant NSCLC Results in Divergent Resistance Mechanisms in Response to EGFR Tyrosine Kinase Inhibition*. Cancer Res, 2015. **75**(20): p. 4372-83.
56. Brabletz, T., Kalluri, R., Nieto, M. A. and Weinberg, R. A., *EMT in cancer*. Nat Rev Cancer, 2018. **18**(2): p. 128-134.
57. Uramoto, H., Iwata, T., Onitsuka, T., Shimokawa, H., Hanagiri, T. and Oyama, T., *Epithelial-mesenchymal transition in EGFR-TKI acquired resistant lung adenocarcinoma*. Anticancer Res, 2010. **30**(7): p. 2513-7.
58. Weinstein, R.S., F.B. Merck, and J. Alroy, *The structure and function of intercellular junctions in cancer*. Adv Cancer Res, 1976. **23**: p. 23-89.
59. Gabbert, H., Wagner, R., Moll, R. and Gerharz, C. D., *Tumor dedifferentiation: an important step in tumor invasion*. Clin Exp Metastasis, 1985. **3**(4): p. 257-79.
60. Lyons, J.G., Lobo, E., Martorana, A. M. and Myerscough, M. R., *Clonal diversity in carcinomas: its implications for tumour progression and the contribution made to it by epithelial-mesenchymal transitions*. Clin Exp Metastasis, 2008. **25**(6): p. 665-77.

61. Mahmood, M.Q., Ward, C., Muller, H. K., Sohal, S. S. and Walters, E. H., *Epithelial mesenchymal transition (EMT) and non-small cell lung cancer (NSCLC): a mutual association with airway disease*. Med Oncol, 2017. **34**(3): p. 45.
62. Brabletz, T., *EMT and MET in metastasis: where are the cancer stem cells?* Cancer Cell, 2012. **22**(6): p. 699-701.
63. Davenport, A.P. and J.J. Maguire, *Endothelin*. Handb Exp Pharmacol, 2006(176 Pt 1): p. 295- 329.
64. Boldrini, L., Gisfredi, S., Ursino, S., Faviana, P., Lucchi, M., Melfi, F., Mussi, A., Basolo, F. and Fontanini, G., *Expression of endothelin-1 is related to poor prognosis in non-small cell lung carcinoma*. Eur J Cancer, 2005. **41**(18): p. 2828-35.
65. Arun, C., N.J. London, and D.M. Hemingway, *Prognostic significance of elevated endothelin-1 levels in patients with colorectal cancer*. Int J Biol Markers, 2004. **19**(1): p. 32-7.
66. Asham, E., Shankar, A., Loizidou, M., Fredericks, S., Miller, K., Boulos, P. B., Burnstock, G. and Taylor, I., *Increased endothelin-1 in colorectal cancer and reduction of tumour growth by ET(A) receptor antagonism*. Br J Cancer, 2001. **85**(11): p. 1759-63.
67. Dhaun, N., J. Goddard, and D.J. Webb, *The endothelin system and its antagonism in chronic kidney disease*. J Am Soc Nephrol, 2006. **17**(4): p. 943-55.
68. Smollich, M., Gotte, M., Kersting, C., Fischgrabe, J., Kiesel, L. and Wulfing, P., *Selective ETAR antagonist atrasentan inhibits hypoxia-induced breast cancer cell invasion*. Breast Cancer Res Treat, 2008. **108**(2): p. 175-82.
69. Salani, D., Di Castro, V., Nicotra, M. R., Rosano, L., Tecce, R., Venuti, A., Natali, P. G. and Bagnato, A., *Role of endothelin-1 in neovascularization of ovarian carcinoma*. Am J Pathol, 2000. **157**(5): p. 1537-47.
70. Iijima, K., Lin, L., Nasjletti, A. and Goligorsky, M. S., *Intracellular signaling pathway of endothelin-1*. J Cardiovasc Pharmacol, 1991. **17 Suppl 7**: p. S146-9.
71. Li, X., Dai, D., Chen, B., Tang, H., Xie, X. and Wei, W., *Efficacy of PI3K/AKT/mTOR pathway inhibitors for the treatment of advanced solid cancers: A literature-based meta-analysis of 46 randomised control trials*. PLoS One, 2018. **13**(2): p. e0192464.

72. Mandal, A., Shahidullah, M., Beimgraben, C. and Delamere, N. A., *The effect of endothelin-1 on Src-family tyrosine kinases and Na,K-ATPase activity in porcine lens epithelium*. J Cell Physiol, 2011. **226**(10): p. 2555-61.
73. Petreaca, M.L., Yao, M., Liu, Y., Defea, K. and Martins-Green, M., *Transactivation of vascular endothelial growth factor receptor-2 by interleukin-8 (IL-8/CXCL8) is required for IL-8/CXCL8-induced endothelial permeability*. Mol Biol Cell, 2007. **18**(12): p. 5014-23.
74. Shah, B.H., Farshori, M. P., Jambusaria, A. and Catt, K. J., *Roles of Src and epidermal growth factor receptor transactivation in transient and sustained ERK1/2 responses to gonadotropin-releasing hormone receptor activation*. J Biol Chem, 2003. **278**(21): p. 19118-26.
75. Oda, K., Matsuoka, Y., Funahashi, A. and Kitano, H., *A comprehensive pathway map of epidermal growth factor receptor signaling*. Mol Syst Biol, 2005. **1**: p. 2005 0010.
76. Koch, S., Tugues, S., Li, X., Gualandi, L. and Claesson-Welsh, L., *Signal transduction by vascular endothelial growth factor receptors*. Biochem J, 2011. **437**(2): p. 169-83.
77. Maurey, C., Hislop, A. A., Advenier, C., Vouhe, P. R., Israel-Biet, D. and Levy, M., *Interaction of KATP channels and endothelin-1 in lambs with persistent pulmonary hypertension of the newborn*. Pediatr Res, 2006. **60**(3): p. 252-7.
78. Baumgart, B., Guha, M., Hennan, J., Li, J., Woicke, J., Simic, D., Graziano, M., Wallis, N., Sanderson, T. and Bunch, R. T., *In vitro and in vivo evaluation of dasatinib and imatinib on physiological parameters of pulmonary arterial hypertension*. Cancer Chemother Pharmacol, 2017. **79**(4): p. 711-723.
79. Harsing, L., Bartha, J., Harza, T. and Kover, G., *[Blood flow and PAH-extraction of the isolated kidney in osmotic diuresis and during ureteral occlusion]*. Pflugers Arch, 1969. **308**(1): p. 47-56.
80. D'Alto, M., M., Romeo, E., Argiento, P., Paciocco, G., Prediletto, R., Ghio, S., Correale, M., Lo Giudice, F., Badagliacca, R., Greco, A. and Vizza, C. D., *Initial tadalafil and ambrisentan combination therapy in pulmonary arterial hypertension: cLinical and haemodyNamic long-term efficacy (ITALY study)*. J Cardiovasc Med (Hagerstown), 2018. **19**(1): p. 12-17.
81. Henrie, A.M., J.J. Nawarskas, and J.R. Anderson, *Clinical utility of tadalafil in the treatment of pulmonary arterial hypertension: an evidence-based review*. Core Evid, 2015. **10**: p. 99-109.

82. Morbidelli, L., Orlando, C., Maggi, C. A., Ledda, F. and Ziche, M., *Proliferation and migration of endothelial cells is promoted by endothelins via activation of ETB receptors*. Am J Physiol, 1995. **269**(2 Pt 2): p. H686-95.
83. Salani, D., Taraboletti, G., Rosano, L., Di Castro, V., Borsotti, P., Giavazzi, R. and Bagnato, A., *Endothelin-1 induces an angiogenic phenotype in cultured endothelial cells and stimulates neovascularization in vivo*. Am J Pathol, 2000. **157**(5): p. 1703-11.
84. Wu, M.H., Huang, C. Y., Lin, J. A., Wang, S. W., Peng, C. Y., Cheng, H. C. and Tang, C. H., *Endothelin-1 promotes vascular endothelial growth factor-dependent angiogenesis in human chondrosarcoma cells*. Oncogene, 2014. **33**(13): p. 1725-35.
85. Weydert, C.J., Esser, A. K., Mejia, R. A., Drake, J. M., Barnes, J. M. and Henry, M. D., *Endothelin-1 inhibits prostate cancer growth in vivo through vasoconstriction of tumor-feeding arterioles*. Cancer Biol Ther, 2009. **8**(8): p. 720-9.
86. Lahav, R., Suva, M. L., Rimoldi, D., Patterson, P. H. and Stamenkovic, I., *Endothelin receptor B inhibition triggers apoptosis and enhances angiogenesis in melanomas*. Cancer Res, 2004. **64**(24): p. 8945-53.
87. DiSalvo, J., Bayne, M. L., Conn, G., Kwok, P. W., Trivedi, P. G., Soderman, D. D., Palisi, T. M., Sullivan, K. A. and Thomas, K. A., *Purification and characterization of a naturally occurring vascular endothelial growth factor.placenta growth factor heterodimer*. J Biol Chem, 1995. **270**(13): p. 7717-23.
88. Senger, D.R., Galli, S. J., Dvorak, A. M., Perruzzi, C. A., Harvey, V. S. and Dvorak, H. F., *Tumor cells secrete a vascular permeability factor that promotes accumulation of ascites fluid*. Science, 1983. **219**(4587): p. 983-5.
89. Stringer, S.E., *The role of heparan sulphate proteoglycans in angiogenesis*. Biochem SocTrans, 2006. **34**(Pt 3): p. 451-3.
90. Germain, S., Monnot, C., Muller, L. and Eichmann, A., *Hypoxia-driven angiogenesis: role of tip cells and extracellular matrix scaffolding*. Curr Opin Hematol, 2010. **17**(3): p. 245-51.
91. Simons, M., E. Gordon, and L. Claesson-Welsh, *Mechanisms and regulation of endothelial VEGF receptor signalling*. Nat Rev Mol Cell Biol, 2016. **17**(10): p. 611-25.

92. Shalaby, F., Rossant, J., Yamaguchi, T. P., Gertsenstein, M., Wu, X. F., Breitman, M. L. and Schuh, A. C., *Failure of blood-island formation and vasculogenesis in Flk-1-deficient mice*. Nature, 1995. **376**(6535): p. 62-6.
93. Doebele, R.C., Spigel, D., Tehfe, M., Thomas, S., Reck, M., Verma, S., Eakle, J., Bustin, F., Goldschmidt, J., Jr., Cao, D., Alexandris, E., Yurasov, S., Camidge, D. R. and Bonomi, P., *Phase 2, randomized, open-label study of ramucirumab in combination with first-line pemetrexed and platinum chemotherapy in patients with nonsquamous, advanced/metastatic non-small cell lung cancer*. Cancer, 2015. **121**(6): p. 883-92.
94. Villaruz, L.C. and M.A. Socinski, *The role of anti-angiogenesis in non-small-cell lung cancer: an update*. Curr Oncol Rep, 2015. **17**(6): p. 26.
95. Mori, R., Fujimoto, D., Ito, M. and Tomii, K., *Bevacizumab for ramucirumab refractory malignant pleural effusion in non-small cell lung cancer: a case report and review of the literature*. Oncotarget, 2017. **8**(29): p. 48521-48524.
96. Wang, J., Chen, J., Guo, Y., Wang, B. and Chu, H., *Strategies targeting angiogenesis in advanced non-small cell lung cancer*. Oncotarget, 2017. **8**(32): p. 53854-53872.
97. Caraglia, M., Santini, D., Bronte, G., Rizzo, S., Sortino, G., Rini, G. B., Di Fede, G. and Russo, A., *Predicting efficacy and toxicity in the era of targeted therapy: focus on anti-EGFR and anti-VEGF molecules*. Curr Drug Metab, 2011. **12**(10): p. 944-55.
98. Brunner, M., Thurnher, D., Pammer, J., Geleff, S., Heiduschka, G., Reinisch, C. M., Petzelbauer, P. and Erovic, B. M., *Expression of VEGF-A/C, VEGF-R2, PDGF-alpha/beta, c-kit, EGFR, Her-2/Neu, Mcl-1 and Bmi-1 in Merkel cell carcinoma*. Mod Pathol, 2008. **21**(7): p. 876-84.
99. Weber, D.C., Tille, J. C., Combescure, C., Egger, J. F., Laouiti, M., Hammad, K., Granger, P., Rubbia-Brandt, L. and Miralbell, R., *The prognostic value of expression of HIF1alpha, EGFR and VEGF-A, in localized prostate cancer for intermediate- and high-risk patients treated with radiation therapy with or without androgen deprivation therapy*. Radiat Oncol, 2012. **7**: p. 66.
100. Chen, S., Liu, X., Gong, W., Yang, H., Luo, D., Zuo, X., Li, W., Wu, P., Liu, L., Xu, Q. and Ji, A., *Combination therapy with VEGFR2 and EGFR siRNA enhances the antitumor effect of cisplatin in non-small cell lung cancer xenografts*. Oncol Rep, 2013. **29**(1): p. 260-8.
101. Pan, Y., Xu, Y., Feng, S., Luo, S., Zheng, R., Yang, J., Wang, L., Zhong, L., Yang, H. Y., Wang, B. L., Yu, Y., Liu, J., Cao, Z., Wang, X., Ji, P., Wang, Z., Chen, X., Zhang, S., Wei, Y. Q. and Yang, S. Y., *SKLB1206, a novel orally available multikinase inhibitor targeting EGFR activating and T790M mutants, ErbB2, ErbB4, and VEGFR2, displays potent antitumor activity both in vitro and in vivo*. Mol Cancer Ther, 2012. **11**(4): p. 952-62.

102. Morabito, A., Piccirillo, M. C., Costanzo, R., Sandomenico, C., Carillio, G., Daniele, G., Giordano, P., Bryce, J., Carotenuto, P., La Rocca, A., Di Maio, M., Normanno, N., Rocco, G. and Perrone, F., *Vandetanib: An overview of its clinical development in NSCLC and other tumors*. *Drugs Today (Barc)*, 2010. **46**(9): p. 683-98.
103. Massarelli, E., Onn, A., Marom, E. M., Alden, C. M., Liu, D. D., Tran, H. T., Mino, B., Wistuba, II, Faiz, S. A., Bashoura, L., Eapen, G. A., Morice, R. C., Jack Lee, J., Hong, W. K., Herbst, R. S. and Jimenez, C. A., *Vandetanib and indwelling pleural catheter for non-small-cell lung cancer with recurrent malignant pleural effusion*. *Clin Lung Cancer*, 2014. **15**(5): p. 379-86.
104. Pietanza, M.C., Lynch, T. J., Jr., Lara, P. N., Jr., Cho, J., Yanagihara, R. H., Vrindavanam, N., Chowhan, N. M., Gadgeel, S. M., Pennell, N. A., Funke, R., Mitchell, B., Wakelee, H. A. and Miller, V. A., *XL647--a multitargeted tyrosine kinase inhibitor: results of a phase II study in subjects with non-small cell lung cancer who have progressed after responding to treatment with either gefitinib or erlotinib*. *J Thorac Oncol*, 2012. **7**(1): p. 219-26.
105. Groen, H.J., Socinski, M. A., Grossi, F., Juhasz, E., Gridelli, C., Baas, P., Butts, C. A., Chmielowska, E., Usari, T., Selaru, P., Harmon, C., Williams, J. A., Gao, F., Tye, L., Chao, R. C. and Blumenschein, G. R., Jr., *A randomized, double-blind, phase II study of erlotinib with or without sunitinib for the second-line treatment of metastatic non-small-cell lung cancer (NSCLC)*. *Ann Oncol*, 2013. **24**(9): p. 2382-9.
106. Cell Biolabs, I. *293LTV Cell Line*. 2011 [cited 2018; Available from: <https://www.cellbiolabs.com/sites/default/files/LTV-100-lentivirus-293-cell-line.pdf>].
107. Carpentier, G. *Angiogenesis Analyzer for ImageJ*. in *ImageJ User and Developer Conference*. 2012. Mondorf-les-Bains, Luxembourg.
108. Weidner, N., *Current pathologic methods for measuring intratumoral microvessel density within breast carcinoma and other solid tumors*. *Breast Cancer Res Treat*, 1995. **36**(2): p. 169- 80.
109. Weidner, N., Carroll, P. R., Flax, J., Blumenfeld, W. and Folkman, J., *Tumor angiogenesis correlates with metastasis in invasive prostate carcinoma*. *Am J Pathol*, 1993. **143**(2): p. 401-9.
110. Weidner, N., Folkman, J., Pozza, F., Bevilacqua, P., Allred, E. N., Moore, D. H., Meli, S. and Gasparini, G., *Tumor angiogenesis: a new significant and independent prognostic indicator in early-stage breast carcinoma*. *J Natl Cancer Inst*, 1992. **84**(24): p. 1875-87.

111. Puztaszeri, M.P., W. Seelentag, and F.T. Bosman, *Immunohistochemical expression of endothelial markers CD31, CD34, von Willebrand factor, and Fli-1 in normal human tissues*. J Histochem Cytochem, 2006. **54**(4): p. 385-95.
112. Chen, H.F., Chuang, C. Y., Lee, W. C., Huang, H. P., Wu, H. C., Ho, H. N., Chen, Y. J. and Kuo, H. C., *Surface marker epithelial cell adhesion molecule and E-cadherin facilitate the identification and selection of induced pluripotent stem cells*. Stem Cell Rev, 2011. **7**(3): p. 722-35.
113. Sawano, A., Takahashi, T., Yamaguchi, S. and Shibuya, M., *The phosphorylated 1169-tyrosine containing region of flt-1 kinase (VEGFR-1 is a major binding site for PLCgamma*. Biochem Biophys Res Commun, 1997. **238**(2): p. 487-91.
114. Wu, Q., Li, M. Y., Li, H. Q., Deng, C. H., Li, L., Zhou, T. Y. and Lu, W., *Pharmacokinetic-pharmacodynamic modeling of the anticancer effect of erlotinib in a human non-small cell lung cancer xenograft mouse model*. Acta Pharmacol Sin, 2013. **34**(11): p. 1427-36.
115. Nowell, P.C., *The clonal evolution of tumor cell populations*. Science, 1976. **194**(4260): p. 23-8.
116. Shlush, L.I. and D. HersHKovitz, *Clonal evolution models of tumor heterogeneity*. Am Soc Clin Oncol Educ Book, 2015: p. e662-5.
117. Bae, G.Y., Choi, S. J., Lee, J. S., Jo, J., Lee, J., Kim, J. and Cha, H. J., *Loss of E-cadherin activates EGFR-MEK/ERK signaling, which promotes invasion via the ZEB1/MMP2 axis in non-small cell lung cancer*. Oncotarget, 2013. **4**(12): p. 2512-22.
118. Miller, K., Moul, J. W., Gleave, M., Fizazi, K., Nelson, J. B., Morris, T., Nathan, F. E., McIntosh, S., Pemberton, K. and Higano, C. S., *Phase III, randomized, placebo-controlled study of once-daily oral zibotentan (ZD4054) in patients with non-metastatic castration-resistant prostate cancer*. Prostate Cancer Prostatic Dis, 2013. **16**(2): p. 187-92.
119. Zeng, Q., Li, X., Zhong, G., Zhang, W. and Sun, C., *Endothelin-1 induces intracellular [Ca<sup>2+</sup>] increase via Ca<sup>2+</sup> influx through the L-type Ca<sup>2+</sup> channel, Ca<sup>2+</sup> -induced Ca<sup>2+</sup> release and a pathway involving ET A receptors, PKC, PKA and AT1 receptors in cardiomyocytes*. Sci China C Life Sci, 2009. **52**(4): p. 360-70.
120. Marek, L., Ware, K. E., Fritzsche, A., Hercule, P., Helton, W. R., Smith, J. E., McDermott, L. A., Coldren, C. D., Nemenoff, R. A., Merrick, D. T., Helfrich, B. A., Bunn, P. A., Jr. and Heasley, L. E., *Fibroblast growth factor (FGF) and FGF receptor-mediated autocrine signaling in non-small-cell lung cancer cells*. Mol Pharmacol, 2009. **75**(1): p. 196-207.

121. Ouyang, G., Liu, M., Ruan, K., Song, G., Mao, Y. and Bao, S., *Upregulated expression of periostin by hypoxia in non-small-cell lung cancer cells promotes cell survival via the Akt/PKB pathway*. *Cancer Lett*, 2009. **281**(2): p. 213- 9.
122. T. Ninomiya, N. Takigawa, E. Ichihara, N. Ochi, T. Murakami, Y. Honda, T. Kubo, D. Minami, K. Kudo, M. Tanimoto, K. Kiura. *Afatinib prolongs survival compared with gefitinib in an epidermal growth factor receptor-driven lung cancer model* *Mol. Cancer Ther.*, 12 (5) (2013), pp. 589-597
123. Takagi K., Takada T., Amano H. *A high peripheral microvessel density count correlates with a poor prognosis in pancreatic cancer*. *Journal of Gastroenterology*. 2005;40(4):402–408. doi: 10.1007/s00535-004-1556-x.
124. Rajaganeshan, R, Prasad, R., Guillou, P. J., Chalmers, C. R., Scott, N., Sarkar, R., Poston, G. and Jayne, D. G., *The Influence of Invasive Growth Pattern and Microvessel Density on Prognosis in Colorectal Cancer and Colorectal Liver Metastases*. *British Journal of Cancer* 96.7 (2007): 1112–1117. *PMC*. Web. 19 Mar. 2018.
125. Volm M, Koomagi R, Mattern J. *Interrelationships between microvessel density, expression of VEGF and resistance to doxorubicin of non-small lung cell carcinoma*. *Anticancer Res*. 1996;16(1):213–218.
126. Dybdal-Hargreaves, Nicholas F., April L. Risinger, and Susan L. Mooberry. *Regulation of E-Cadherin Localization by Microtubule Targeting Agents: Rapid Promotion of Cortical E-Cadherin through p130Cas/Src Inhibition by Eribulin*. *Oncotarget* 9.5 (2018): 5545–5561. *PMC*. Web. 19 Mar. 2018.



## VITA

Stephen Laszlo Ollosi was born August 16<sup>th</sup>, 1987 in Oak Park, IL. He attended the University of Illinois in Chicago where he earned a Bachelor's of Science in Biological Sciences in 2010. After earning his BS, Stephen worked as a quality control microbiologist in the food safety industry. Stephen then joined the Loyola University Chicago Stritch School of Medicine Biochemistry and Molecular Biology program and began his graduate education in Cancer Biology under Dr. Takeshi Shimamura.

Stephen's Thesis work aims at elucidating the role of Endothelin-1 (EDN1) in non-small cell lung cancer (NSCLC) disease progression and the potential efficacy of targeting angiogenesis during NSCLC treatment. After completion of his Master of Science, Stephen will re-enter industry in a pharmaceutical research company.

